Aus der Medizinischen Klinik und Poliklinik IV

Klinikum der Ludwig-Maximilians-Universität München

Direktor: Prof. Dr. med. Martin Reincke

Novel molecular targeted therapies in pheochromocytomas, paragangliomas and neuroendocrine tumors

Dissertation

zum Erwerb des Doktorgrades der Medizin

an der Medizinischen Fakultät der

Ludwig-Maximilians-Universität München

vorgelegt von

Katharina Wang

aus

Graz

2024

Mit Genehmigung der Medizinischen Fakultät der

Ludwig-Maximilians-Universität zu München

Erstes Gutachten:	Prof. Dr. med. Svenja Nölting
Zweites Gutachten:	Prof. Dr. Thomas Knösel
Drittes Gutachten:	Prof. Dr. Ludwig Schaaf

Dekan:	Prof. Dr. med. Thomas Gudermann

Tag der mündlichen Prüfung:	13.12.2024

Affidavit

I hereby declare that the submitted thesis titled: “Novel molecular targeted therapies in pheochromocytomas, paragangliomas and neuroendocrine tumors” is my own work.

I have only used the sources indicated and have not made unauthorized use of services of a third party. Where the work of others has been quoted or reproduced, the source is always given.

I further declare that the dissertation presented here has not been submitted in the same or similar form to any other institution for the purpose of obtaining an academic degree.

Munich, 15.12.2024

Katharina Wang

_____

Table of content

Affidavit **3**

Table of content **4**

Abbreviations **5**

List of publications **6**

Contribution to the publications **8**

1. Introduction **10**

1.1 Background 10

1.1.1 *Pheochromocytomas and paragangliomas* 10

1.1.2 *Neuroendocrine tumors* 12

1.2 Personalized drug testing in human pheochromocytoma/paraganglioma primary cultures 13

1.3 Impact of the PI3Kalpha inhibitor alpelisib on everolimus resistance and somatostatin receptor expression in an orthotopic pancreatic NEC xenograft mouse model 17

2. Abstract **20**

3. Zusammenfassung **21**

4. References **22**

5. Publication I **26**

6. Publication II **27**

7. Appendix (Publication III) **28**

Acknowledgements **29**

Abbreviations

ECAR	Extracellular acidification rates
GSK3	Glycogen synthase kinase-3
MPC	Mouse pheochromocytoma
NECs	Neuroendocrine carcinomas
NENs	Neuroendocrine neoplasms
NETs	Neuroendocrine tumors
NGS	Next generation sequencing
OCR	Oxygen consumption rates
panNETs	Pancreatic neuroendocrine tumors
PCCs	Pheochromocytomas
PGLs	Paragangliomas
PPGLs	Pheochromocytomas and paragangliomas
PRRT	Peptide (somatostatin) receptor-based radionuclide therapy
SCID	Severe combined immunodeficient
SDHB	Succinate dehydrogenase subunit B
SSTR2	Somatostatin receptor 2

List of publications

Publications that are part of this cumulative dissertation:

Wang K, Schütze I, Gulde S, Bechmann N, Richter S, Helm J, Lauseker M, Maurer J, Reul A, Spoettl G, Klink B, William D, Knösel T, Friemel J, Bihl M, Weber A, Fankhauser M, Schober L, Vetter D, Broglie Däppen M, Ziegler CG, Ullrich M, Pietzsch J, Bornstein SR, Lottspeich C, Kroiss M, Fassnacht M, Wenter VUJ, Ladurner R, Hantel C, Reincke M, Eisenhofer G, Grossman AB, Pacak K, Beuschlein F, Auernhammer CJ, Pellegata NS, **Nölting S**. Personalized drug testing in human pheochromocytoma/paraganglioma primary cultures. Endocr Relat Cancer. 2022 May 9;29(6):285-306. doi: 10.1530/ERC-21-0355. PMID: 35324454.

Mohan AM, Prasad S, Schmitz-Peiffer F, Lange C, Lukas M, Koziolek EJ, Albrecht J, Messroghli D, Stein U, Ilmer M, **Wang K**, Schober L, Reul A, Maurer J, Friemel J, Weber A, Zuellig RA, Hantel C, Fritsch R, Reincke M, Pacak K, Grossman AB, Auernhammer CJ, Beuschlein F, Brenner W, Beindorff N, **Nölting S**. Impact of the PI3Kalpha inhibitor alpelisib on everolimus resistance and somatostatin receptor expression in an orthotopic pancreatic NEC xenograft mouse model. Endocr Relat Cancer. 2023 Nov 1:ERC-23-0041. doi: 10.1530/ERC-23-0041. Epub ahead of print. PMID: 37943630.

Wang K, Crona J, Beuschlein F, Grossman AB, Pacak K, **Nölting S**. Targeted Therapies in Pheochromocytoma and Paraganglioma. J Clin Endocrinol Metab. 2022 Nov 23;107(11):2963-2972. doi: 10.1210/clinem/dgac471. PMID: 35973976; PMCID: PMC9923802.

Other publications:

Fischer A, Kloos S, Maccio U, Friemel J, Remde H, Fassnacht M, Pamporaki C, Eisenhofer G, Timmers HJLM, Robledo M, Fliedner SMJ, **Wang K**, Maurer J, Reul A, Zitzmann K, Bechmann N, Žygienė G, Richter S, Hantel C, Vetter D, Lehmann K, Mohr H, Pellegata NS, Ullrich M, Pietzsch J, Ziegler CG, Bornstein SR, Kroiss M, Reincke M, Pacak K, Grossman AB, Beuschlein F, **Nölting S**. Metastatic Pheochromocytoma and Paraganglioma: Somatostatin Receptor 2 Expression, Genetics, and Therapeutic Responses. J Clin Endocrinol Metab. 2023 Sep 18;108(10):2676-2685. doi: 10.1210/clinem/dgad166. PMID: 36946182; PMCID: PMC10505550.

Pamporaki C, Berends AMA, Filippatos A, Prodanov T, Meuter L, Prejbisz A, Beuschlein F, Fassnacht M, Timmers HJLM, **Nölting S**, Abhyankar K, Constantinescu G, Kunath C, de Haas

RJ, **Wang K**, Remde H, Bornstein SR, Januszewicz A, Robledo M, Lenders JWM, Kerstens MN, Pacak K, Eisenhofer G. Prediction of metastatic pheochromocytoma and paraganglioma: a machine learning modelling study using data from a cross-sectional cohort. Lancet Digit Health. 2023 Sep;5(9):e551-e559. doi: 10.1016/S2589-7500(23)00094-8. Epub 2023 Jul 18. PMID: 37474439.

Fischer A, Kloos S, Remde H, Dischinger U, Pamporaki C, Timmers HJLM, Robledo M, Fliedner SMJ, **Wang K**, Maurer J, Reul A, Bechmann N, Hantel C, Mohr H, Pellegata NS, Bornstein SR, Kroiss M, Auernhammer CJ, Reincke M, Pacak K, Grossman AB, Beuschlein F, **Nölting S**. Responses to systemic therapy in metastatic pheochromocytoma/paraganglioma - A retrospective multi-center cohort study. Eur J Endocrinol. 2023 Nov 9:lvad146. doi: 10.1093/ejendo/lvad146. Epub ahead of print. PMID: 37949483.

Fischer A, Maccio U, **Wang K**, Friemel J, Broglie Daeppen MA, Vetter D, Lehmann K, Reul A, Robledo M, Hantel C, Bechmann N, Pacak K, Zitzmann K, Auernhammer CJ, Grossman AB, Beuschlein F, **Nölting S**. PD-L1 and HIF-2α Upregulation in Head and Neck Paragangliomas after Embolization. Cancers (Basel). 2023 Oct 29;15(21):5199. doi: 10.3390/cancers15215199. PMID: 37958373; PMCID: PMC10650267.

Conference presentations:

The joint 22nd ENS@T and 2nd COST Harmonis@tion meeting 2023: “Responses to systemic therapy in metastatic pheochromocytoma and paraganglioma”

ENDO 2023: “Systemic Treatment of Metastatic Pheochromocytomas and Paragangliomas – Established and Novel Therapeutic Options”

15. Deutsche Nebennierenkonferenz 2023: “Metastatic pheochromocytoma and paraganglioma: Retrospective analysis of therapy responses to current systemic treatment options”

SfE BES conference 2022: “Pre clinical and clinical evaluation of targeted therapies in PPGL”

eYARE meeting 2021: “Combination targeted therapies for malignant tumours – Towards precision medicine”

Contribution to the publications

In this chapter, I present my contributions to the three publications included in this cumulative dissertation:

- Publication I: "Personalized drug testing in human pheochromocytoma/paraganglioma primary cultures" (Original work, shared first author)
- Publication II: "Impact of the PI3Kalpha inhibitor alpelisib on everolimus resistance and somatostatin receptor expression in an orthotopic pancreatic NEC xenograft mouse model" (Original work, co-author)
- Publication III (Appendix): "Targeted therapies in Pheochromocytoma and Paraganglioma" (Mini-review, first author)

Publication I:

My contribution to this publication included the planning, execution and analysis of the primary culture experiments and cell culture experiments in cooperation with the chemical- and medical-technical assistants in the research group of Prof. Nölting in Munich. The primary and cell culture experiments consisted of the collection, isolation, cultivation and testing of the primary tumors with different mono- and combination therapies as well as the cultivation and testing of the cell cultures. Analysis of the data included the assessment of cell viability using cell viability assays, the evaluation and interpretation of the data generated, basic statistical calculations, and consultations with our medical statistician.

Another main part of my contribution comprised the drafting of the manuscript and the creation of the tables and figures. Therefore, I extensively studied the literature in the field of PPGLs. Additionally, I organized the transport of tumor material to a partner laboratory where somatic mutation testing was performed, and I distributed the PPGL primary cultures into molecular clusters based on the patient`s specific mutations. I also collected the medical histories of the patients and identified their biochemical phenotypes based on their laboratory results.

The primary culture data from Zurich were generated and integrated into the manuscript by Ina Schütze, who worked in the research laboratory of Prof. Nölting in the University Hospital Zurich. The manuscript data were therefore obtained from both Munich and Zurich and combined for this publication, justifying the shared authorship of Ina Schütze and myself.

Publication II:

My contribution to the second publication of this cumulative dissertation included the cultivation of the BON1KDMSO and BON1RR2 cells, and the execution of the XF Real-Time ATP Rate

Assay experiments in cooperation with the chemical- and medical-technical assistants in the research group of Prof. Nölting in Munich. The cultivation of the everolimus-resistant BON1KDMSO and BON1RR2 cell lines included maintaining and verifying everolimus resistance. The XF Real-Time ATP Rate Assay experiments included the planning and execution of the experiments, the evaluation and interpretation of the data, as well as literature studies related to the scientific context of the obtained data. I also aided in the organization of the transport of frozen cell vials and drugs to our partner laboratory for the performance of animal experiments.

Additionally, I contributed to the revision and editing of the manuscript.

Publication III (Appendix):

My contribution to this mini-review comprised an extensive literature search on the management and therapy of metastatic PPGLs and the subsequent drafting of the manuscript.

The former included a systematic review of relevant research articles, expert views, and guidelines on targeted therapies in PPGLs. In order to provide an overview on existing therapeutic options for metastatic PPGLs, I also reviewed scientific data on established therapeutics which are not considered targeted therapy.

The latter comprised the drafting of the manuscript and the creation of the tables and figures, which included the molecular signaling pathways of PPGLs, practical therapy standards, and ongoing clinical trials investigating targeted therapies in PPGL patients.

1. Introduction

1.1 Background

Neuroendocrine neoplasms (NENs) are a heterogeneous group of malignancies characterized by a common origin from cells with neuroendocrine phenotypes (1). They can further be categorized into epithelial or non-epithelial NENs (2).

Pheochromocytomas (PCCs) and paragangliomas (PGLs), commonly known as PPGLs, are rare non-epithelial NENs of the adrenal medulla (PCCs) or the sympathetic or parasympathetic extra-adrenal paraganglia (PGLs) (2).

Epithelial NENs are classified into neuroendocrine tumors (NETs) or neuroendocrine carcinomas (NECs), depending on their differentiation – NETs are well-differentiated epithelial NENs, NECs are poorly differentiated epithelial NENs (3). The latest WHO Classification of Neuroendocrine Neoplasms 2022 further divides NETs into G1, G2 or G3 based on proliferative markers and NECs into small or large cell subtypes (4).

Both tumor entities (PPGLs and NETs/NECs) are difficult to treat when metastatic, making the exploration of novel therapies, especially combination therapies, highly necessary.

1.1.1 *Pheochromocytomas and paragangliomas*

PPGLs are distinguished from other endocrine tumors since they show the highest rate of heritability or genetically known causes. With around 30-35% of PPGL patients showing germline mutations and another 35-40% showing somatic driver mutations in known susceptibility genes (5-11), around 70% of all patients can be assigned to one of the three main molecular clusters: Pseudohypoxia-related cluster 1 (1A or 1B), kinase signaling-related cluster 2 or Wnt signaling-related cluster 3 (**Figure 1**) (12, 13). The clusters are associated with distinct biochemical and clinical phenotypes and influence diagnosis as well as the necessary follow-up of PPGL patients (13). For instance, mutations in succinate dehydrogenase subunit B (*SDHB*) are associated with younger age at diagnosis and a high metastatic risk (5, 13, 14).

All PPGLs have the potential to metastasize. There are still no definitive biomarkers available to clearly predict metastatic behavior or recurrence. Therefore, the WHO definition of metastatic disease remains the presence of chromaffin tissue where none would be expected (3). Around 10-15% of PCCs and around 35-40% of PGLs metastasize (5, 15-18). Metastatic PPGLs show 5- and 10-year mortality rates of 37% and 29%, respectively (19). The diagnosis and therapy of metastatic PPGL patients remains challenging. Currently, metastatic potential can be assessed using a multifactorial risk assessment including tumor size ≥ 5 cm, extra-adrenal location, high Ki-67, certain mutations, and a dopaminergic phenotype (13, 16, 20). Recently, it was also found that

the incorporation of a dopamine metabolite, plasma methoxytyramine, into machine-learning models can help to predict metastases in PPGL patients (21). Moreover, SSTR2 expression has recently been reported to be associated with the metastatic behavior of PPGLs (22).

Regarding treatment, non-metastatic PPGLs are regularly treated by curative surgery, but metastatic PPGLs remain difficult to treat as the only FDA-approved therapy option (high-specific activity [^{131}I]-MIBG therapy) will be withdrawn in 2024. Moreover, while personalized, cluster-specific management has already entered clinical routine practice (13), therapy remains largely non-specific, and novel and more effective therapeutic options are needed (12). For instance, molecular targeted therapy plays an increasingly important role in the treatment of metastatic PPGLs (12). My mini-review "Targeted therapies in Pheochromocytoma and Paraganglioma" outlines both existing therapeutic options and the recent development of novel personalized molecular targeted therapies (12). This review thus provides an overview of the broader scientific context of metastatic PPGL therapy, which is the focus of my first original article of this cumulative dissertation.

The establishment of human PPGL cell lines has been proven to be particularly difficult for this tumor entity over the last few decades of research, and there are still no reliable and readily accessible cell models available. This is why we established a pipeline for the evaluation of potential therapies *in vitro* using patient-derived PPGL human primary cultures (23, 24). By establishing a total of 33 primary cultures, including 7 metastatic PPGLs, we were able to assess the efficacy of novel mono- and combination therapies and correlate the drug responsivities of such PPGL primary cultures with the molecular clusters (n=10 cluster 1-related PPGLs, n=14 cluster 2-related PPGLs) (23).

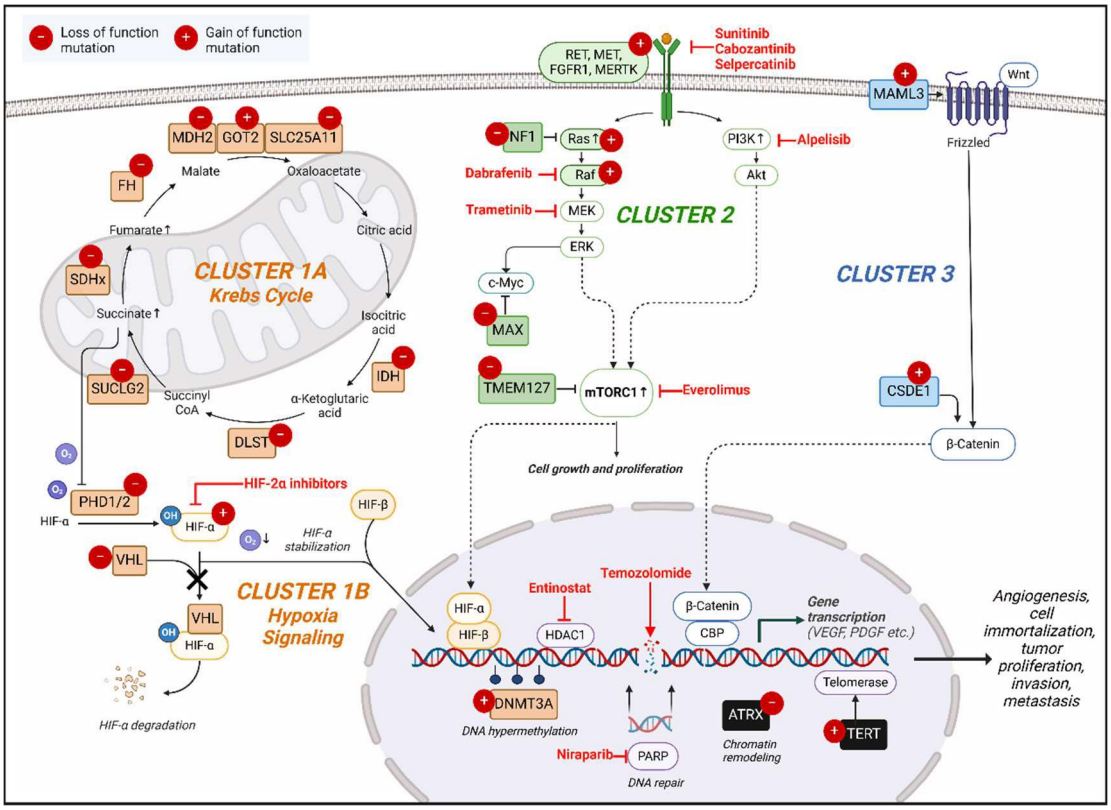

Figure 1: The three main molecular clusters of PPGLs, their associated loss or gain of function mutations, and potential therapies (red). Cluster 1 mutations affect either cluster 1A/Krebs cycle or cluster 1B/hypoxia signaling (orange), cluster 2 mutations lead to overactivation of kinase signaling pathways (green) and cluster 3 mutations affect the Wnt signaling pathway (blue). Additionally, secondary modifier mutations (*ATRX*, *TERT*) play roles in cell immortalization and chromatin remodeling (black). The mentioned mutations can promote tumor proliferation, cell immortalization, invasive behavior, metastasis, and angiogenesis. Activation (↑) and inhibition (⊥). Created with Biorender.com.

1.1.2 *Neuroendocrine tumors*

NETs are frequently located in the gastrointestinal tract and pancreas. Interestingly, pancreatic NETs (panNETs) have shown a significant increase in incidence years in recent years (25-28), making further studies into these tumors highly relevant.

In about 40–45% of panNET patients, liver metastases can already be found at diagnosis (29). However, there are no curative systemic therapies and only few established systemic treatments available for metastatic panNET patients. The latter include the somatostatin analogs octreotide (30) and lanreotide (31), the mTORC1 inhibitor everolimus (32, 33), the tyrosine kinase inhibitor sunitinib (34), systemic chemotherapy (35) and peptide (somatostatin) receptor-based radionuclide therapy (PRRT) (36).

One of these therapies, the mTORC1 inhibitor everolimus, usually inhibits tumor growth initially, but most patients develop drug resistances after less than a year of treatment (37). In order to study long-term resistance to everolimus, two stable everolimus-resistant human panNET cell lines, BON1RR1 and BON1RR2, were previously established by Prof. Nölting's group (38). Results showed that *in vitro* long-term resistance to everolimus was mediated by, among others, an

upregulation of glycogen synthase kinase-3 (GSK3) (38). It was further found that the PI3Kα inhibitor alpelisib, officially approved for the therapy of breast cancer (39), was able to overcome everolimus resistance *in vitro*, led to GSK3 inhibition and increased somatostatin receptor 2 (SSTR2) expression (38, 40).

We have now transferred this previously established everolimus-resistant cell line (BON1RR2) and the corresponding control cell line (BON1KDMSO) to an orthotopic pancreatic NEC xenograft mouse model (41). This enabled an evaluation of the mechanisms of everolimus resistance and an investigation as to whether alpelisib might overcome everolimus resistance *in vivo*. Additionally, in order to further characterize the role of GSK3 activation in everolimus resistance and evaluate potential mitochondrial involvement, we selectively inhibited GSK3 in BON1KDMSO and BON1RR2 cells and evaluated oxygen consumption rates and extracellular acidification rates.

1.2 Personalized drug testing in human pheochromocytoma/paraganglioma primary cultures

We established both two- and three-dimensional primary cultures of 33 PPGL patients (25 PCCs, 8 PGLs) by obtaining and isolating PPGL tumor tissue directly following surgery (23). As the Materials and Methods and Results are described in detail in the publication (23), they will be briefly summarized here.

The PPGL primary cultures were generated and treated with 18 different drugs alone and in combination for 72h (23). These included drugs most likely targeting cluster 2 (tyrosine kinase inhibitors cabozantinib, sunitinib and selpercatinib, PI3Kα inhibitor alpelisib, mTORC1 inhibitor everolimus, RAF inhibitor dabrafenib, MEK inhibitor trametinib, GSK3 inhibitor AR-A014418), drugs probably targeting cluster 1 (PARP inhibitor niraparib, HDAC1 inhibitor entinostat, chemotherapeutics temozolomide, gemcitabine and 5-fluorouracil, somatostatin analog octreotide, HIF2α inhibitors TC-S 7009 and belzutifan), and certain other drugs (bisphosphonate zoledronic acid, hormone estradiol) (23). Drug concentrations close to the clinically relevant levels were chosen for all drugs (23). Furthermore, mouse PCC (MPC) cell lines were also cultivated and treated with chosen inhibitors for up to 14 days (23). Cell viabilities of primary cultures and murine cell lines were then assessed as previously described (24). A robust statistical analysis was undertaken and significance was set at $p < 0.05$ (23).

Somatic mutation testing was performed using targeted next-generation sequencing (NGS) (23). Known PPGL susceptibility genes and commonly accepted oncogenes or tumor suppressor genes, were included in the panels used (10, 23). Germline mutation testing was performed in the respective centers of human genetics when patient consent had been given (23).

We found germline or somatic mutations in 79% (26/33) of tumors, 76% (25/33) of which in known PPGL susceptibility genes (**Figure 2**) (23). These included 10 cluster 1 mutations, 14

cluster 2 mutations, and two secondary modifier mutations (*ATRX*) (23). We additionally found two potential driver mutations which have not been described in PPGLs before (*ATM*, *MPL*) (23). Two tumors showed double mutations (23). In total, seven tumors showed no identifiable mutations (23). The biochemical phenotypes correlated with the mutations/cluster affiliations, with only few exceptions (23).

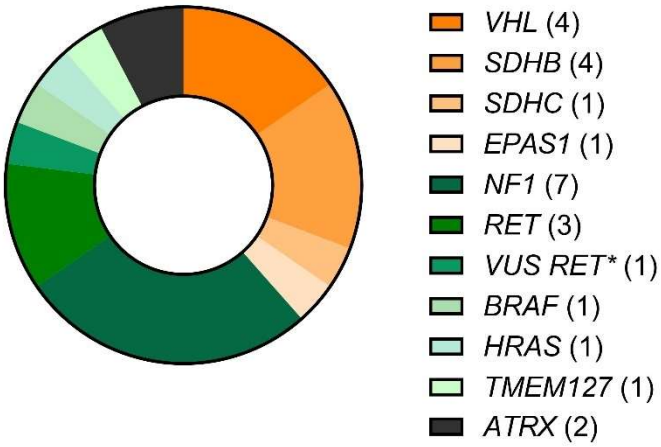

Figure 2: Distribution of driver mutations in known PPGL susceptibility genes (25/33 tumors). Cluster 1 mutations in orange, cluster 2 mutations in green, secondary modifier mutations in black. Number (*n*) of samples with each mutation in brackets. Two samples showed double mutations. Not shown: Two samples with mutations in unknown PPGL susceptibility genes (*MPL*, *ATM*). *Most likely pathogenic mutation. Data from Wang et al. (23).

We then correlated primary culture drug responsivity with the underlying mutation/cluster affiliation and compared drug responsivities of cluster 1-related and cluster 2-related tumors (23). Furthermore, we performed Western blot analysis in n=16 PPGL primary cultures in order to identify baseline and therapy-induced differences (23).

Cabozantinib/everolimus combination therapy was the most effective combination therapy and showed overall synergistic effects (**Figure 3**) (23). We performed a stratification according to the molecular clusters and malignancy (**Figure 4**), and found that cabozantinib/everolimus showed synergistic effects and significantly stronger efficacy in cluster 2-related PPGL (23). Additionally, we cross-validated these results in murine MPC cell spheroids, which were generated and cultivated as previously described (23, 42, 43). We found significant reductions in spheroid diameter after treatment with cabozantinib/everolimus (23). These results are particularly interesting, since NET patients treated with everolimus usually develop resistance after less than one year (37), which is possibly also enabled through c-Met activation (38, 44). The combination of c-Met inhibitor cabozantinib with everolimus might, therefore, be able to overcome everolimus resistance (23).

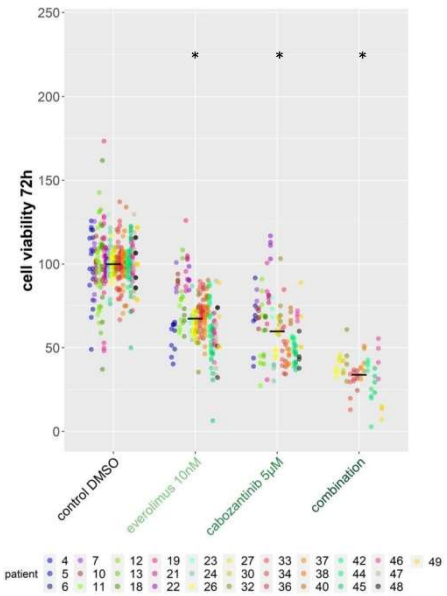

Figure 3: 72h cell viability results of tyrosine kinase inhibitor cabozantinib (n=29) in combination with the mTORC inhibitor everolimus (n=31) in all PPGL primary cultures tested for these therapies. Both monotherapies and the combination therapy significantly decreased cell viability (compared to control DMSO $p<0.05$). Moreover, cabozantinib/everolimus combination therapy (n=14) led to an overall synergistic decrease of cell viability. Data from Wang et al. (23).

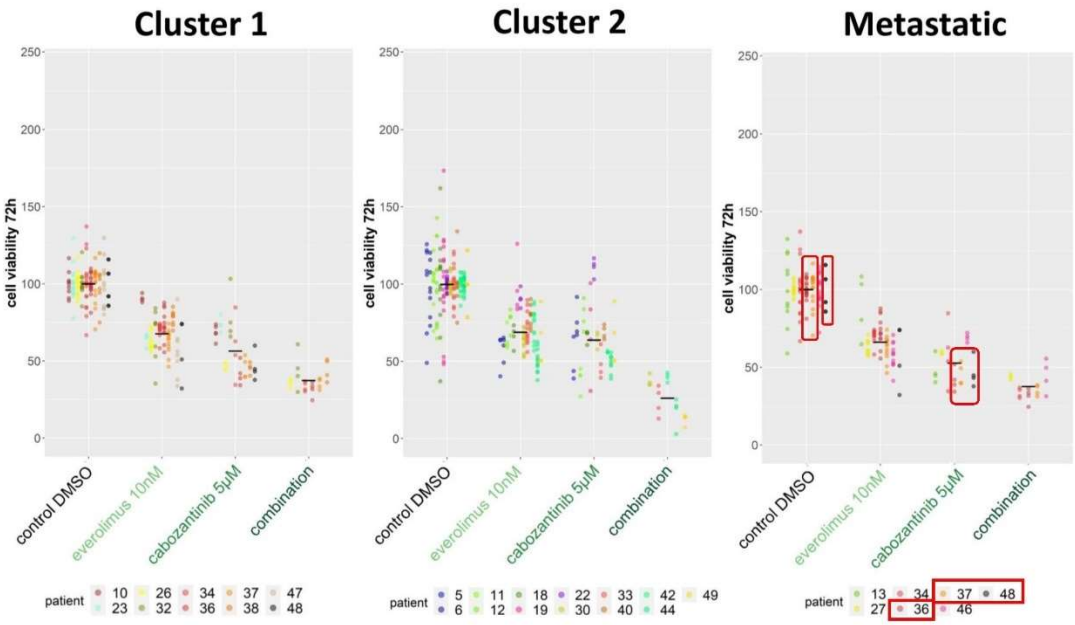

Figure 4: Stratification of cabozantinib/everolimus 72h cell viability results depending on molecular clusters and malignancy. Each patient is represented by a different color. Cabozantinib/everolimus combination therapy led to an additive decrease of cell viability in cluster 1-related (n=6) and metastatic tumors (n=5) and a synergistic decrease of cell viability in cluster 2-related tumors (n=5). Cabozantinib also led to a strong reduction of cell viability particularly in the *SDHB*-mutant, metastatic tumors of patients 36, 37 and 49 (red). Data from Wang et al. (23).

Other strongly effective combination therapies in PPGL primary cultures included alpelisib/everolimus and alpelisib/trametinib (23). The efficacy of alpelisib/everolimus *in vitro* has been described previously (24). The efficacy of alpelisib/trametinib might be due to an alpelisib-mediated attenuation of trametinib-induced AKT activation and trametinib-mediated MEK/ERK inhibition, as shown by our Western blot analysis (23). Similarly, the effects of alpelisib on

trametinib-induced AKT activation have also been reported in meningioma cell lines (45). However, while alpelisib/trametinib is a highly effective combination *in vitro*, it is possible that the simultaneous inhibition of two essential kinase signaling pathways (PI3K/AKT/mTOR signaling and MAPK/ERK signaling) might induce significant side effects *in vivo* which might limit their clinical application (46).

Our stratification according to clusters revealed that most of the single substances evaluated in the PPGL primary cultures showed similar efficacy in both clusters (everolimus, sunitinib, alpelisib, trametinib, niraparib, entinostat, gemcitabine, AR-A014418, high-dose zoledronic acid) (23); only cabozantinib, selpercatinib and 5-FU were significantly more effective in cluster 1 and only high-dose estrogen and low-dose zoledronic acid were significantly more effective in cluster 2 (23). Targeted combination treatments (cabozantinib/everolimus, alpelisib/everolimus, alpelisib/trametinib) showed significantly higher efficacy in cluster 2 (23).

Interestingly, particularly promising therapeutic options with high efficacy in *SDHB*-mutant and metastatic tumors included cabozantinib/everolimus combination therapy, gemcitabine, and high-dose zoledronic acid (23).

Drugs that were shown to be effective in PPGL patients (47), but not in PPGL primary cultures, included temozolomide and octreotide (23). While the somatostatin analog octreotide showed no efficacy *in vitro*, including in the *SDHB*-mutant primary cultures (23), it is clinically effective in patients with pathogenic variants in *SDHB* (47). Other drugs in clinical use that showed no efficacy *in vitro* included HIF2α inhibitors and dabrafenib (23). The reason for efficacy of some drugs in patients, but not in primary cultures, may be the fact that efficacy in primary cultures indicates tumor cell death and not disease stabilization, which is an important parameter of drug efficacy *in vivo* (23).

Of the drugs that we tested, several are already being studied for therapy of metastatic PPGL patients (12). These include tyrosine kinase inhibitors sunitinib (NCT01371201) and cabozantinib (NCT02302833) with promising preliminary results (48, 49), belzutifan (NCT04924075) and temozolomide in combination with PARP inhibitors (NCT04394858, NCT05142241). Our results therefore provide relevant and novel information, particularly regarding personalized, cluster-dependent treatment, of metastatic PPGLs. However, since our data also have certain limitations, e.g., a lack of the evaluation of drug toxicity particularly for combination therapies, as a next step *in vivo* studies are needed.

In conclusion, while both diagnosis and therapy of these tumors remain challenging in clinical practice, novel diagnostic markers and therapeutic strategies are constantly being studied and optimized. This enables a range of treatment possibilities and a promising outlook for metastatic PPGL patients.

These results were published in *Endocrine-Related Cancer* in 2022 (23).

1.3 Impact of the PI3Kalpha inhibitor alpelisib on everolimus resistance and somatostatin receptor expression in an orthotopic pancreatic NEC xenograft mouse model

As both the Materials and Methods and the Results have been described in detail previously (41), they are only briefly summarized in the following paragraphs.

Human pancreatic NET cell lines BON1KDMSO (everolimus-sensitive) and BON1RR2 (everolimus-resistant) were cultivated in supplemented DMEM medium (41). In the BON1RR2 cells, stable everolimus resistance has been proven previously (38). However, in preparation for the mouse experiments, BON1RR2 cells were regularly administered 10 nM everolimus to ensure stable resistance *in vivo* (41). This was discontinued 48h prior to tumor cell inoculation into the mice (41).

BON1KDMSO and BON1RR2 cells were then transplanted into the pancreas of 74 female severe combined immunodeficient (SCID) mice (BON1KDMSO: n=38 mice, RR2: n=36 mice) (**Figure 5**) (41).

Oral therapy using placebo, everolimus, alpelisib, or the combination of everolimus plus alpelisib, was started after a minimum tumor size of around 140 mm^3 was reached, and continued until a tumor size of 1900 - 2000 mm^3 or other termination criteria appeared (41). BON1KDMSO mice were treated with placebo (n=10), everolimus (n=10), alpelisib (n=8) and everolimus/alpelisib (n=10) (41). BON1RR2 mice were treated with placebo (n=10), everolimus (n=8), alpelisib (n=8) and everolimus/alpelisib (n=10) (**Figure 5**) (41). Drug concentrations were chosen according to the recommended doses in humans producing therapeutic levels (41). A full statistical analysis was performed and significance was set at $p \leq 0.05$ (41).

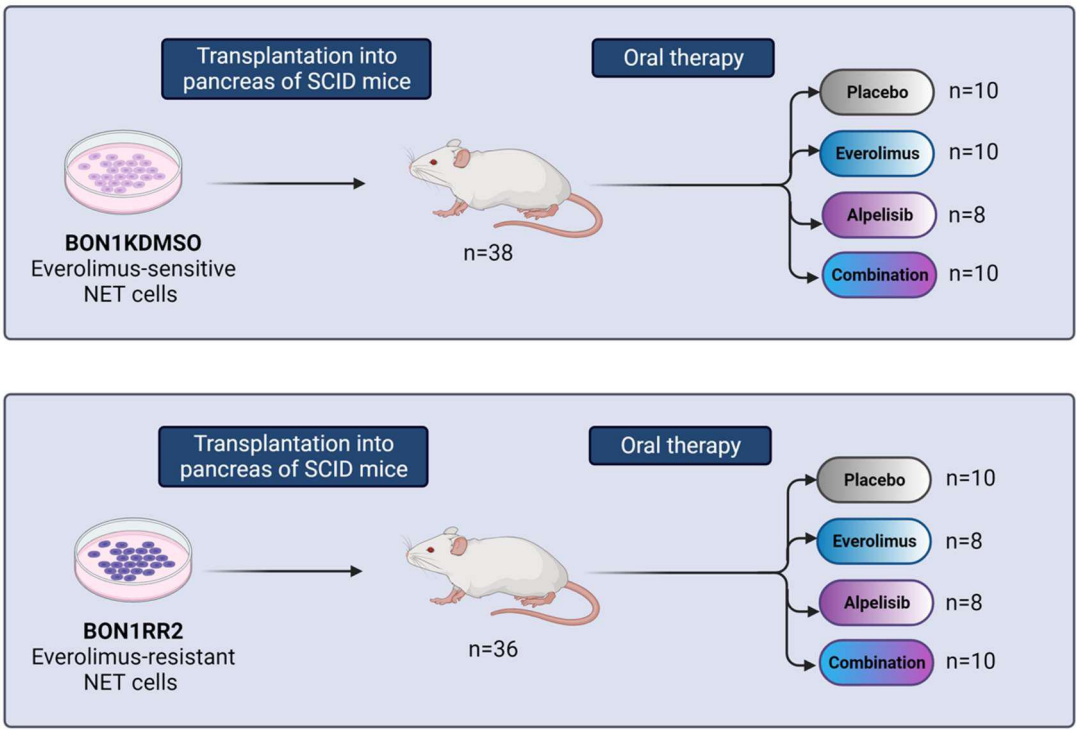

Figure 5: Establishment of an orthotopic pancreatic NEC xenograft mouse model. Everolimus-sensitive BON1KDMSO cells were transplanted into the pancreas of 38 mice (top figure) and everolimus-resistant BON1RR2 cells were transplanted into the pancreas of 36 mice (bottom figure). The mice then received oral therapy with either placebo, everolimus, alpelisib or the combination everolimus/alpelisib. Created with Biorender.com.

Median survival of the everolimus-sensitive mice and the everolimus-resistant mice under treatment with placebo differed significantly, with the everolimus-resistant mice showing longer survival (53d in everolimus-resistance vs. 42d in everolimus-sensitive mice) (41). On treatment with everolimus or alpelisib, only the everolimus-sensitive mice showed significantly longer survival compared to placebo (44d everolimus, 53d alpelisib) (41). Everolimus treatment in the everolimus-resistant mice showed no significant survival benefit, demonstrating everolimus-resistance *in vivo* (41). However, everolimus/alpelisib combination therapy prolonged survival both in the everolimus-sensitive (52d) and in the everolimus-resistant animals (69d) (41). Therefore, supporting the *in vitro* data (38), we could show that combination treatment with alpelisib may also overcome everolimus resistance *in vivo*. Further, both groups showed the longest median survival under combination treatment, with the everolimus-resistant combination-treated group showing the longest survival overall (41).

To assess potential treatment effects on renal function in the mice, renal scintigraphy was performed, as formerly described (50). No adverse effects on renal function were found after treatment with everolimus or combination therapy (41). Only alpelisib monotherapy led to delayed excretion time after 4 weeks of treatment, consistent with increased serum creatinine levels found in breast cancer patients after alpelisib treatment (51).

Conventional staining with hematoxylin-eosin as well as immunohistochemistry was performed on 66 tumors to evaluate tumor morphology, necrosis, Ki-67 and SSTR2 status (41). A high Ki-67 index >20% (in the majority Ki-67 >55%), necrosis, and small cell morphology were found in all tumors, classifying the tumors as NECs (41). Eight of these tumors were classified as mixed endocrine/exocrine tumors based on the presence of gland formation and cystic features (41).

Oxygen consumption rates (OCR), representing mitochondrial respiration, and extracellular acidification rates (ECAR), representing aerobic glycolysis (Warburg effect), of the BON1KDMSO and BON1RR2 cells were assessed by performing XF Real-Time ATP Rate Assay experiments in order to further characterize the role of GSK3 in everolimus-resistance (41). These results showed that GSK3 inhibition by AR-A014418 led to a significant increase of OCR and a significant decrease of ECAR in both BON1KDMSO and BON1RR2 cells, suggesting a role of GSK3 in the impairment of mitochondrial respiration and a shift towards increased aerobic glycolysis (Warburg effect) in these tumor cells (41). These data are consistent with previous studies where increased GSK3 activation was shown to be associated with depleted mitochondrial function (52-54).

Both everolimus and alpelisib are FDA-approved for cancer therapy (everolimus in NET patients, alpelisib in breast cancer patients) (33, 51). Our results now provide novel data regarding their combination therapy *in vivo*: The everolimus/alpelisib combination treatment can overcome everolimus resistance in NECs. Synergistic effects of the alpelisib/everolimus combination were also demonstrated in cluster 2 PPGL primary cultures (23) due to a complementary signaling pathway inhibition.

However, due to the limited direct transferability of the mouse data to humans, the results should be further validated in a clinical phase 2 study in NET/NEC patients. While a dose-finding phase 1 study investigating alpelisib in combination with everolimus in solid tumors has already demonstrated a manageable safety profile and encouraging preliminary efficacy (55), as a next step, a phase 2 study examining this combination therapy should be performed. Additionally, since alpelisib as a single drug has demonstrated high efficacy with few side effects in our study, it may also be evaluated in a clinical phase 2 study in NET/NEC patients.

All data were published in *Endocrine-Related Cancer* in 2023 (41).

2. Abstract

This cumulative dissertation evaluates therapeutic options for pheochromocytomas and paragangliomas (PPGLs) and for neuroendocrine tumors and carcinomas (NETs/NECs) – tumor entities for which treatment remains challenging when advanced or metastatic. Therefore, research into novel therapies and potential combination therapies is urgently needed.

Since there is a lack of reliable human PPGL cell lines, we established a total of 33 patient-derived PPGL primary cultures to investigate the efficacy of established and novel molecular-targeted drugs and chemotherapeutic agents *in vitro* (23). Germline or somatic mutations were identified in 79% of PPGLs, which allowed us to assess potential differences in drug responsivity between pseudohypoxia cluster 1-related (n=10) and kinase signaling cluster 2-related (n=14) PPGL primary cultures (23). While we found only minor differences between drug responsivity of cluster 1- and cluster 2-related PPGLs, some monotherapies showed higher efficacy in cluster 1-related tumors and some targeted combination treatments showed higher efficacy in cluster 2-related tumors (23). Additionally, the tumors showed differences in therapy responses depending on the individual mutations (23). Therefore, our data pave the way for personalized therapy of these tumors.

In the case of NETs, most patients develop resistance to the mTORC1 inhibitor everolimus, one of few officially approved therapies in NETs, within one year of treatment (41). Therefore, we established an everolimus-resistant orthotopic pancreatic NEC xenograft mouse model, enabling us to study resistance mechanisms *in vivo* and to evaluate the possibility of overcoming everolimus-resistance through the addition of PI3Kα inhibitor alpelisib (41). A total of 74 severe combined immunodeficient mice underwent transplantations of everolimus-sensitive (BON1KDMSO) or everolimus-resistant (BON1RR2) pancreatic NET cells, and were subsequently orally treated with either placebo, everolimus, alpelisib or the combination everolimus/alpelisib (41). We found that alpelisib/everolimus combination treatment overcame everolimus resistance *in vivo* and significantly prolonged survival (41). In the next step, a clinical phase 2 study is now needed to validate these preclinical results and to offer additional information on efficacy, toxicity, and tolerability of these therapies in patients.

3. Zusammenfassung

Diese kumulative Dissertation evaluiert Therapieoptionen für Phäochromozytome und Paragangliome (PPGLs) und für neuroendokrine Tumore und Karzinome (NETs/NECs) – Tumorentitäten welche eine therapeutische Herausforderung darstellen, wenn sie bereits fortgeschritten oder metastasiert sind. Daher ist die Erforschung neuer Therapiemöglichkeiten und potenzieller Kombinationstherapien dringend notwendig.

Aufgrund eines Mangels an zuverlässigen humanen PPGL-Zelllinien, etablierten wir 33 humane PPGL Primärkulturen um die Wirksamkeit von etablierten und neuen molekular gezielten Medikamenten und Chemotherapeutika *in vitro* zu evaluieren (23). Wir identifizierten in 79% der PPGLs somatische Mutationen oder Keimbahnmutationen, welche es uns ermöglichten die potentiellen Unterschiede im Therapieansprechen zwischen Cluster 1- (n=10) und Cluster 2-assoziierten (n=14) PPGL Primärkulturen zu beurteilen (23). Zusammenfassend fanden wir nur geringe Unterschiede, jedoch zeigten einige Einzelsubstanzen vermehrte Wirksamkeit in Cluster 1-assoziierten Tumoren und einige molekular gezielte Kombinationstherapien vermehrte Wirksamkeit in Cluster 2-assoziierten Tumoren (23). Zudem zeigten sich individuelle Unterschiede im Therapieansprechen zwischen den einzelnen Tumoren in Abhängigkeit von ihrer spezifischen Mutation (23). Somit ebnen unsere Daten den Weg zur personalisierten Therapie dieser Tumore.

Im Falle von NETs stellt der mTORC1 Inhibitor Everolimus eine der wenigen offiziell zugelassenen Therapiemöglichkeiten dar, jedoch entwickelt ein Großteil der Patienten bereits innerhalb eines Jahres eine Resistenz gegenüber Everolimus (41). Um diese Resistenzmechanismen und die Möglichkeit der Resistenzüberwindung über die zusätzliche Gabe von PI3Kα Inhibitor Alpelisib, *in vivo* zu erforschen, etablierten wir ein Everolimus-resistentes orthotopes pankreatisches NEC Xenograft-Mausmodell. Insgesamt 74 immundefiziente Mäuse erhielten eine Transplantation mit Everolimus-sensitiven (BON1KDMSO) oder Everolimus-resistenten (BON1RR2) pankreatischen NET-Zellen und im Anschluss eine Therapie mit Placebo, Everolimus, Alpelisib oder der Kombination Everolimus/Alpelisib (41). Es zeigte sich, dass die Alpelisib/Everolimus Kombinationstherapie die Everolimus-Resistenz *in vivo* überwinden und das Überleben signifikant verlängern konnte (41). Im nächsten Schritt wird eine klinische Phase 2 Studie benötigt, um diese präklinischen Resultate zu validieren und zusätzliche Daten bezüglich Wirksamkeit, Toxizität und Verträglichkeit dieser Therapien am Patienten zu liefern.

4. References

1. Klöppel G. Neuroendocrine Neoplasms: Dichotomy, Origin and Classifications. Visc Med. 2017;33(5):324-30.

2. Rindi G, Klimstra DS, Abedi-Ardekani B, Asa SL, Bosman FT, Brambilla E, et al. A common classification framework for neuroendocrine neoplasms: an International Agency for Research on Cancer (IARC) and World Health Organization (WHO) expert consensus proposal. Mod Pathol. 2018;31(12):1770-86.

3. Mete O, Wenig BM. Update from the 5th Edition of the World Health Organization Classification of Head and Neck Tumors: Overview of the 2022 WHO Classification of Head and Neck Neuroendocrine Neoplasms. Head Neck Pathol. 2022;16(1):123-42.

4. Rindi G, Mete O, Uccella S, Basturk O, La Rosa S, Brosens LAA, et al. Overview of the 2022 WHO Classification of Neuroendocrine Neoplasms. Endocr Pathol. 2022;33(1):115-54.

5. Crona J, Lamarca A, Ghosal S, Welin S, Skogseid B, Pacak K. Genotype-phenotype correlations in pheochromocytoma and paraganglioma: a systematic review and individual patient meta-analysis. Endocr Relat Cancer. 2019;26(5):539-50.

6. Fishbein L, Leshchiner I, Walter V, Danilova L, Robertson AG, Johnson AR, et al. Comprehensive Molecular Characterization of Pheochromocytoma and Paraganglioma. Cancer Cell. 2017;31(2):181-93.

7. Luchetti A, Walsh D, Rodger F, Clark G, Martin T, Irving R, et al. Profiling of somatic mutations in phaeochromocytoma and paraganglioma by targeted next generation sequencing analysis. Int J Endocrinol. 2015;2015:138573.

8. Jiang J, Zhang J, Pang Y, Bechmann N, Li M, Monteagudo M, et al. Sino-European Differences in the Genetic Landscape and Clinical Presentation of Pheochromocytoma and Paraganglioma. J Clin Endocrinol Metab. 2020;105(10).

9. Burnichon N, Vescovo L, Amar L, Libé R, de Reynies A, Venisse A, et al. Integrative genomic analysis reveals somatic mutations in pheochromocytoma and paraganglioma. Hum Mol Genet. 2011;20(20):3974-85.

10. Gieldon L, William D, Hackmann K, Jahn W, Jahn A, Wagner J, et al. Optimizing Genetic Workup in Pheochromocytoma and Paraganglioma by Integrating Diagnostic and Research Approaches. Cancers (Basel). 2019;11(6).

11. Jochmanova I, Pacak K. Genomic Landscape of Pheochromocytoma and Paraganglioma. Trends Cancer. 2018;4(1):6-9.

12. Wang K, Crona J, Beuschlein F, Grossman AB, Pacak K, Nolting S. Targeted therapies in Pheochromocytoma and Paraganglioma. J Clin Endocrinol Metab. 2022.

13. Nölting S, Bechmann N, Taieb D, Beuschlein F, Fassnacht M, Kroiss M, et al. Personalized Management of Pheochromocytoma and Paraganglioma. Endocr Rev. 2022;43(2):199-239.

14. Taieb D, Jha A, Treglia G, Pacak K. Molecular imaging and radionuclide therapy of pheochromocytoma and paraganglioma in the era of genomic characterization of disease subgroups. Endocr Relat Cancer. 2019;26(11):R627-R52.

15. Bechmann N, Moskopp ML, Ullrich M, Calsina B, Wallace PW, Richter S, et al. HIF2alpha supports pro-metastatic behavior in pheochromocytomas/paragangliomas. Endocr Relat Cancer. 2020;27(11):625-40.

16. Eisenhofer G, Lenders JW, Siegert G, Bornstein SR, Friberg P, Milosevic D, et al. Plasma methoxytyramine: a novel biomarker of metastatic pheochromocytoma and paraganglioma in relation to established risk factors of tumour size, location and SDHB mutation status. Eur J Cancer. 2012;48(11):1739-49.

17. Mannelli M, Ianni L, Cilotti A, Conti A. Pheochromocytoma in Italy: a multicentric retrospective study. Eur J Endocrinol. 1999;141(6):619-24.

18. Goldstein RE, O'Neill JA, Jr., Holcomb GW, 3rd, Morgan WM, 3rd, Neblett WW, 3rd, Oates JA, et al. Clinical experience over 48 years with pheochromocytoma. Ann Surg. 1999;229(6):755-64; discussion 64-6.

19. Hamidi O, Young WF, Jr., Gruber L, Smestad J, Yan Q, Ponce OJ, et al. Outcomes of patients with metastatic phaeochromocytoma and paraganglioma: A systematic review and meta-analysis. Clin Endocrinol (Oxf). 2017;87(5):440-50.

20. Lenders JWM, Kerstens MN, Amar L, Prejbisz A, Robledo M, Taieb D, et al. Genetics, diagnosis, management and future directions of research of phaeochromocytoma and paraganglioma: a position statement and consensus of the Working Group on Endocrine Hypertension of the European Society of Hypertension. J Hypertens. 2020;38(8):1443-56.

21. Pamporaki C, Berends AMA, Filippatos A, Prodanov T, Meuter L, Prejbisz A, et al. Prediction of metastatic pheochromocytoma and paraganglioma: a machine learning modelling study using data from a cross-sectional cohort. Lancet Digit Health. 2023;5(9):e551-e9.

22. Fischer A, Kloos S, Maccio U, Friemel J, Remde H, Fassnacht M, et al. Metastatic pheochromocytoma and paraganglioma: Somatostatin receptor 2 expression, genetics and therapeutic responses. J Clin Endocrinol Metab. 2023.

23. Wang K, Schutze I, Gulde S, Bechmann N, Richter S, Helm J, et al. Personalized drug testing in human pheochromocytoma/paraganglioma primary cultures. Endocr Relat Cancer. 2022.

24. Fankhauser M, Bechmann N, Lauseker M, Goncalves J, Favier J, Klink B, et al. Synergistic Highly Potent Targeted Drug Combinations in Different Pheochromocytoma Models Including Human Tumor Cultures. Endocrinology. 2019;160(11):2600-17.

25. White BE, Rous B, Chandrakumaran K, Wong K, Bouvier C, Van Hemelrijck M, et al. Incidence and survival of neuroendocrine neoplasia in England 1995-2018: A retrospective, population-based study. Lancet Reg Health Eur. 2022;23:100510.

26. Wyld D, Wan MH, Moore J, Dunn N, Youl P. Epidemiological trends of neuroendocrine tumours over three decades in Queensland, Australia. Cancer Epidemiol. 2019;63:101598.

27. Dasari A, Shen C, Halperin D, Zhao B, Zhou S, Xu Y, et al. Trends in the Incidence, Prevalence, and Survival Outcomes in Patients With Neuroendocrine Tumors in the United States. JAMA Oncol. 2017;3(10):1335-42.

28. Lu L, Shang Y, Mullins CS, Zhang X, Linnebacher M. Epidemiologic trends and prognostic risk factors of patients with pancreatic neuroendocrine neoplasms in the US: an updated population-based study. Future Oncol. 2021;17(5):549-63.

29. Frilling A, Modlin IM, Kidd M, Russell C, Breitenstein S, Salem R, et al. Recommendations for management of patients with neuroendocrine liver metastases. Lancet Oncol. 2014;15(1):e8-21.

30. Rinke A, Muller HH, Schade-Brittinger C, Klose KJ, Barth P, Wied M, et al. Placebo-controlled, double-blind, prospective, randomized study on the effect of octreotide LAR in the control of tumor growth in patients with metastatic neuroendocrine midgut tumors: a report from the PROMID Study Group. J Clin Oncol. 2009;27(28):4656-63.

31. Caplin ME, Pavel M, Cwikla JB, Phan AT, Raderer M, Sedlackova E, et al. Lanreotide in metastatic enteropancreatic neuroendocrine tumors. N Engl J Med. 2014;371(3):224-33.

32. Yao JC, Fazio N, Singh S, Buzzoni R, Carnaghi C, Wolin E, et al. Everolimus for the treatment of advanced, non-functional neuroendocrine tumours of the lung or gastrointestinal tract (RADIANT-4): a randomised, placebo-controlled, phase 3 study. Lancet. 2016;387(10022):968-77.

33. Yao JC, Shah MH, Ito T, Bohas CL, Wolin EM, Van Cutsem E, et al. Everolimus for advanced pancreatic neuroendocrine tumors. N Engl J Med. 2011;364(6):514-23.

34. Raymond E, Dahan L, Raoul JL, Bang YJ, Borbath I, Lombard-Bohas C, et al. Sunitinib malate for the treatment of pancreatic neuroendocrine tumors. N Engl J Med. 2011;364(6):501-13.

35. Pavel M, Oberg K, Falconi M, Krenning EP, Sundin A, Perren A, et al. Gastroenteropancreatic neuroendocrine neoplasms: ESMO Clinical Practice Guidelines for diagnosis, treatment and follow-up. Ann Oncol. 2020;31(7):844-60.

36. Strosberg JR, Caplin ME, Kunz PL, Ruszniewski PB, Bodei L, Hendifar A, et al. (177)Lu-Dotatate plus long-acting octreotide versus high-dose long-acting octreotide in patients with midgut neuroendocrine tumours (NETTER-1): final overall survival and long-term safety results from an open-label, randomised, controlled, phase 3 trial. Lancet Oncol. 2021;22(12):1752-63.

37. Lee L, Ito T, Jensen RT. Everolimus in the treatment of neuroendocrine tumors: efficacy, side-effects, resistance, and factors affecting its place in the treatment sequence. Expert Opin Pharmacother. 2018;19(8):909-28.

38. Aristizabal Prada ET, Spottl G, Maurer J, Lauseker M, Koziolek EJ, Schrader J, et al. The role of GSK3 and its reversal with GSK3 antagonism in everolimus resistance. Endocr Relat Cancer. 2018;25(10):893-908.

39. Andre F, Ciruelos E, Rubovszky G, Campone M, Loibl S, Rugo HS, et al. Alpelisib for PIK3CA-Mutated, Hormone Receptor-Positive Advanced Breast Cancer. N Engl J Med. 2019;380(20):1929-40.

40. Nölting S, Rentsch J, Freitag H, Detjen K, Briest F, Mobs M, et al. The selective PI3Kalpha inhibitor BYL719 as a novel therapeutic option for neuroendocrine tumors: Results from multiple cell line models. PLoS One. 2017;12(8):e0182852.

41. Mohan AM, Prasad S, Schmitz-Peiffer F, Lange C, Lukas M, Koziolek EJ, et al. Impact of the PI3Kalpha inhibitor alpelisib on everolimus resistance and somatostatin receptor expression in an orthotopic pancreatic NEC xenograft mouse model. Endocr Relat Cancer. 2023.

42. Bechmann N, Ehrlich H, Eisenhofer G, Ehrlich A, Meschke S, Ziegler CG, et al. Anti-Tumorigenic and Anti-Metastatic Activity of the Sponge-Derived Marine Drugs Aeroplysinin-1 and Isofistularin-3 against Pheochromocytoma In Vitro. Mar Drugs. 2018;16(5).

43. Bechmann N, Poser I, Seifert V, Greunke C, Ullrich M, Qin N, et al. Impact of Extrinsic and Intrinsic Hypoxia on Catecholamine Biosynthesis in Absence or Presence of Hif2alpha in Pheochromocytoma Cells. Cancers (Basel). 2019;11(5).

44. Van den Bossche V, Jadot G, Grisay G, Pierrard J, Honoré N, Petit B, et al. c-MET as a Potential Resistance Mechanism to Everolimus in Breast Cancer: From a Case Report to Patient Cohort Analysis. Target Oncol. 2020;15(1):139-46.

45. Mondielli G, Mougel G, Darriet F, Roche C, Querdray A, Lisbonis C, et al. Co-Targeting MAP Kinase and Pi3K-Akt-mTOR Pathways in Meningioma: Preclinical Study of Alpelisib and Trametinib. Cancers (Basel). 2022;14(18).

46. Tolcher AW, Bendell JC, Papadopoulos KP, Burris HA, 3rd, Patnaik A, Jones SF, et al. A phase IB trial of the oral MEK inhibitor trametinib (GSK1120212) in combination with everolimus in patients with advanced solid tumors. Ann Oncol. 2015;26(1):58-64.

47. Fischer A, Kloos S, Remde H, Dischinger U, Pamporaki C, Timmers H, et al. Responses to systemic therapy in metastatic pheochromocytoma/paraganglioma: a retrospective multicenter cohort study. Eur J Endocrinol. 2023;189(5):546-65.

48. Baudin E, Goichot B, Berruti A, Hadoux J, Moalla S, Laboureau S, et al. First International Randomized Study in Malignant Progressive Pheochromocytoma and Paragangliomas

(FIRSTMAPPP): An academic double-blind trial investigating sunitinib. Annals of Oncology. 2021;32:S621-S5. 10.1016/annonc/annonc700.

49. Jimenez C, Busaidy N, Habra M, Waguespack S, Jessop A. A phase 2 study to evaluate the effects of cabozantinib in patients with unre- sectable metastatic pheochromocytomas and paragangliomas. International Symposium on Pheochromocytoma and Paraganglioma Sydey, Australia2017.

50. Huang K, Lukas M, Steffen IG, Lange C, Huang EL, Dorau V, et al. Normal Values of Renal Function measured with 99mTechnetium Mercaptoacetyltriglycine SPECT in Mice with Respect to Age, Sex and Circadian Rhythm. Nuklearmedizin. 2018;57(6):224-33.

51. Markham A. Alpelisib: First Global Approval. Drugs. 2019;79(11):1249-53.

52. Chiara F, Rasola A. GSK-3 and mitochondria in cancer cells. Front Oncol. 2013;3:16.

53. Papadopoli D, Pollak M, Topisirovic I. The role of GSK3 in metabolic pathway perturbations in cancer. Biochim Biophys Acta Mol Cell Res. 2021;1868(8):119059.

54. Yang K, Chen Z, Gao J, Shi W, Li L, Jiang S, et al. The Key Roles of GSK-3beta in Regulating Mitochondrial Activity. Cell Physiol Biochem. 2017;44(4):1445-59.

55. Curigliano G, Martin M, Jhaveri K, Beck JT, Tortora G, Fazio N, et al. Alpelisib in combination with everolimus +/- exemestane in solid tumours: Phase Ib randomised, open-label, multicentre study. Eur J Cancer. 2021;151:49-62.

5. Publication I

RESEARCH

Personalized drug testing in human pheochromocytoma/paraganglioma primary cultures

Katharina Wang[1,*], Ina Schütze[2,*], Sebastian Gulde[3], Nicole Bechmann[4,5], Susan Richter[4], Jana Helm[5], Michael Lauseker[6], Julian Maurer[1], Astrid Reul[2], Gerald Spoettl[1], Barbara Klink[7,8,9], Doreen William[9], Thomas Knösel[10], Juliane Friemel[11], Michel Bihl[11], Achim Weber[11], Maria Fankhauser[1], Laura Schober[1], Diana Vetter[12], Martina Broglie Däppen[13], Christian G Ziegler[5], Martin Ullrich[14], Jens Pietzsch[14,15], Stefan R Bornstein[5], Christian Lottspeich[1], Matthias Kroiss[1,16], Martin Fassnacht[16], Vera Ursula Julia Wenter[17], Roland Ladurner[18], Constanze Hantel[2,5], Martin Reincke[1], Graeme Eisenhofer[4,5], Ashley B Grossman[19,20], Karel Pacak[21], Felix Beuschlein[1,2], Christoph J Auernhammer[1], Natalia S Pellegata[3] and **Svenja Nölting[1,2]**

[1]Department of Internal Medicine IV, University Hospital, LMU Klinikum, Ludwig Maximilian University of Munich, Munich, Germany
[2]Department of Endocrinology, Diabetology and Clinical Nutrition, University Hospital Zurich (USZ) and University of Zurich (UZH), Zurich, Switzerland
[3]Institute for Diabetes and Cancer (IDC), Helmholtz Center Munich, German Research Center for Environmental Health, Neuherberg, Germany
[4]Institute of Clinical Chemistry and Laboratory Medicine, University Hospital Carl Gustav Carus, Technische Universität Dresden, Dresden, Germany
[5]Department of Internal Medicine III, University Hospital Carl Gustav Carus Dresden, Technische Universität Dresden, Dresden, Germany
[6]Institute for Medical Information Processing, Biometry, and Epidemiology (IBE), Ludwig Maximilian University of Munich, Munich, Germany
[7]Institute for Clinical Genetics, Faculty of Medicine Carl Gustav Carus, Technische Universität Dresden, Dresden, Germany
[8]National Center of Genetics, Laboratoire National de Santé, Dudelange, Luxembourg
[9]German Cancer Consortium, Dresden, Germany
[10]Institute of Pathology, Ludwig Maximilian University of Munich, Munich, Germany
[11]Department of Pathology and Molecular Pathology, University Hospital Zurich, Zurich, Switzerland
[12]Department of Visceral and Transplantation Surgery, University Hospital, Zurich, Switzerland
[13]Department of Otorhinolaryngology, University Hospital Zurich, Zurich, Switzerland
[14]Department of Radiopharmaceutical and Chemical Biology, Institute of Radiopharmaceutical Cancer Research, Helmholtz-Zentrum Dresden-Rossendorf (HZDR), Dresden, Germany
[15]Faculty of Chemistry and Food Chemistry, School of Science, Technische Universität Dresden, Dresden, Germany
[16]Division of Endocrinology and Diabetes, Department of Medicine I, University Hospital Würzburg, University of Würzburg, Würzburg, Germany
[17]Department of Nuclear Medicine, University Hospital, LMU Klinikum, Ludwig Maximilian University of Munich, Munich, Germany
[18]Department of General-, Visceral-, and Transplant-Surgery, University Hospital, LMU Klinikum, Ludwig Maximilian University of Munich, Munich, Germany
[19]Green Templeton College, University of Oxford, Oxford, UK
[20]NET Unit, ENETS Centre of Excellence, Royal Free Hospital, London, UK
[21]Eunice Kennedy Shriver National Institute of Child Health and Human Development, National Institutes of Health, Bethesda, Maryland, USA

Correspondence should be addressed to S Nölting: svenja.noelting@usz.ch

*(K Wang and I Schütze contributed equally to this work)

Abstract

Aggressive pheochromocytomas and paragangliomas (PPGLs) are difficult to treat, and molecular targeting is being increasingly considered, but with variable results. This study investigates established and novel molecular-targeted drugs and chemotherapeutic agents for the treatment of PPGLs in human primary cultures and murine cell line spheroids. In PPGLs from 33 patients, including 7 metastatic PPGLs, we identified germline or somatic driver mutations in 79% of cases, allowing us to assess potential differences in drug responsivity between pseudohypoxia-associated cluster 1-related (n = 10) and kinase signaling-associated cluster 2-related (n = 14) PPGL primary

Key Words

- personalized drug testing
- pheochromocytoma/paraganglioma
- human primary cultures
- 3D spheroid models
- somatic mutations

https://erc.bioscientifica.com
https://doi.org/10.1530/ERC-21-0355

© 2022 Society for Endocrinology
Published by Bioscientifica Ltd.
Printed in Great Britain

Downloaded from Bioscientifica.com at 05/11/2022 04:19:32PM
via Bodleian Library

cultures. Single anti-cancer drugs were either more effective in cluster 1 (cabozantinib, selpercatinib, and 5-FU) or similarly effective in both clusters (everolimus, sunitinib, alpelisib, trametinib, niraparib, entinostat, gemcitabine, AR-A014418, and high-dose zoledronic acid). High-dose estrogen and low-dose zoledronic acid were the only single substances more effective in cluster 2. Neither cluster 1- nor cluster 2-related patient primary cultures responded to HIF-2a inhibitors, temozolomide, dabrafenib, or octreotide. We showed particular efficacy of targeted combination treatments (cabozantinib/everolimus, alpelisib/everolimus, alpelisib/trametinib) in both clusters, with higher efficacy of some targeted combinations in cluster 2 and overall synergistic effects (cabozantinib/everolimus, alpelisib/trametinib) or synergistic effects in cluster 2 (alpelisib/everolimus). Cabozantinib/everolimus combination therapy, gemcitabine, and high-dose zoledronic acid appear to be promising treatment options with particularly high efficacy in *SDHB*-mutant and metastatic tumors. In conclusion, only minor differences regarding drug responsivity were found between cluster 1 and cluster 2: some single anti-cancer drugs were more effective in cluster 1 and some targeted combination treatments were more effective in cluster 2.

Endocrine-Related Cancer (2022) **29**, 285–306

Introduction

Pheochromocytomas (PCCs) and paragangliomas (PGLs), collectively referred to as PPGLs, are rare endocrine tumors originating from neural crest-derived cells of the adrenal medulla or the sympathetic or parasympathetic paraganglia. Approximately 10–15% of PCCs and 35–40% of PGLs are metastatic (Goldstein *et al.* 1999, Mannelli *et al.* 1999, Eisenhofer *et al.* 2012, Crona *et al.* 2019, Bechmann *et al.* 2020), defined as the presence of metastases in lymph nodes or other distant sites, particularly bones (Lam 2017). The median overall survival of patients with metastatic PPGLs has been reported to be 7 years (Hescot *et al.* 2019), with a 5-year mortality rate of 37% (Turkova *et al.* 2016, Hamidi *et al.* 2017).

PPGLs have the highest degree of heritability among all tumor entities: 30–35% show identifiable germline mutations and another 35–40% somatic driver mutations in known susceptibility genes (Burnichon *et al.* 2011, Luchetti *et al.* 2015, Fishbein *et al.* 2017, Gieldon *et al.* 2019, Jiang *et al.* 2020). Therefore, around 70% of all PPGLs can be assigned to one of three main molecular clusters with different gene expression signatures and clinical behavior (Fig. 1). Pseudohypoxia-associated cluster 1 is subdivided into cluster 1A (Krebs cycle-related) and cluster 1B (hypoxia signaling related). Cluster 1-related mutations lead to hypoxia-inducible factor (HIF) 2α stabilization and accumulation which promote angiogenesis, tumor cell migration and invasion, extravasation, and metastasis (Keith *et al.* 2011, Bechmann *et al.* 2020). Accounting for around 50–60% of all metastatic tumors, cluster 1-related PPGLs have the highest metastatic risk, with up to 75% showing metastases (John *et al.* 1999, Turkova *et al.* 2016, Crona *et al.* 2019, Bechmann *et al.* 2020). Around 2–4% of metastatic tumors belong to the kinase signaling-associated cluster 2 (metastatic risk 2–12%) (Crona *et al.* 2019, Bechmann *et al.* 2020). Cluster 3 mutations of Wnt signaling-related genes have been revealed to play an active role in PPGL pathogenesis and are associated with aggressive behavior and high metastatic risk (Fishbein *et al.* 2017, Alzofon *et al.* 2021). Knowledge of a tumor's molecular cluster guides informed personalized management of PPGLs. Although cluster-specific diagnostics (biochemistry, imaging) and follow-up have entered clinical routine (Nölting *et al.* 2019, 2022), therapy is largely not as yet cluster-specific.

Apart from high-specific activity [^{131}I]-MIBG therapy – approved only in the United States – there are neither approved nor highly effective therapies available for metastatic PPGLs. In clinical practice, conventional chemotherapy with cyclophosphamide, vincristine, and dacarbazine (CVD) is used in patients with rapidly progressive metastatic PPGL with a high tumor burden, while watchful waiting or radionuclide therapy is the recommended first-line option for patients with slow or moderate disease progression (Fassnacht *et al.* 2020, Lenders *et al.* 2020, Nölting *et al.* 2022). In the cases of further progression, the tyrosine kinase inhibitors (TKI) sunitinib or cabozantinib, or the chemotherapeutic temozolomide, can be used (Ayala-Ramirez *et al.* 2012, Hadoux *et al.* 2014, Jimenez *et al.* 2017, O'Kane *et al.* 2019, Baudin *et al.* 2021).

https://erc.bioscientifica.com
https://doi.org/10.1530/ERC-21-0355
© 2022 Society for Endocrinology
Published by Bioscientifica Ltd.
Printed in Great Britain

Downloaded from Bioscientifica.com at 05/11/2022 04:19:32PM
via Bodleian Library

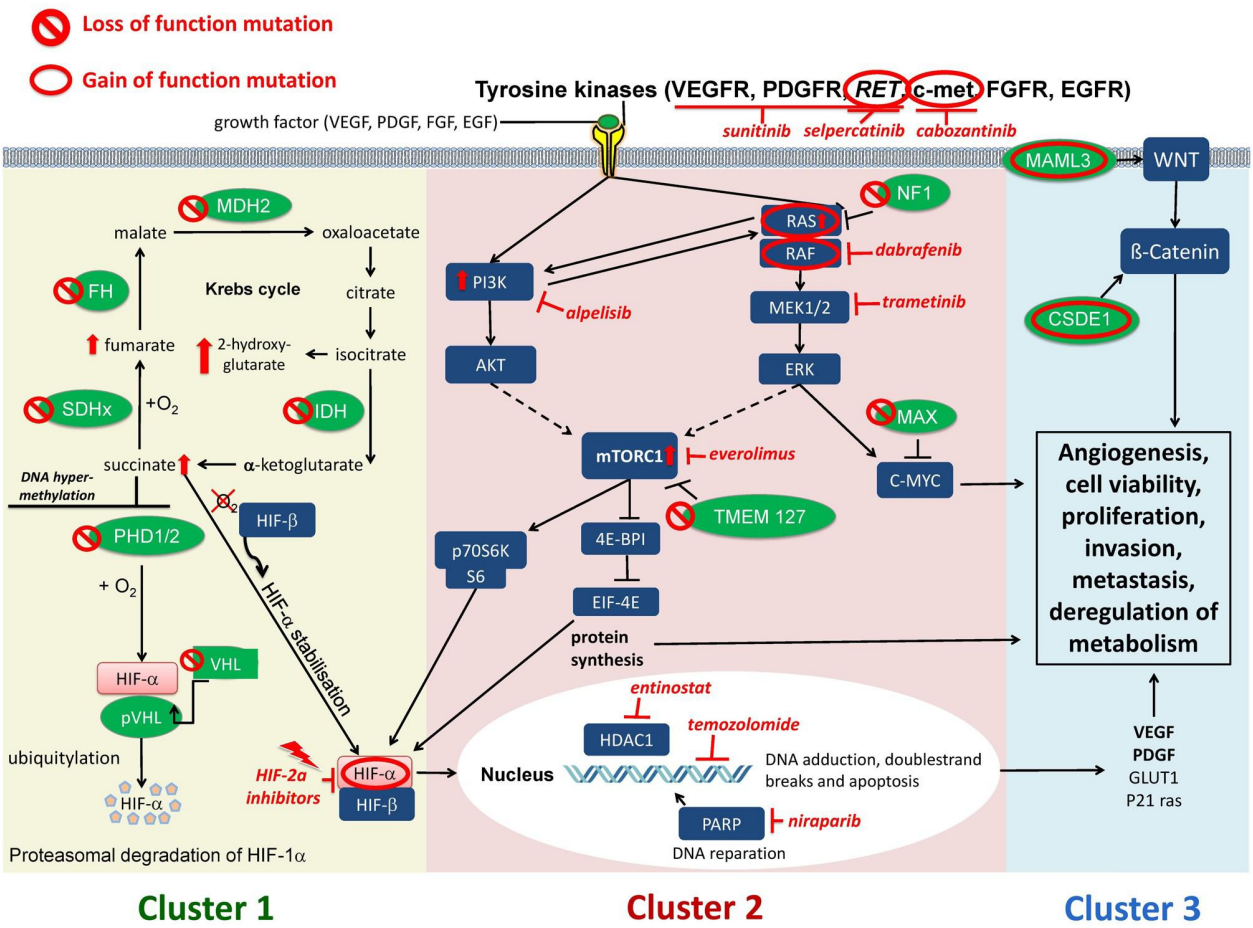

Figure 1

PPGL molecular clusters 1, 2, and 3, including their associated loss- or gain-of-function mutations (green), and potential informed targeted treatment options (red). Pseudohypoxia-associated cluster 1 is subdivided into cluster 1A (Krebs cycle related) and cluster 1B (*VHL/EPAS1* hypoxia signaling related). Cluster 1A involves mutations in genes encoding for succinate dehydrogenase subunits and succinate dehydrogenase complex assembly factor-2 (*SDHA[AF2]/B/C/D*), fumarate hydratase (*FH*), malate dehydrogenase 2 (*MDH2*), isocitrate dehydrogenase 1 (*IDH*), mitochondrial glutamicoxaloacetic transaminase (*GOT2*), 2-oxoglutarate-malate carrier (*SLC25A11*), dihydrolipoamide S-succinyltransferase (*DLST*), and succinate-CoA ligase GDP-forming subunit beta (*SUCLG2*). Cluster 1B comprises mutations in Egl-9 prolyl hydroxylase-1 and -2 (*EGLN1/2* encoding *PHD1/2*), von Hippel-Lindau (*VHL*), hypoxia-inducible factor 2α (*HIF2A/EPAS1*), and iron regulatory protein 1 (*IRP1*). The kinase signaling-associated cluster 2 includes mutations in the rearranged during transfection proto-oncogene (*RET*), neurofibromin 1 (*NF1*), *HRAS,* transmembrane protein 127 (*TMEM127*), Myc-associated factor X (*MAX*), and fibroblast growth factor receptor 1 (*FGFR1*), and in rare cases in *Met, MERTK, BRAF*, and the nerve growth factor receptor (*NGFR*), which leads to overactivation of the PI3K/AKT, mTORC1/p70S6K, and RAS/RAF/MEK/ERK (MAPK) signaling pathways. Wnt signaling-associated cluster 3 comprises mutations in cold shock domain-containing E1 (*CSDE1*), 'mastermind-like' transcriptional coactivator 3 (*MAML3*). ⇧ denotes protein activation/upregulation; ⊥ denotes protein inhibition; ⊘ denotes tumor-promoting loss-of-function mutation; ◯ denotes tumor-promoting gain-of-function mutation.

Therefore, there is a considerable clinical need for novel therapeutic strategies and more effective treatment options, especially for metastatic PPGLs, which would ideally be individualized. Given the lack of reliable human PPGL cell models, we have established a model to perform individualized drug testing in patient-derived PPGL primary cultures (Fankhauser *et al.* 2019), which has been designated as a very promising *in vitro* model (Bayley & Devilee 2020).

After publishing preliminary data from six non-metastatic tumors (Fankhauser *et al.* 2019), we have now expanded our studies (n = 33) allowing us to compare the drug responsivity of cluster 1- (n = 10) with the drug responsivity of cluster 2-related PPGLs (n = 14). Seven of the included primary cultures are from metastatic PPGLs (n = 3 cluster 1, n = 4 non-defined).

Materials and methods

This study was approved by the local ethics committee of both partaking centers (Ethikkommission der Medizinischen Fakultät der LMU München, Projekt-Nr.

https://erc.bioscientifica.com
https://doi.org/10.1530/ERC-21-0355
© 2022 Society for Endocrinology
Published by Bioscientifica Ltd.
Printed in Great Britain

Downloaded from Bioscientifica.com at 05/11/2022 04:19:32PM
via Bodleian Library

379-10 and Kantonale Ethikkommission Zürich, BASEC 2017-00771) and by ENS@T (European Network for the Study of Adrenal Tumors). Written informed consent was obtained from each patient prior to participation.

Human PPGL two-dimensional primary cultures and murine MPC cell lines

Fresh primary tumor tissues were obtained directly after surgery from 33 PPGL patients at the University Hospitals of LMU Munich ($n = 25$) and USZ Zurich ($n = 8$) and numbered consecutively. PPGL primary cultures were isolated using collagenase and red blood cell lysis buffer, incubated for 72 h after seeding and then treated for 72 h with inhibitors listed below (DMSO used as control). Murine pheochromocytoma cell lines (MPC) were cultivated and treated with inhibitors for up to 14 days. Both primary and murine cell viabilities were assessed as previously described (Fankhauser *et al.* 2019). In order to avoid fibroblast overgrowth in the primary cultures, we performed these short-term experiments. We did not observe fibroblast overgrowth on day 8 of cultivation, but it was seen on day 16 of cultivation in the untreated PPGL primary cultures. Other studies have also described fibroblast overgrowth after 15 days of cultivation (April-Monn *et al.* 2021).

Human PPGL three-dimensional primary cultures

Primary cell isolation was carried out using the gentleMACS™ Octo Dissociator with Heaters (Miltenyi Biotec, Germany) together with the human Tumor Dissociation Kit (Miltenyi Biotec). Single-cell suspensions were incubated with RBCLB for 3 min. Primary cells (2×10^4 per well) were plated in a 96-well Ultra-Low Attachment plate (Corning) and incubated for 6 days to allow spheroid formation. Subsequently, cells were treated with drugs for 72 h, and cell viability was assessed after 0, 24, 48, and 72 h using RealTime-Glo™ MT Cell Viability Assay (Promega).

Inhibitors and treatment concentrations

Eighteen different drugs were tested alone and in combination. Drugs targeting cluster 2 include cabozantinib and sunitinib, selpercatinib (LOXO-292), alpelisib (BYL719), everolimus, dabrafenib, trametinib, and AR-A014418. Drugs targeting cluster 1 include temozolomide, niraparib, entinostat, gemcitabine and 5-fluorouracil (5-FU), octreotide, TC-S 7009, and belzutifan (MK6482/PT2977). Other drugs include zoledronic acid and estradiol. The drugs were purchased from Selleckchem (Houston, TX, USA), Hycultec (Beutelsbach, Germany), and Lucerna-Chem (Lucerne, Switzerland) and dissolved in DMSO. In general, we used drug concentrations to approximate the average plasma concentrations measured in patients after therapy (Supplementary Table 1, see section on supplementary materials given at the end of this article). If this information was not available from previous studies or if these doses were not effective (in rare cases), we then performed drug dose–response curves to identify the effective concentrations *in vitro* (Supplementary Fig. 1).

Genetic testing

Targeted next-generation sequencing (NGS), used to identify somatic variants in tumors, was conducted with a custom multi-gene panel covering 84 genes (Gieldon *et al.* 2019) or the human comprehensive cancer panel (Qiagen, DHS-3501Z), covering 306 cancer-associated genes. In both panels, known PPGL susceptibility genes (*NF1, RET, TMEM127, VHL, FH, SDHA, SDHB, SDHC, SDHD, SDHAF2,* and *MAX*), as well as commonly known oncogenes and tumor suppressor genes, were included. Sequencing and analysis were performed as previously described (Gieldon *et al.* 2019). Classification of identified variants was performed following the standards and guidelines of the American College of Medical Genetics and Genomics and the Association for Molecular Pathology (ACMG-AMP) (Richards *et al.* 2015).

Germline testing was performed during routine clinical practice in the respective centers of human genetics using patient blood samples.

Generation and validation of *Sdhb* knockdowns in murine MPC cells

Mouse PCC cells, MPC 4/30/PRR, and MPC cells with stable expression of HIF-2a (MPC mCherry H2A/EV) were cultivated as previously described (Bechmann *et al.* 2019). Five single-guide RNA (sgRNA) specific to *Sdhb* were cloned into pLenti SpBsmBI sgRNA Puro (provided by Rene Maehr; Addgene plasmid #62207) (Pham *et al.* 2016). After initial testing, two sgRNA were chosen for further use (sgRNA-2: ACCTCGAATGCAGACGTACG; sgRNA-3: TGCGCCATGAACATCAACGG). Components of the CRISPR/Cas9 system were stably introduced into MPC cells by two subsequent lentiviral transductions. First Cas9 from *Streptococcus pyogenes* was transduced using vector Lenti-Cas9-2A-Blast (provided by Jason Moffat; Addgene

Downloaded from Bioscientifica.com at 05/11/2022 04:19:32PM
via Bodleian Library

plasmid) (Hart *et al.* 2015). Positively transduced cells were selected by 2 µg/mL blasticidin treatment and then transduced with sgRNA specific for *Sdhb* or with the vector without sgRNA. After puromycin (0.5 µg/mL) selection, cell lines MPC-Cas9-sgRNA2, MPC-Cas9-sgRNA3, and MPC-Cas9-control were obtained (Supplementary Fig. 2).

Spheroid cultivation and treatment

Spheroids of different MPC sub-cell lines were generated (500 cells/spheroid) and cultivated as previously described (Bechmann *et al.* 2018, 2019). Four days after seeding, spheroids were treated with selected drugs. DMSO was used as the control. Average spheroid diameters were measured 14 days after seeding using ImageJ Software (single treatment). Diameters were given relative to DMSO-treated spheroids to account for different growth behaviors of the different cell lines.

SDS-PAGE and Western blot analysis

Cells were seeded into six-well plates (300,000–500,000 cells/well) and treated with selected inhibitors the following day. After 24 or 72 h, cell lysis was performed using a 1:100 dilution of Halt™ Protease and Phosphatase Inhibitor Cocktail (100×) with M-PER™ Mammalian Protein Extraction Reagent, both purchased from Thermo Scientific. Western blotting was then conducted as previously described (Jin *et al.* 2020). Supplementary Table 2 lists the applied antibodies. Protein bands were visualized using chemiluminescence imaging system ECL Chemocam imager (INTAS, Göttingen, Germany) and Western blot quantification was performed.

For the validation of *Sdhb* knockouts in MPC cells, SDHB protein levels were quantified in three different passages of the cell lines by Western blotting using anti-SDHB (ab14714, Abcam) and anti-actin (MAB1501R, Millipore) antibodies. Densitometry on Western blot images was performed using ImageJ software.

Statistical analysis

Each cell viability experiment consisted of four samples per drug concentration. All results are displayed as the mean ± s.d. Efficacy was described as poor (<25% cell viability reduction), moderate (25–50% cell viability reduction), and strong (>50% cell viability reduction). Statistical calculations were made using R 4.0 (R Foundation for Statistical Computing, Vienna, Austria). Wald tests were used for the treatment comparisons. Synergism was assessed as previously described (Slinker 1998, Fankhauser *et al.* 2019). 'Synergistic effects' were confirmed when single effects were significant and interaction effects were both negative and significant. 'Additive effects' were defined as significant single effects but non-significant interaction effects. 'Antagonistic effects' were defined as significant single effects and both positive and significant interaction effects. Statistical significance was set at $P < 0.05$. Due to the exploratory nature of the study, no adjustment for multiple testing was done.

Results

Tumor characteristics, mutational status, and biochemical phenotypes

Genetics

We established human PPGL primary cultures (25 PCCs, 8 PGLs) from 33 individual patients, including 7 metastatic PPGLs (21%, 3 PGLs, 4 PCCs; Table 1). Germline or somatic mutations were found in 79% (26/33) of tumors, with 76% (25/33) in known PPGL susceptibility genes (Fig. 2). The somatic and germline mutations identified in the different tumors are summarized in Table 1. Altogether, 10 clusters 1 mutations (36%), 14 clusters 2 mutations (50%), 2 secondary modifier mutations (*ATRX*; 7%), and 2 potential driver mutations which have not previously been described in PPGL (*ATM*, *MPL*; 7%) were identified. Two tumors showed double mutations. In seven tumors, no known PPGL driver mutations were found.

Biochemical and clinical phenotypes in different clusters

Cluster 1 PPGLs are regularly associated with noradrenergic (elevated plasma concentrations of normetanephrine and no or relatively small increases in metanephrine) and cluster 2 PPGLs with adrenergic (plasma metanephrines that exceed 5% relative to the sum of metanephrines and normetanephrines) phenotypes.

All cluster 1-associated PPGL patients ($n = 10$) presented with noradrenergic phenotypes, except for two biochemically silent head-and-neck PGL (HNPGL) patients (47 and 48). All cluster 2-associated PPGL patients ($n = 14$), apart from patients 30 (*TMEM127*-mutant, noradrenergic), 42 (*RET* (VUS)-mutant, noradrenergic), and 49 (*NF1*-mutant HNPGL, biochemically silent), showed adrenergic phenotypes. In patients without cluster affiliations, *ATRX* mutations were associated with noradrenergic and the *MPL* mutation with adrenergic phenotypes. As expected from

https://erc.bioscientifica.com
https://doi.org/10.1530/ERC-21-0355
© 2022 Society for Endocrinology
Published by Bioscientifica Ltd.
Printed in Great Britain

Downloaded from Bioscientifica.com at 05/11/2022 04:19:32PM
via Bodleian Library

Table 1 Human PPGL primary cultures patient cohort (n = 33).

Patient ID	Sex	Age (years)	Histology and tumor characteristics	Ki-67 (%)	Biochemical phenotype	Tumor sequencing	Germline status
4[a]	m	82	PCC, 1.5 cm, capsule infiltration	1–2	Adrenergic	No mutation	No mutation
5[a]	m	50	PCC, 12.9 cm	1–2	Adrenergic	*NF1*	n/a
6[a]	f	73	PCC, 3.9 cm	2	Adrenergic	*NF1*	Somatic
7[a]	m	26	PCC, 4 cm, angioinvasion	<5	Noradrenergic	No mutation	No mutation
10[a]	m	65	PCC, bilateral, right 5.7 cm and left 2.1 cm, PASS 3	<1	Noradrenergic	*VHL, ATRX*	n/a
11[a]	m	59	PCC, 5.5 cm, capsule infiltration, angioinvasion, PASS 2	<1	Adrenergic	*BRAFV601*	n/a
12	f	36	PCC, 6 cm	<2	Adrenergic	*RET:p.C618S*	Germline (MEN2A)
13	f	58	PGL, metastatic (liver, lymph node, muscle), max. 9.5 cm, muscle infiltration, angioinvasion	n/a	Noradrenergic	No mutation	No mutation
16	m	58	PCC, 3.7 cm	low	Noradrenergic	*SDHC*	Germline
18	m	25	PCC, 2.6 cm or 1.9 cm	1–2	Adrenergic	*RET:p.C634A, ATM*	Germline (MEN2A)
19	f	41	PCC, 9 cm	1–2	Adrenergic	*NF1*	Somatic
20	m	52	PCC, 8.2 cm	<1	Adrenergic	*NF1*	Somatic
21	f	70	PGL, nonfunctioning, abdominal, 4.2 cm, R1	1	Silent	No mutation	No mutation
22	f	41	PGL, extra/periadrenal, 1.7 cm, and PCC 6 mm, R1	1	Adrenergic	*RET:p.C634T*	Germline (MEN2A)
23	f	19	PCC, max. 6.1 cm	n/a	Noradrenergic	*VHL*	Somatic
24	m	57	PCC, 2.7 cm	<1	Adrenergic	*MPL*	Somatic
26	f	34	PGL, abdominal, max. 4.5 cm	4	Noradrenergic	*VHL*	Germline
27	m	53	PCC, metastatic (lung, bone), 5.2 cm, angioinvasion, PASS 15	80	Noradrenergic	*ATRX*	Somatic
30	m	62	PCC, max. 6.7 cm, PASS 0	n/a	Noradrenergic	*TMEM127*	Somatic
32	f	58	PCC, max. 3.3 cm	n/a	Noradrenergic	*VHL*	n/a
33	f	55	PCC, max. 12.6 cm	<1	Adrenergic	*NF1*	n/a
34	f	50	PCC, metastatic (liver, lymph node, bone), 16.9 cm, GAPP 8	10	Noradrenergic	No mutation (VUS *SDHA*[b])	No mutation
36	f	33	PCC, metastatic (bone, paravertebral)	15	Noradrenergic	*SDHB*	Germline
37	m	38	PGL, metastatic (liver, lymph node, bone), 8 cm, infiltration of liver and vena cava, GAPP 8, immunohistochemical *SDHB*-loss	5	Noradrenergic	*SDHB*	Germline
38	f	63	PCC, max. 2.2 cm	1–2	Noradrenergic	*EPAS1*	Somatic
40	f	38	PCC, 7 cm, PASS 3	<1	Adrenergic	*NF1*	Somatic
42	f	74	PCC, 5.4 cm, lymphatic invasion	10	Noradrenergic	VUS *RET*[c]	Somatic
44	f	49	PCC, 4 cm	<2	Adrenergic	*HRAS*	Somatic
45	m	76	PCC, 2.8 cm, angioinvasion, SSTR2 expression negative	<1	Noradrenergic	No mutation	No mutation
46	f	62	PCC, micrometastases (lung), 9.8 cm, angioinvasion	2–3	Adrenergic	No mutation	No mutation
47	f	27	PGL, head/neck, 2.7 cm, immunohistochemical *SDHB*-loss	n/a	Silent	*SDHB*	Germline
48	f	47	PGL, head/neck, metastatic (bone), 1.2 cm	n/a	Silent	*SDHB* (VUS *EPAS1*[d])	Germline
49	m	36	PGL, head/neck, 2.1 cm	n/a	Silent	*NF1*	Somatic
Total	**14 m, 19 f**	**median age: 52**	**25 PCCs, 8 PGLs, 7 metastatic PPGLs**		**14 adrenergic, 15 noradrenergic, 4 silent**		**12 somatic, 9 germline, 5 unknown**

[a]Previously published data (Fankhauser *et al.* 2019). [b]SDHA:c.1232G>A (p.Gly411Asp). Succinate:fumarate unremarkable. [c]Most likely pathogenic mutation. [d]Clinical interpretation unclear, mutation mentioned for information.
Male (m), female (f), pheochromocytoma (PCC), paraganglioma (PGL), pheochromocytoma and paraganglioma (PPGL), next-generation sequencing (NGS), not available (n/a).

https://erc.bioscientifica.com
https://doi.org/10.1530/ERC-21-0355
© 2022 Society for Endocrinology
Published by Bioscientifica Ltd.
Printed in Great Britain

Downloaded from Bioscientifica.com at 05/11/2022 04:19:32PM
via Bodleian Library

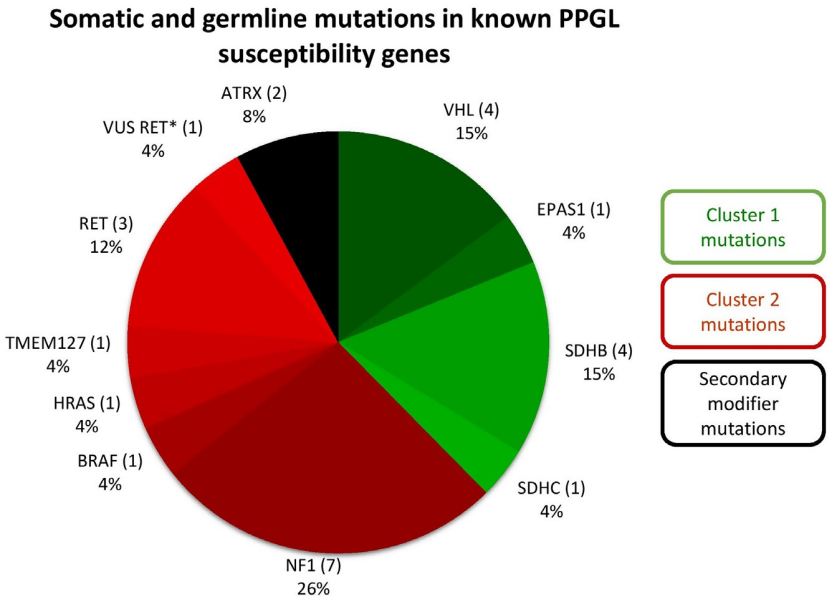

Figure 2
Distribution of somatic and germline mutations in 25/33 PPGL samples with mutations in known PPGL susceptibility genes (76%). Cluster 1 mutations were identified in 10 samples, cluster 2 mutations were identified in 14 samples, and secondary modifier mutations were identified in 2 samples. Double mutations were found in 2 samples. Not shown: two samples with mutations in unknown PPGL susceptibility genes (*MPL*, *ATM*). *Most likely pathogenic mutation.

other studies, metastatic PPGLs - except for one (patient 46) - had noradrenergic phenotypes.

SSTR2 baseline expression in patient primary cultures

Currently there is no evidence for direct transferability of primary culture data to patient care. Two anecdotal reports indicate transferability of primary culture data to patient management.

PGL patient 13

Patient 13, without a known PPGL susceptibility mutation, presented with recurrent liver, lymph node, and abdominal metastases from a primarily resected PGL. Somatostatin receptor (SSTR)-based radionuclide imaging showed SSTR2 positivity. Baseline SSTR2 expression by Western blot analysis was notably higher compared to most other primary cultures (n = 16; Fig. 3A and B). SSTR2-targeted radionuclide therapy (PRRT) was clinically applied as first-line systemic therapy; follow-up staging indicated a complete biochemical (decrease of plasma free normetanephrines from 1020 ng/L to 239 ng/L) and almost complete radiological response (Fig. 3C).

PCC patient 34

Primarily metastatic patient 34 also showed SSTR2-positivity in clinical imaging but, in contrast to patient 13, very low SSTR2 protein levels in Western blot analysis (Fig. 3A). Due to multiple lymph node and bone metastases, patient 34 received two cycles of PRRT after primary tumor resection but showed no radiological response with instead mildly progressive disease (Fig. 3C).

Drug treatment of patient primary cultures

We correlated drug responsivity with the underlying mutation/cluster affiliation, performed Western blot analysis where sufficient cell material was available (n = 16), and identified baseline and therapy-induced differences. Table 2 shows drug responsivity of the PPGL primary cultures, defined as the mean percentage of cell viability reduction after drug treatment, stratified depending on the underlying mutation and cluster affiliation. Statistical significance was assessed overall and for cluster 1, cluster 2, and metastatic primary cultures. We also compared drug responsivity of cluster 1-related with drug responsivity of cluster 2-related tumors.

Kinase signaling inhibitors in clinical use: targeting cluster 2?

Multi-TKIs cabozantinib and sunitinib alone and in combination with mTORC1 inhibitor everolimus Cabozantinib and sunitinib are currently in clinical use as therapeutic options for progressive metastatic PPGLs. In our PPGL primary cultures, we tested both drugs alone and in combination with everolimus, which is clinically used for progressive neuroendocrine tumors (NETs). Clinically relevant doses of cabozantinib (5 µM), sunitinib (0.5 µM), and everolimus (10 nM) significantly

https://erc.bioscientifica.com
https://doi.org/10.1530/ERC-21-0355
© 2022 Society for Endocrinology
Published by Bioscientifica Ltd.
Printed in Great Britain

Downloaded from Bioscientifica.com at 05/11/2022 04:19:32PM
via Bodleian Library

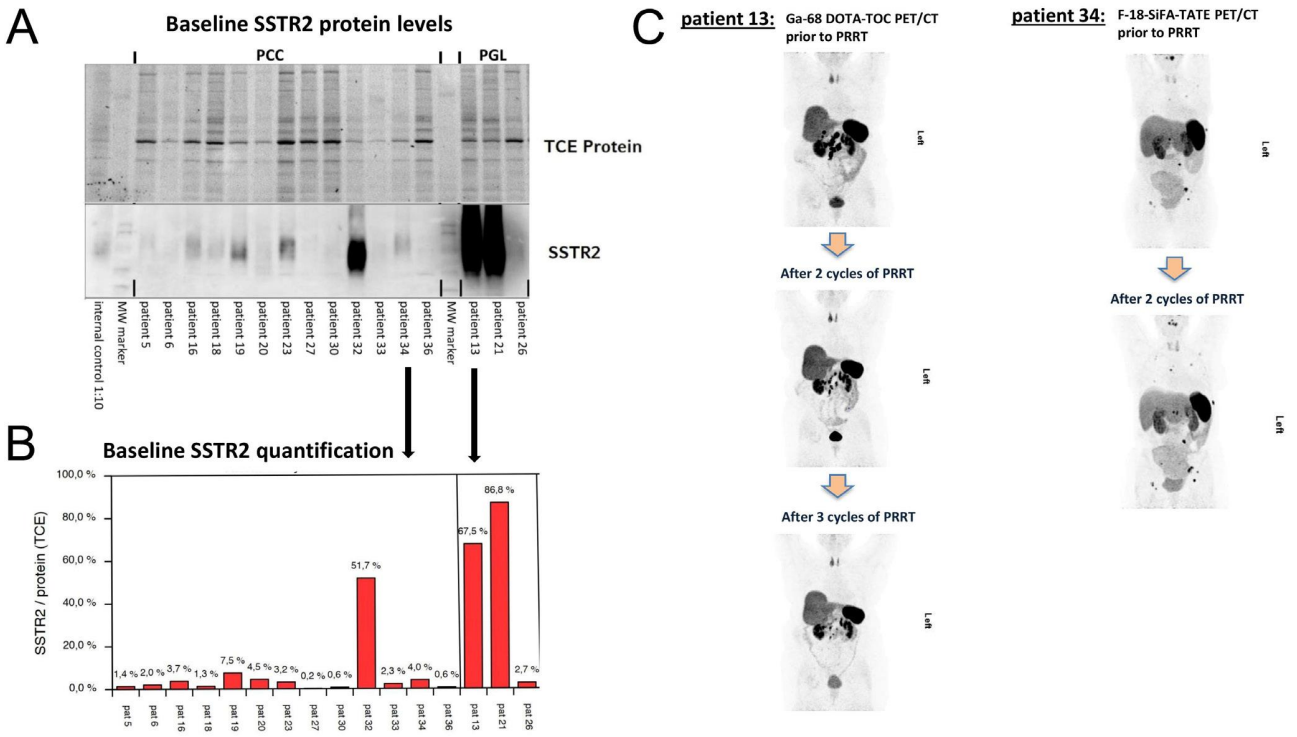

Figure 3

Baseline SSTR2 protein levels in relation to TCE protein levels (A) and baseline SSTR2 quantification (B) of the PPGL primary cultures (n = 16). Significantly higher SSTR2 expressions were found in the metastatic PGL primary cultures of patients 13 and 21 and the PCC primary culture of patient 32 compared to the other PPGL primary cultures. (C) Ga-68 DOTA-TOC PET/CT imaging of patient 13 prior to and after two and three cycles of SSTR2-guided peptide receptor radionuclide therapy (PRRT) and F-18-SiFA-TATE PET/CT imaging of patient 34 prior to and after two cycles of PRRT. After two to three cycles of PRRT, Ga-DOTA-TOC PET/CT of patient 13 showed a significant decrease of tumor burden. Patient 13 also had a strong biochemical therapy response with a near normalization of plasma free normetanephrines (239 ng/L) from initial values of 1020 ng/L. In contrast, F-18-SiFA-TATE PET/CT of patient 34 showed slightly progressive disease after two cycles of PRRT.

reduced primary culture cell viability. Cabozantinib showed the strongest efficacy. Unexpectedly, cabozantinib was significantly more effective in cluster 1- (n = 8) compared to cluster 2-related PPGLs (n = 13) (−44% vs −35% viability reduction), especially in *SDHB*-mutant metastatic PPGLs (−55%, n = 3) (Fig. 4A). Everolimus was similarly effective in both clusters (-28%, n = 31) but showed stronger efficacy in *SDHB*-mutant PPGLs (−36%, n = 4).

Cabozantinib/everolimus combination treatment was highly effective in both clusters and showed an overall synergistic effect (−66%, n = 14) with slightly but significantly stronger efficacy in cluster 2 (−74%, n = 5) compared to cluster 1 (−62%, n = 5; Fig. 4A). Combination treatment resulted in attenuation of everolimus-induced AKT activation and a strong inhibition of mTOR downstream effectors 4EBP1, p70S6K, and S6 (n = 6) as a potential explanation for the synergism of the two drugs (Supplementary Fig. 2). Supporting this finding, we confirmed the strong efficacy of cabozantinib/everolimus combination treatment in a MPC spheroid model, with significant spheroid shrinkage and no regrowth 10 days after combination treatment (Fig. 4B, C and D).

Sunitinib showed low overall efficacy (−15%, n = 30) with best efficacy in *SDHB*-mutant tumors (−20%, n = 3) (Fig. 5). Sunitinib/everolimus combination treatment was significantly more effective in cluster 2 (−43%, n = 11) compared to cluster 1 (−36%, n = 7) and showed additive effects (Fig. 5). However, the efficacy of sunitinib/everolimus was overall much weaker compared to other targeted combinations tested (cabozantinib/everolimus, alpelisib/everolimus, alpelisib/trametinib (see below)), especially in metastatic *SDHB*-mutant primary cultures 36 and 37 (Figs 4, 5 and 6, red-labeled).

PI3K inhibitor alpelisib alone and in combination with everolimus We have previously shown synergistic effects of alpelisib in combination with everolimus in a few patients' primary cultures (n = 6) and in human progenitor

https://erc.bioscientifica.com
https://doi.org/10.1530/ERC-21-0355
© 2022 Society for Endocrinology
Published by Bioscientifica Ltd.
Printed in Great Britain

Downloaded from Bioscientifica.com at 05/11/2022 04:19:32PM
via Bodleian Library

Table 2 Reduction in mean cell viability[a] following individual treatment according to the underlying mutation/cluster affiliation.

Drug		Mean cell viability reduction in total[b] [%] (*n*) ± s.d.	Mean cell viability reduction in cluster 1 tumors[b] (%) (*n*) ± s.d.			Mean cell viability reduction in cluster 2 tumors[b] (%) (*n*) ± s.d.			Mean cell viability reduction in metastatic tumors[b] [%] (*n*) ± s.d.
			Total (*n*)	*SDHB*-mutant	*VHL*-mutant	Total (*n*)	*RET*-mutant	*NF1*-mutant	
Kinase signaling inhibitors	Cabozantinib (5 μM)	39[c] (29) ± 0.19	44[c]† (8) ± 0.16	55 (3) ± 0.08	33 (4) ± 0.15	35[c] (13) ± 0.21	22 (4) ± 0.22	37 (6) ± 0.18	47[c] (7) ± 0.13
	Everolimus (10 nM)	28[c] (31) ± 0.15	29[c] (9) ± 0.13	36 (4) ± 0.13	25 (4) ± 0.11	29[c] (13) ± 0.16	23 (4) ± 0.12	28 (6) ± 0.19	31[c] (7) ± 0.14
	Sunitinib (0.5 μM)	15[c] (30) ± 0.12	18[c] (8) ± 0.12	20 (3) ± 0.13	17 (4) ± 0.12	14[c] (13) ± 0.11	15 (4) ± 0.11	12 (6) ± 0.13	15[c] (6) ± 0.13
	Cabozantinib (5 μM)/ Everolimus (10 nM)	66[c] (14) ± 0.11	62[c] (5) ± 0.08	67 (2) ± 0.04	60 (2) ± 0.1	74[c]† (5) ± 0.13	60 (1) ± 0.03	82 (2) ± 0.09	62[c] (5) ± 0.07
	Sunitinib (0.5 μM)/ Everolimus (10 nM)	39[c] (26) ± 0.15	36[c] (7) ± 0.08	42 (2) ± 0.04	33 (4) ± 0.07	43[c]† (11) ± 0.17	36 (4) ± 0.12	47 (5) ± 0.21	38[c] (6) ± 0.12
	Alpelisib (5 μM)	34[c] (31) ± 0.12	34[c] (9) ± 0.11	34 (4) ± 0.09	36 (4) ± 0.12	33[c] (13) ± 0.12	30 (4) ± 0.15	29 (6) ± 0.08	33[c] (7) ± 0.09
	Alpelisib (5 μM)/ Everolimus (10 nM)	55[c] (31) ± 0.15	54[c] (9) ± 0.13	60 (4) ± 0.14	51 (4) ± 0.11	58[c] (13) ± 0.16	49 (4) ± 0.13	60 (6) ± 0.18	56[c] (7) ± 0.12
	Trametinib (1 μM)	29[c] (25) ± 0.19	34[c] (7) ± 0.11	36 (3) ± 0.06	28 (3) ± 0.12	27[c] (11) ± 0.23	21 (4) ± 0.14	26 (5) ± 0.3	31[c] (6) ± 0.11
	Trametinib (1 μM)/ Alpelisib (5 μM)	65[c] (18) ± 0.15	63[c] (7) ± 0.09	71 (3) ± 0.07	56 (3) ± 0.06	65[c]† (6) ± 0.23	57 (1) ± 0.03	60 (3) ± 0.31	65[c] (5) ± 0.07
	Dabrafenib (10 μM)	Increase by 16[+] (20) ± 0.25	Increase by 12[+] (6) ± 0.12	Increase by 19 (2) ± 0.07	Increase by 10 (3) ± 0.14	Increase by 13 (8) ± 0.32	Increase by 9 (4) ± 0.38	Increase by 12 (3) ± 0.24	Increase by 23 (6) ± 0.23
	Trametinib (1 μM)/ Dabrafenib (10 μM)	22[c] (17) ± 0.14	21[c] (6) ± 0.09	19 (2) ± 0.08	20 (3) ± 0.11	22[c] (6) ± 0.14	15 (2) ± 0.09	25 (3) ± 0.18	22 (5) ± 0.17
	Selpercatinib (5 μM)	33[c] (22) ± 0.16	41[c]† (6) ± 0.13	46 (3) ± 0.13	37 (2) ± 0.09	28[c] (9) ± 0.13	20 (3) ± 0.1	31 (4) ± 0.14	37[c] (6) ± 0.12
	AR-A014418 (20 μM)	50[c] (15) ± 0.19	49[c] (6) ± 0.19	56 (4) ± 0.17	22 (1) ± 0.04	50[c] (6) ± 0.21	59 (1) ± 0.03	56 (3) ± 0.13	49[c] (5) ± 0.17
Chemotherapeutics, HIF-2a Inhibitors, SSTR2 Analogues	Temozolomide (100 μM)	2 (19) ± 0.2	3 (5) ± 0.11	4 (2) ± 0.11	2 (2) ± 0.13	6 (8) ± 0.18	0 (1) ± 0.12	4 (5) ± 0.21	2 (5) ± 0.1
	Niraparib (10 μM)	27[c] (27) ± 0.19	30 (7) ± 0.1	37 (2) ± 0.1	28 (4) ± 0.09	23[c] (12) ± 0.24	12 (4) ± 0.16	27 (5) ± 0.33	35[c] (6) ± 0.13
	Temozolomide (100 μM)/Niraparib (10 μM)	37[c] (19) ± 0.14	41 (5) ± 0.13	52 (2) ± 0.07	35 (2) ± 0.11	36[c] (8) ± 0.17	20 (1) ± 0.04	39 (5) ± 0.19	41 (5) ± 0.12
	Entinostat (1 μM)	40[c] (28) ± 0.18	44 (7) ± 0.14	45 (3) ± 0.15	44 (4) ± 0.15	38[c] (13) ± 0.2	36 (4) ± 0.16	34 (6) ± 0.23	42[c] (6) ± 0.12
	Niraparib (10 μM)/ Entinostat (1 μM)	46[c] (23) ± 0.16	44 (6) ± 0.11	52 (3) ± 0.07	40 (3) ± 0.11	46[c] (10) ± 0.18	45 (4) ± 0.17	38 (3) ± 0.22	53[c] (6) ± 0.09
	Gemcitabine (30 μM)	47[c] (14) ± 0.2	52[c] (5) ± 0.19	60 (3) ± 0.19	30 (1) ± 0.05	49[c] (6) ± 0.21	45 (1) ± 0.07	58 (2) ± 0.27	51[c] (4) ± 0.23
	Gemcitabine (30 μM)/ AR-A014418 (20 μM)	54[c] (13) ± 0.19	52[c] (5) ± 0.2	62 (3) ± 0.18	25 (1) ± 0.02	55[c] (5) ± 0.21	65 (1) ± 0.09	55 (2) ± 0.14	62[c] (4) ± 0.13
	5-fluorouracile (20 μM)	27[c] (21) ± 0.23	36[c]† (6) ± 0.11	40 (3) ± 0.08	29 (2) ± 0.14	20[c] (8) ± 0.3	Increase by 4 (3) ± 0.29	35 (3) ± 0.27	34[c] (6) ± 0.13
	TCS-7009 (20 μM)	8[c] (17) ± 0.15	9[c] (5) ± 0.1	9 (1) ± 0.07	8 (4) ± 0.11	8 (7) ± 0.2	Increase by 1 (3) ± 0.21	7 (2) ± 0.19	9 (4) ± 0.14
	TCS-7009 (40 μM)	19[c] (17) ± 0.18	18[c] (5) ± 0.17	15 (1) ± 0.07	18 (4) ± 0.18	22[c] (7) ± 0.19	13 (3) ± 0.16	21 (2) ± 0.21	17[c] (4) ± 0.18
	Belzutifan (10 μM)	1 (8) ± 0.14	Increase by 2 (2) ± 0.18	Increase by 2 (2) ± 0.18	-	1 (4) ± 0.13	Increase by 2 (1) ± 0.04	1 (2) ± 0.18	1 (3) ± 0.16
	Belzutifan (20 μM)	7 (9) ± 0.11	5 (3) ± 0.14	5 (2) ± 0.15	-	6 (4) ± 0.1	12 (1) ± 0.08	7 (2) ± 0.1	7 (3) ± 0.12
	Octreotide (40 μM)	2 (19) ± 0.13	3 (6) ± 0.13	7 (3) ± 0.13	Increase by 1 (2) ± 0.1	2 (7) ± 0.15	7 (2) ± 0.19	3 (3) ± 0.16	2 (5) ± 0.08

(*Continued*)

https://erc.bioscientifica.com
https://doi.org/10.1530/ERC-21-0355
© 2022 Society for Endocrinology
Published by Bioscientifica Ltd.
Printed in Great Britain

Downloaded from Bioscientifica.com at 05/11/2022 04:19:32PM
via Bodleian Library

Table 2 Continued.

Drug		Mean cell viability reduction in total[b] [%] (*n*) ± s.d.	Mean cell viability reduction in cluster 1 tumors[b] (%) (*n*) ± s.d.			Mean cell viability reduction in cluster 2 tumors[b] (%) (*n*) ± s.d.			Mean cell viability reduction in metastatic tumors[b] [%] (*n*) ± s.d.
			Total (*n*)	*SDHB*-mutant	*VHL*-mutant	Total (*n*)	*RET*-mutant	*NF1*-mutant	
Others	Zoledronic acid (5 µM)	26[c] (20) ± 0.2	21[c] (6) ± 0.2	35 (3) ± 0.19	7 (2) ± 0.05	32[c]† (8) ± 0.21	19 (2) ± 0.07	38 (4) ± 0.28	29[c] (5) ± 0.2
	Zoledronic acid (40 µM)	45* (18) ± 0.22	50* (5) ± 0.22	64 (3) ± 0.11	38 (1) ± 0.03	46* (8) ± 0.25	31 (2) ± 0.07	49 (4) ± 0.32	53* (5) ± 0.18
	Estradiol (1 µM)	10* (12) ± 0.15	4 (4) ± 0.12	5 (3) ± 0.14	-	12* (5) ± 0.15	4 (1) ± 0.1	25 (2) ± 0.13	1 (4) ± 0.1
	Estradiol (10 µM)	26* (12) ± 0.18	16* (4) ± 0.2	23 (3) ± 0.17	-	28*† (5) ± 0.09	29 (1) ± 0.01	25 (2) ± 0.12	23* (4) ± 0.15

[a]Efficacy is described as poor (<25% cell viability reduction), moderate (25–50% cell viability reduction), and strong (>50% cell viability reduction). [b]Statistical significance was assessed for total primary cultures, total cluster 1 tumors, total cluster 2 tumors and metastatic tumors. Significance could not be assessed for temozolomide, niraparib, entinostat, temozolomide/niraparib, niraparib/entinostat in cluster 1. Significance could not be assessed for dabrafenib, trametinib/dabrafenib, temozolomide, temozolomide/niraparib in metastatic tumors. [c]Significant decrease of cell viability compared to control DMSO $P < 0.05$. *Significant increase of cell viability compared to control DMSO $P < 0.05$. †Significantly higher efficacy of the listed therapy in the marked cluster compared to the other cluster.

pheochromocytoma (hPheo1) cells (Fankhauser *et al.* 2019, Helm *et al.* 2022). We have now extended these investigations by analyzing cluster-specific drug responsivity in a larger cohort ($n = 31$).

Clinically relevant doses of alpelisib (5 µM) led to a similar cell viability decrease in both clusters (−34% and −33%, respectively). Alpelisib/everolimus combination therapy showed strong efficacy (−55%) with an additive effect overall and in cluster 1 (−54%, $n = 9$) but a synergistic effect in cluster 2 (−58%, $n = 13$; Fig. 6). Notably, the strongest decrease in viability was found in metastatic *SDHB*-mutant tumors (−64%, $n = 3$). We cross-validated the efficacy of alpelisib/everolimus in three out of four 3D primary cultures. One of those was cluster 1-related (*VHL*-mutant), one was cluster 2-related (*TMEM127*-mutant), and one was metastatic (*ATRX*-mutant) (Fig. 7). Alpelisib/everolimus combination treatment attenuated everolimus-induced AKT activation and strongly inhibited 4EBP1, p70S6K, and S6 signaling ($n = 16$) (Supplementary Fig. 3).

Alpelisib in combination with MEK inhibitor trametinib We evaluated the combination of trametinib, which is in clinical use for metastatic melanoma, with alpelisib. Trametinib (1 µM) showed a moderate overall viability decrease (−29%, $n = 25$), with a slightly higher efficacy in cluster 1 than cluster 2 (−34%, $n = 7$ and −27%, $n = 11$). Trametinib/alpelisib combination resulted in an overall synergistic cell viability decrease in both clusters (−65%, $n = 18$), with strongest efficacy in *SDHB*-mutant PPGLs (−71%, $n = 3$), and significantly stronger efficacy in cluster 2 compared to cluster 1 (Fig. 8A).

This synergism may be explained by alpelisib-mediated attenuation of trametinib-induced AKT activation and simultaneous trametinib-mediated inhibition of ERK ($n = 2$) (Fig. 8B and C). Unexpectedly, trametinib alone and in combination with alpelisib led to strong increases of phosphorylated MEK (pMEK), possibly be due to feedback induction of upstream signaling (Yaeger & Corcoran 2019).

Trametinib in combination with the RAF inhibitor dabrafenib In contrast to trametinib, dabrafenib (10 µM) significantly promoted overall cell survival (+16%, $n = 20$), especially in metastatic PPGLs (+23%, $n = 6$; Fig. 9A), possibly through increased activation of ERK ($n = 6$; Fig. 9B). Dabrafenib/trametinib combination treatment led to a weaker decrease of cell viability than trametinib alone (−22%, $n = 17$ vs −29%, $n = 25$).

Selective RET inhibitor selpercatinib Clinically relevant doses of selpercatinib (5 µM) showed overall

https://erc.bioscientifica.com
https://doi.org/10.1530/ERC-21-0355
© 2022 Society for Endocrinology
Published by Bioscientifica Ltd.
Printed in Great Britain

Downloaded from Bioscientifica.com at 05/11/2022 04:19:32PM
via Bodleian Library

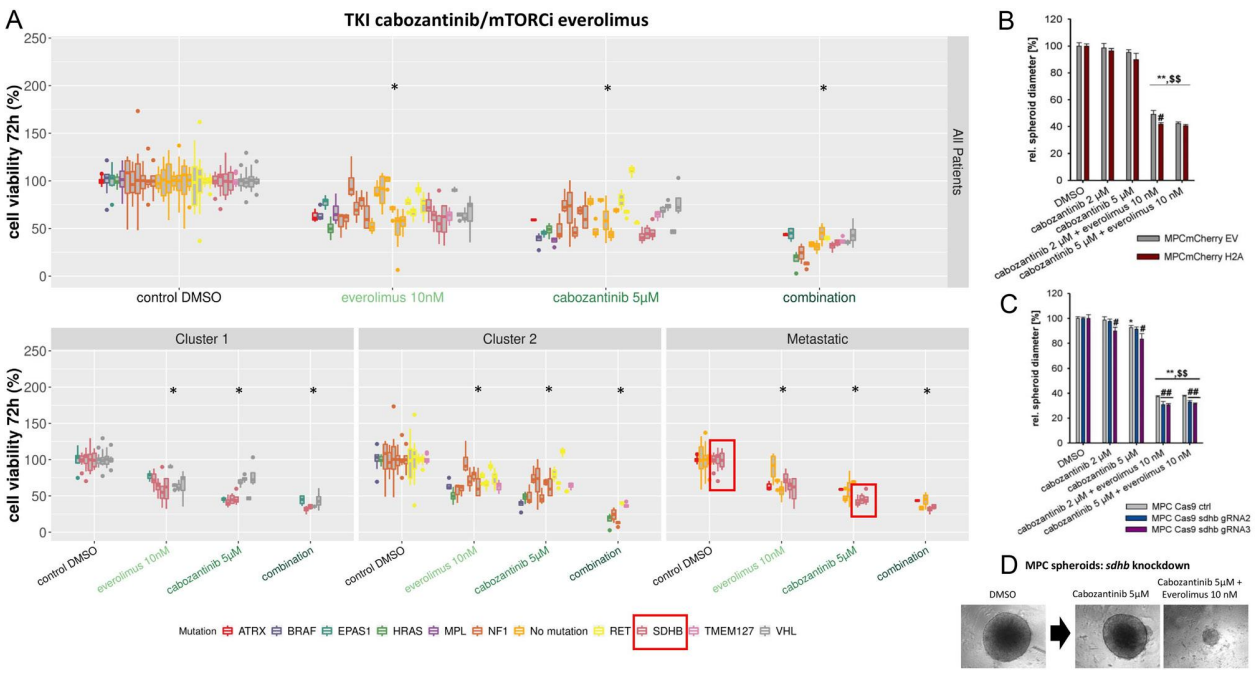

Figure 4

The tyrosine kinase inhibitor (TKI) cabozantinib tested in combination with the mTORC1 inhibitor everolimus in 2D PPGL primary cultures and in MPC cell spheroids. (A) Stratification depending on molecular clusters and malignancy. Patients with the same mutation are represented by the same color. Seventy-two-hour cell viability assay: Treatment with cabozantinib (n = 29) alone and in combination with everolimus (n = 31). Cabozantinib at a dose close to the clinically relevant doses significantly reduced cell viability, particularly in the *SDHB*-mutant metastatic tumors of patients 36, 37, and 49 (red frame). Cabozantinib/everolimus combination therapy led to an overall synergistic decrease of cell viability (n = 14). An additive decrease was found in cluster 1-related (n = 5) and metastatic tumors (n = 5) while a synergistic decrease was found in cluster 2-related tumors (n = 5). *Significant decrease of cell viability compared to control DMSO $P < 0.05$. (B) Combination treatment with cabozantinib and everolimus in MPC cell spheroids with expression of *Hif2α* resulted in a significant reduction in spheroid diameter and showed superiority to treatment with cabozantinib alone. (C) Cabozantinib/everolimus significantly reduced the spheroid diameter, compared to the untreated controls, with slightly higher efficacy in *Sdhb* knockdown spheroids compared to the control spheroids. Mean ± s.e.m. ANOVA and Bonferroni *post hoc* test comparison vs DMSO control $^{*}P < 0.05$, $^{**}P < 0.01$ vs MPCmCherry EV or MPC Cas9 ctrl $^{\#}P < 0.05$, $^{\#\#}P < 0.01$, vs cabozantinib alone $^{\$}P < 0.05$, $^{\$\$}P < 0.01$. (D) Cabozantinib/everolimus combination treatment significantly diminished the growth of MPC *Sdhb* knockdown spheroids compared to the untreated DMSO control or single treatment with cabozantinib.

moderate efficacy with significantly higher efficacy in cluster 1-related (n = 6) and slightly higher efficacy in metastatic, compared to cluster 2-related primary cultures (n = 9) (−41%, −37%, and −28%, respectively), including *RET*-mutant patients (−20%, n = 3). Selpercatinib inhibited ERK signaling in most (9/12) PPGL primary cultures, including *RET*-mutant PCC from patient 18 (Fig. 9B).

Chemotherapeutics, inhibitors of PARP, HDAC1 and HIF-2a, somatostatin analogs: targeting cluster 1?

Chemotherapeutic temozolomide, PARP inhibitor niraparib, and HDAC1 inhibitor entinostat As previously published (n = 5) (Fankhauser *et al.* 2019), temozolomide (100 µM) – currently in clinical use for metastatic PPGLs – showed poor overall efficacy in human primary cultures (−2%, n = 19). Niraparib (10 µM) and entinostat (1 µM) were moderately effective (−27%, n = 27 and −40%, n = 28) with slightly higher efficacy in cluster 1 and metastatic PPGLs, compared to cluster 2. Temozolomide/niraparib combination therapy showed overall synergistic effects (−37%, n = 19) while niraparib/entinostat combination therapy showed antagonistic effects (−46%, n = 23), with no relevant difference between both clusters. Both combination therapies showed strong efficacy in *SDHB*-mutant PPGLs (−52%, n = 2 and −52%, n = 3).

Chemotherapeutic gemcitabine alone and in combination with GSK3 inhibitor AR-A014418 Clinically relevant doses of gemcitabine (30 µM) led to a moderate viability decrease (−47%, n = 14) in both clusters, with strong efficacy in *SDHB*-mutant cases (−60% n = 3, −72% in two metastatic *SDHB*-mutant cases; Fig. 10A). MPC spheroid models confirmed the strong efficacy of gemcitabine with a strong shrinkage/destruction

https://erc.bioscientifica.com
https://doi.org/10.1530/ERC-21-0355
© 2022 Society for Endocrinology
Published by Bioscientifica Ltd.
Printed in Great Britain

Downloaded from Bioscientifica.com at 05/11/2022 04:19:32PM
via Bodleian Library

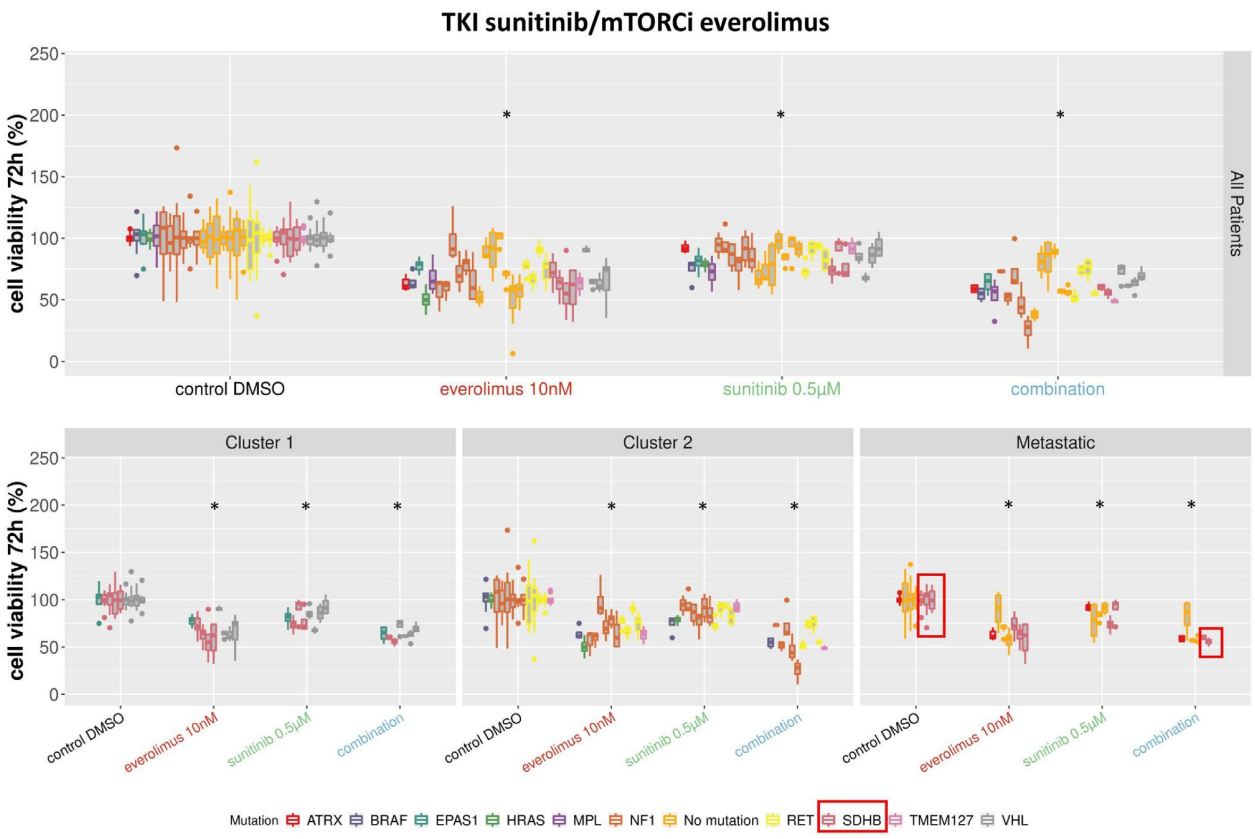

Figure 5
Stratification depending on molecular clusters and malignancy. Patients with the same mutation are represented by the same color. Seventy-two-hour cell viability assay: Treatment with the tyrosine kinase inhibitor (TKI) sunitinib (n = 30) alone and in combination with the mTORC1 inhibitor everolimus (n = 31). Sunitinib/everolimus combination therapy (n = 26) led to an additive but weaker decrease of cell viability compared to other targeted combination therapies, especially in the metastatic *SDHB*-mutant primary cultures 36 and 37 (red frame). An additive decrease of cell viability was also found in cluster 2-related (n = 11) and metastatic (n = 6) tumors. However, in cluster 1-related (n = 7) tumors, sunitinib/everolimus showed antagonistic effects. *Significant decrease of cell viability compared to control DMSO $P < 0.05$.

of all cell line spheroids and no regrowth 10 days after treatment (*Sdhb* knockdown and control cells; Fig. 10B and C). Since GSK3 inhibition may sensitize cancer cells to chemotherapy with gemcitabine, we tested the GSK3 inhibitor AR-A014418 in combination with gemcitabine. However, while AR-A014418 (20 µM) alone significantly decreased overall cell viability (−50%, n = 15), gemcitabine/AR-A014418 combination therapy showed antagonistic effects (−54%, n = 13).

Chemotherapeutic 5-FU 5-FU (20 µM) moderately decreased cell viability in the primary cultures (−27%, n = 21). Significantly higher efficacy was detected in cluster 1-related (−36%, n = 6), with the highest efficacy in *SDHB*-mutant (−40%, n = 3), compared to cluster 2-related tumors (−20%, n = 8). In *RET*-mutant tumors, 5-FU treatment even led to a promotion of tumor cell survival (+4%, n = 3).

HIF-2a inhibitors TC-S 7009 (20 µM, 40 µM, n = 17) and belzutifan (10 µM, 20 µM, n = 9) showed low overall efficacy in the primary cultures and no difference between both clusters (TC-S 7009: −8% (20 µM) and −19% (40 µM); belzutifan: −1% (10 µM) and −7% (20 µM)).

Somatostatin analog octreotide Octreotide has been approved for the therapy of metastatic NETs but data on PPGLs is still lacking. Octreotide (40 µM) showed no efficacy in the primary cultures (−2%, n = 19) and no difference between clusters, including patients 13 and 21 with high SSTR2 expression.

Others

Bisphosphonate zoledronic acid Zoledronic acid, which is regularly applied to PPGL patients with bone metastases, significantly decreased cell viability at clinically relevant

https://erc.bioscientifica.com
https://doi.org/10.1530/ERC-21-0355
© 2022 Society for Endocrinology
Published by Bioscientifica Ltd.
Printed in Great Britain

Downloaded from Bioscientifica.com at 05/11/2022 04:19:32PM
via Bodleian Library

Figure 6
Stratification depending on molecular clusters and malignancy. Patients with the same mutation are represented by the same color. Seventy-two-hour cell viability assay of the PI3K inhibitor alpelisib (n = 31) and the mTORC1 inhibitor everolimus (n = 31). Additive decrease of overall cell viability by alpelisib/everolimus combination therapy (n = 31) as well as in cluster 1-related (n = 9) and metastatic tumors (n = 7). Synergistic decrease of cell viability by alpelisib/everolimus combination therapy in cluster 2-related tumors (n = 13). Notably, the highest viability decrease was found in metastatic *SDHB*-mutant primary cultures 36, 37, and 48 (red frame). *Significant decrease of cell viability compared to control DMSO P < 0.05.

(5 µM) (−26%, n = 20) and higher doses (40 µM) (−45%, n = 18). At low doses, efficacy was significantly higher in cluster 2 (−32%, n = 8; cluster 1: −21%, n = 6), while high doses were slightly more effective in cluster 1 and metastatic PPGLs (−50%, n = 5 and −53%, n = 5; cluster 2: 46%, n = 8; Fig. 10D). The highest efficacy was found in *SDHB*-mutant PPGLs (−64%, n = 3). In MPC spheroids, we found an approximately 1.5-fold decrease of spheroid diameter 10 days after treatment with high-dose zoledronic acid and no regrowth, but no significant difference between *Sdhb* knockdown and control cells (Fig. 10E and F).

Estrogen In order to assess the reason for potential sex differences with regards to PPGL growth, we investigated estrogen in primary cultures. High-dose (10 µM) estradiol led to a significantly stronger cell viability reduction in cluster 2-related (−28%, n = 5), compared to cluster 1-related tumors (−16%, n = 4) and low-dose (1 µM) estradiol led to a slightly higher effect in cluster 2 (−12%, n = 5), compared to cluster 1 (−4%, n = 4).

Validation of primary culture data in MPC cells

In order to evaluate the effects of longer treatment times on tumor cell (re-)growth, we also performed MPC cell line experiments applying gemcitabine, cabozantinib/everolimus, alpelisib/trametinib, alpelisib/everolimus, and zoledronic acid with extended treatment times over 14 days (change of medium and drug treatment every 3 days; Supplementary Fig. 4). After long-term treatment (6, 10, and 14 days) with gemcitabine (30 µM), cabozantinib (5 µM), cabozantinib (5 µM)/everolimus (10 nM), alpelisib (5 µM), trametinib (1 µM), alpelisib (2.5 µM)/trametinib (1 µM), or alpelisib (5 µM)/everolimus (10 nM), almost no surviving MPC cells and no tumor cell regrowth were observed. For high-dose zoledronic acid (40 µM), there was also a strong significant cell viability reduction (to 15.5%)

https://erc.bioscientifica.com
https://doi.org/10.1530/ERC-21-0355
© 2022 Society for Endocrinology
Published by Bioscientifica Ltd.
Printed in Great Britain

Downloaded from Bioscientifica.com at 05/11/2022 04:19:32PM
via Bodleian Library

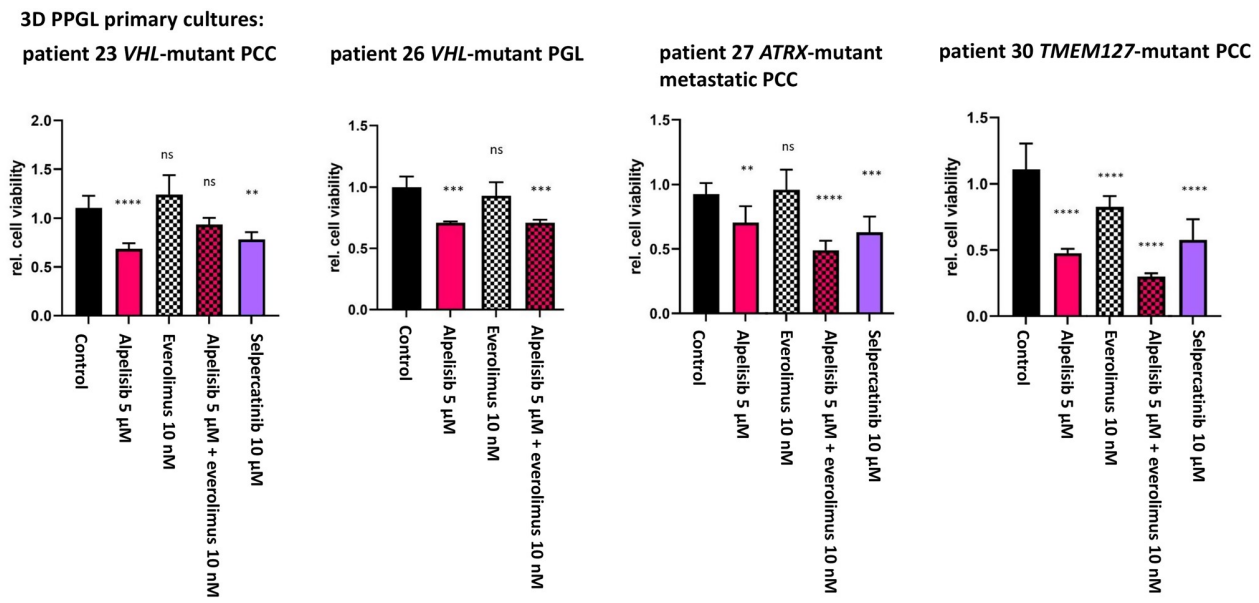

Figure 7

Three dimensional PPGL primary cultures (n = 4). Significant decrease of cell viability compared to the control was achieved by PI3K inhibitor alpelisib (n = 4) and RET inhibitor selpercatinib (n = 3) monotherapies, but mTORC1 inhibitor everolimus monotherapy significantly decreased cell viability in only 1/4 3D primary cultures (patient 30). Alpelisib/everolimus combination therapy led to a highly significant decrease of cell viability in 3/4 3D primary cultures – one cluster 1-related (*VHL*-mutant), one cluster 2-related (*TMEM127*-mutant), and one metastatic (*ATRX*-mutant). Significant decrease of cell viability compared to the untreated control: *$P \leq 0.05$, **$P \leq 0.01$, ***$P \leq 0.001$, ****$P \leq 0.0001$.

and no regrowth; however, there was no efficacy of low dose zoledronic acid (5 µM).

Discussion

There is a considerable clinical need for novel more optimal therapeutic strategies for metastatic PPGLs (Nölting *et al.* 2022). Given the lack of available human PPGL cell line models, we have established a method for multiple drug testing in patient-derived PPGL primary cultures (Fankhauser *et al.* 2019), which we have now expanded to a larger number of 33 PPGL primary cultures, including several metastatic tumors. This enables us for the first time to assess cluster-specific drug responsivities.

Consistent with other studies (Burnichon *et al.* 2011, Yao *et al.* 2011, 2016, Luchetti *et al.* 2015, Fishbein *et al.* 2017, Gieldon *et al.* 2019, Jiang *et al.* 2020), we could identify driver mutations in 79% of cases. Noradrenergic phenotypes correlated with cluster 1 mutations and adrenergic phenotypes with cluster 2 mutations, with only a few exceptions.

Kinase signaling inhibitors

Surprisingly, kinase signaling inhibitors – expected to be more effective in cluster 2-related tumors – showed similar efficacy in both clusters (sunitinib, everolimus, alpelisib, trametinib, and GSK3 inhibitor AR-A014418) or even stronger efficacy in cluster 1-related PPGLs (cabozantinib and selpercatinib).

We found strong efficacy of targeted combination treatments (cabozantinib/everolimus, alpelisib/everolimus, alpelisib/trametinib) in both clusters, with a slightly but significantly better responsivity of cluster 2 (cabozantinib/everolimus, alpelisib/trametinib), compared to cluster 1. Cabozantinib/everolimus was the most effective combination therapy with overall synergistic effects. Everolimus alone leads to development of resistance after less than one year in NET patients (Yao *et al.* 2011, 2016) – possibly amongst others through c-MET activation (Aristizabal Prada *et al.* 2018, Van den Bossche *et al.* 2020). The combination of everolimus with the c-MET inhibitor cabozantinib might therefore overcome everolimus resistance.

The second most effective combination alpelisib/trametinib showed overall synergistic effects, most likely due to an alpelisib-mediated attenuation of trametinib-induced AKT activation and simultaneous trametinib-mediated ERK inhibition. However, similar to everolimus/trametinib combination treatment (Tolcher *et al.* 2015), alpelisib/trametinib may lead to increased toxicity in patients through the inhibition of two essential signaling pathways.

https://erc.bioscientifica.com
https://doi.org/10.1530/ERC-21-0355
© 2022 Society for Endocrinology
Published by Bioscientifica Ltd.
Printed in Great Britain

Downloaded from Bioscientifica.com at 05/11/2022 04:19:32PM
via Bodleian Library

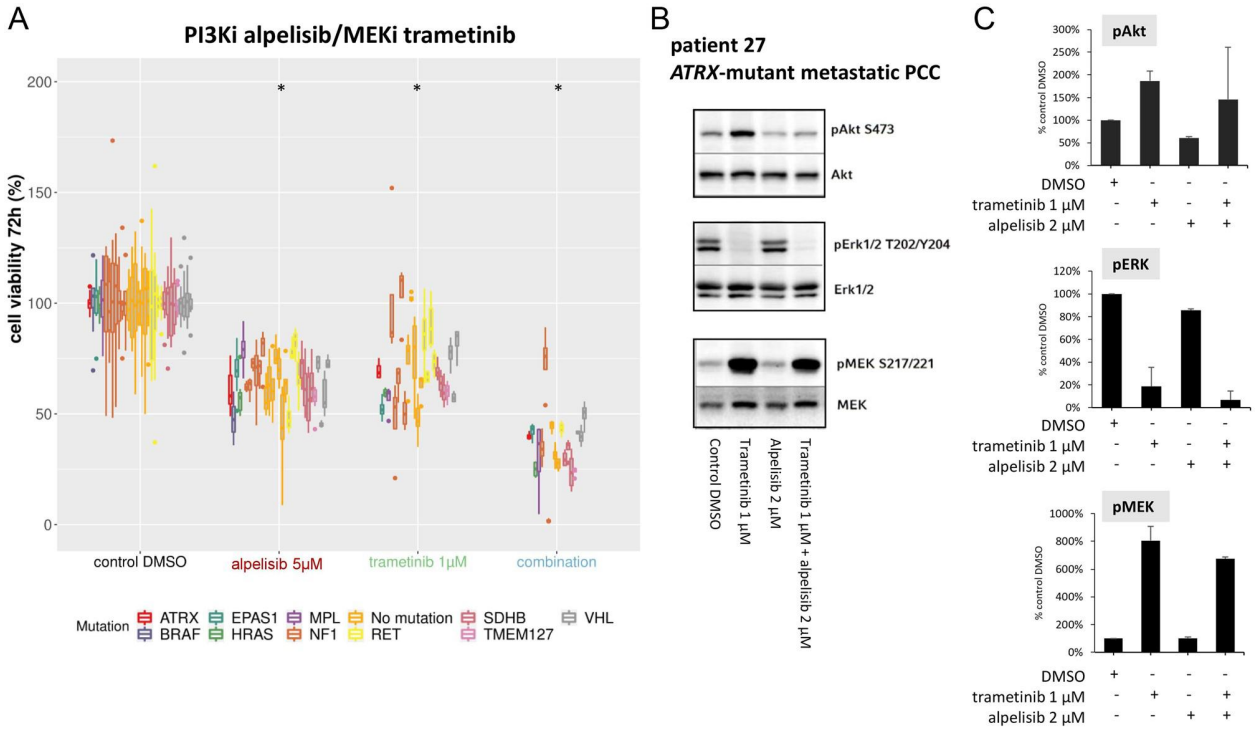

Figure 8

Seventy-two-hour cell viability assay, 24-h Western blot analysis and Western blot quantification after treatment with the PI3K inhibitor alpelisib and the MEK inhibitor trametinib. (A) Patients with the same mutation are represented by the same color. Significant decrease of cell viability by alpelisib (n = 31), trametinib (n = 25) and the combination of alpelisib and trametinib (n = 18) compared to control DMSO *P < 0.05. Alpelisib/trametinib combination showed an overall synergistic effect in clinically relevant doses. (B) Representative western blot of metastatic PCC patient 27: Alpelisib/trametinib combination therapy led to an attenuation of trametinib-induced AKT activation. Trametinib and the alpelisib/trametinib combination also inhibited ERK and strongly activated MEK. (C) Western blot quantification of phosphorylated AKT, ERK, and MEK of primary cultures tested with trametinib and alpelisib (n = 2).

Nevertheless, combination treatment with sunitinib and the mTORC1 inhibitor rapamycin was clinically well tolerated and effective at low doses (Ayala-Ramirez *et al.* 2012, Waqar *et al.* 2013). Consistent with our previously published data (Fankhauser *et al.* 2019, Helm *et al.* 2022), alpelisib/everolimus treatment showed strong efficacy with synergism in cluster 2 through dual inhibition of PI3K/AKT and mTORC1 pathways.

However, not all of the drugs/drug combinations targeting kinase signaling pathways were effective. While trametinib/dabrafenib combination therapy is approved for the treatment of *BRAF*-mutant melanoma and non-small cell lung cancer (Planchard *et al.* 2016, Long *et al.* 2017), it showed no beneficial effects in PPGL primary cultures. Dabrafenib alone even led to a promotion of tumor growth, possibly via a paradoxical ERK activation (Del Curatolo *et al.* 2018).

There are only a few published clinical studies on molecular-targeted therapies (sunitinib, cabozantinib, everolimus) in PPGLs, with none of them distinguishing between the different molecular clusters. For sunitinib, a prospective clinical trial in PPGLs (n = 25) reported a response rate of 13% and a disease control rate (DCR) of 83% over 3 months (DCR 61% over 6 months); all patients with *SDHx*-related disease showed a partial response or stable disease (O'Kane *et al.* 2019). One retrospective clinical trial (n = 17) described a partial response to sunitinib in 21% and a DCR of 57% over 6 months; 62.5% (5/8) of cases with stable disease or partial response were *SDHB* mutation carriers (Ayala-Ramirez *et al.* 2012). The results of the first randomized placebo-controlled clinical trial (FIRST-MAPPP) (n = 78) were recently presented at the ESMO conference and suggested that sunitinib is significantly superior to placebo (Baudin *et al.* 2021). Whether patients with *SDHB*-mutant tumors are the best candidates for sunitinib, as suggested by a small number of *SDHB*-related PPGL primary cultures (n = 3), is not yet known from the FIRST-MAPPP study but was also indicated by the above-mentioned small series.

For cabozantinib, an abstract of the preliminary results of a prospective clinical trial (n = 10) demonstrated a DCR of 90% (all minor or partial response) over 3 months (DCR 70% over 6 months, DCR 30% over 12 months) (PFS 11.1

https://erc.bioscientifica.com
https://doi.org/10.1530/ERC-21-0355
© 2022 Society for Endocrinology
Published by Bioscientifica Ltd.
Printed in Great Britain

Downloaded from Bioscientifica.com at 05/11/2022 04:19:32PM
via Bodleian Library

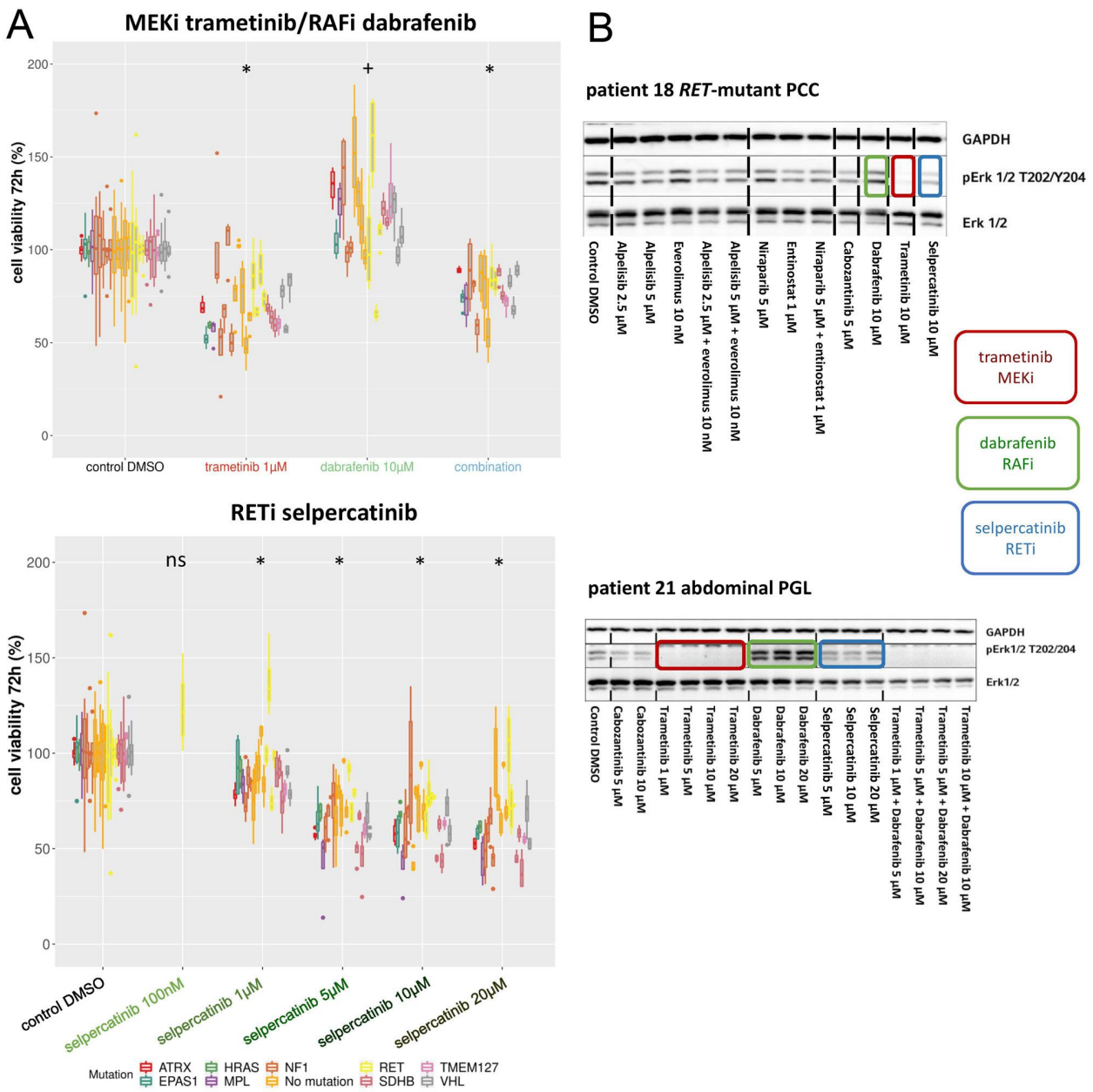

Figure 9

Seventy-two-hour cell viability assays and 24-h Western blots of the RAF inhibitor dabrafenib, the MEK inhibitor trametinib and the RET inhibitor selpercatinib. (A) Patients with the same mutation are represented by the same color. Dabrafenib in combination with trametinib had opposite effects on cell viability (n = 17): While trametinib significantly decreased cell viability (n = 25), dabrafenib significantly promoted PPGL primary culture survival (n = 20). Selpercatinib also significantly decreased cell viability in concentrations of 120 µM (n = 22). *Significant decrease of cell viability compared to control DMSO $P < 0.05$, +significant increase of cell viability compared to control DMSO $P < 0.05$. (B) Representative Western blots of PCC patient 18 and abdominal PGL patient 21: While trametinib strongly inhibited ERK and effectively decreased tumor cell survival, dabrafenib induced paradoxical ERK activations in most PPGL primary cultures which may explain its lack of efficacy and its beneficial effect on tumor survival. Selpercatinib inhibited ERK in the primary culture of patient 18 with a high-risk *RET* mutation but not in the primary culture of patient 21.

© 2022 Society for Endocrinology
Published by Bioscientifica Ltd.
Printed in Great Britain

Downloaded from Bioscientifica.com at 05/11/2022 04:19:32PM
via Bodleian Library

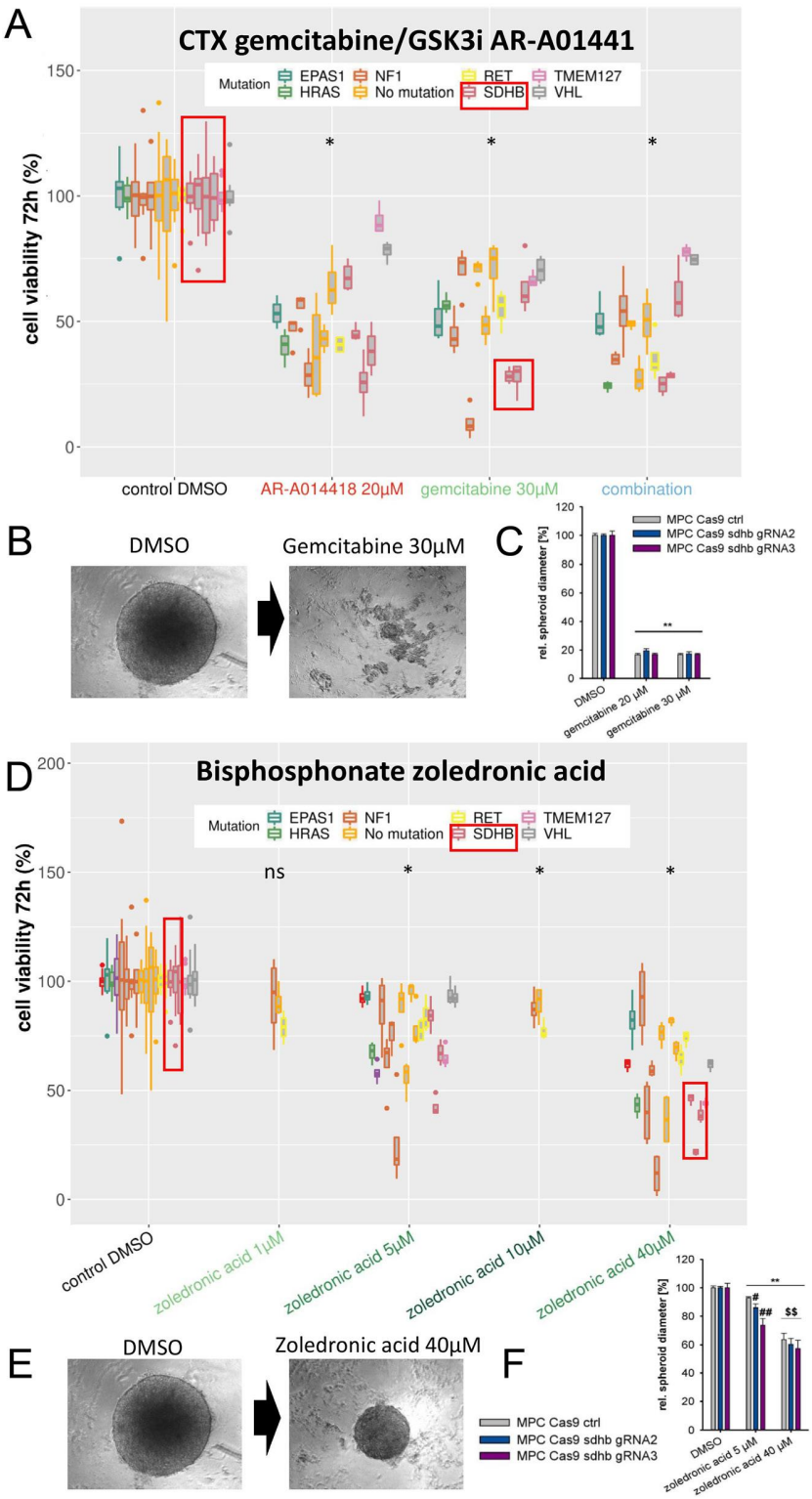

Figure 10

The chemotherapeutic agent (CTX) gemcitabine alone and in combination with the GSK3 inhibitor AR-A014418, and the antiresorptive agent zoledronic acid: 72-h cell viability assays. Patients with the same mutation are represented by the same color. (A) The combination of AR-A01441 and gemcitabine showed antagonistic effects in the PPGL primary cultures (n = 13). Clinically relevant doses of gemcitabine significantly decreased cell viability in all PPGL primary cultures tested (n = 14) but particularly in the metastatic *SDHB*-mutant primary cultures 36 and 37 (red frame). *Significant decrease of cell viability compared to control DMSO $P < 0.05$. (B) Single treatment with gemcitabine significantly diminished the growth of MPC *Sdhb* knockdown spheroids compared to the DMSO control. (C) Gemcitabine showed high efficacy to reduce the diameter of MPC *Sdhb* knockdown spheroids at both concentrations tested. Mean ± s.e.m. ANOVA and Bonferroni *post hoc* test comparison vs DMSO control $^{**}P < 0.01$. (D) Zoledronic acid also significantly decreased cell viability at concentrations of 5–40 µM (n = 18–20) and especially in the *SDHB*-mutant primary cultures of patients 36, 37, and 47 (red frame). *Significant decrease of cell viability compared to control DMSO $P < 0.05$. (E) Single treatment with zoledronic acid significantly reduced the diameter of MPC *Sdhb* knockdown spheroids compared to the DMSO control. (F) Zoledronic acid showed increased efficacy to reduce diameter of MPC *Sdhb* knockdown spheroids compared with MPC Cas9 crtl spheroids. Mean ± s.e.m. ANOVA and Bonferroni *post hoc* test comparison vs DMSO control $^{*}P < 0.05$, $^{**}P < 0.01$, vs MPC Cas9 ctrl $^{\#}P < 0.05$, $^{\#\#}P < 0.01$, vs zoledronic acid 5 µM $^{\$}P < 0.05$, $^{\$\$}P < 0.01$.

https://erc.bioscientifica.com
https://doi.org/10.1530/ERC-21-0355
© 2022 Society for Endocrinology
Published by Bioscientifica Ltd.
Printed in Great Britain

Downloaded from Bioscientifica.com at 05/11/2022 04:19:32PM
via Bodleian Library

months). All *SDHB*-mutant patients ($n = 5$) showed minor/partial responses (Jimenez *et al.* 2017). This is consistent with the primary culture data with better responsivity to cabozantinib (viability reduction by 39%) compared to sunitinib (viability reduction by 15%), and significantly stronger responsivity of cluster 1-related, compared to cluster 2-related tumors, with the best responsivity in *SDHB*-related tumors. It is worth mentioning that the anti-angiogenic properties of sunitinib and cabozantinib are part of their efficacy *in vivo* but clearly cannot be investigated in our primary culture model.

The low to moderate responsivity of human primary cultures (viability reduction by 28%) to everolimus seems somewhat more promising, compared to response rates of 0% published in one prospective and one retrospective study ($n = 7$, DCR 71% and $n = 4$, DCR 25%, respectively) (Druce *et al.* 2009, Oh *et al.* 2012).

The selective RET inhibitor selpercatinib has shown promising effects in a phase I/II clinical study in *RET*-mutant medullary thyroid carcinoma (LIBRETTO-001, NCT03157128 (Wirth *et al.* 2020)). Interestingly, selpercatinib showed poor efficacy in *RET*-related PPGL primary cultures and even significantly stronger efficacy in cluster 1 than in cluster 2. Since the sub-groups of tumor samples with the same mutation only contain small numbers (Table 2), there are not enough data to draw a valid conclusion for each specific mutation. For instance, we only treated three tumors with *RET* mutations with selpercatinib, one of which was a VUS of *RET*. Therefore, our data are not strong enough to interrogate the selective efficacy of selpercatinib. Additionally, it is important to mention that in a clinical setting, the efficacy of a drug represents growth inhibition as well as tumor cell death. However, in our primary culture model, neither pure growth inhibition, due to low PPGL cell growth rates and short treatment intervals (72 h), nor microenvironmental effects, including vascularization (see above), are assessable.

Chemotherapeutics, HIF-2a inhibitors, and other drugs

Apart from AR-A014418 (see above), which is not yet in clinical use, gemcitabine and high-dose zoledronic acid were the most effective single agents in both clusters, with the best responsivity of cluster 1 *SDHB*-related tumors. 5-FU, with significantly stronger efficacy in cluster 1, may also be an interesting therapy option for cluster 1 tumors.

The literature on chemotherapeutic treatment of PPGL other than CVD is still scarce. Consistent with our data, case reports of metastatic PPGL patients treated with gemcitabine (Pipas & Krywicki 2000, Mora *et al.* 2009, Costello *et al.* 2014) and 5-FU (Bukowski & Vidt 1984, Srimuninnimit & Wampler 1991) showed good therapy responses.

The good responsivity of the primary cultures to zoledronic acid, clinically used for the treatment of bone metastases, is consistent with a significant cancer risk reduction to 67% in osteopenic postmenopausal women treated with zoledronic acid, compared to placebo (Reid *et al.* 2020) and a reported inhibition of cancer cell proliferation by zoledronic acid (Wang *et al.* 2020).

Poorly effective agents in PPGL primary cultures included temozolomide, HIF-2a inhibitors, octreotide, and estrogen (moderate efficacy only at supraphysiological doses). As mentioned above, drug responsivity of PPGL primary cultures rather represents tumor cell death (partial response *in vivo*), but this neither measures disease stabilization, an important parameter of drug efficacy *in vivo*, nor the effects on the microenvironment. This may result in discrepancies between the primary culture and *in vivo* data.

In contrast to the primary culture data, a retrospective study investigating temozolomide treatment in 15 PPGL patients showed a high DCR of 80% (Hadoux *et al.* 2014). However, indirect antitumoral effects of temozolomide on the immune system (Di Ianni *et al.* 2021) or the gut microbiota (Li *et al.* 2021) have been discussed in glioblastoma patients/glioma cells, which are not reflected in our model. It has been shown that temozolomide in combination with PARP inhibitors may be a novel therapeutic approach in *SDHB*-mutant PPGLs (Pang *et al.* 2018). A clinical phase II study on PARP inhibitor olaparib plus temozolomide (NCT04394858) is recruiting. We confirmed a synergistic effect of the PARP inhibitor niraparib together with temozolomide in the primary cultures with highest efficacy in *SDHB*-related tumors.

With regards to HIF-2a inhibitors, a phase II study on *VHL*-associated renal cell carcinoma (RCC) treated with HIF-2a inhibitor belzutifan has shown promising preliminary results (Jonasch *et al.* 2021) resulting in FDA approval of belzutifan in patients with *VHL*-related disease (Deeks 2021). A clinical phase II trial on advanced PPGLs and pancreatic NETs (MK-6482-015, NCT04924075) is ongoing. However, consistent with our data, other preclinical studies have shown a lack of efficacy of HIF-2a inhibitors in *HIF2A*-related PPGLs (Bechmann *et al.* 2020) and *VHL*-mutant RCC cell lines due to the appearance of resistance (Courtney *et al.* 2020, Bechmann & Eisenhofer 2021).

While the somatostatin analogs octreotide and lanreotide are well established growth inhibitory agents

t hpspph / doi .rhg/ 1h053/ d1o5/ E7 Rr
Published by Bioscientifica Ltd.
Printed in Great Britain

Downloaded from Bioscientifica.com at 05/11/2022 04:19:32PM
via Bodleian Library

in the treatment algorithms of NET patients (Pavel *et al.* 2020, Rinke *et al.* 2021), the preclinical *in vitro* data could not demonstrate significant growth inhibition in NET cells (Exner *et al.* 2018, Herrera-Martinez *et al.* 2019). Similarly, we observed no significant effect of octreotide on PPGL primary cultures. However, strong SSTR2 expression in the molecular analysis of some primary cultures indicates the potential importance of SSTR2-guided treatment depending on SSTR2 expression. Only a few case reports of somatostatin analogs in PPGL patients have been published (Tonyukuk *et al.* 2003, van Hulsteijn *et al.* 2013, Tena *et al.* 2018, Jha *et al.* 2020) and data are still lacking (Patel *et al.* 2021), but one phase II study investigating lanreotide in PPGL patients is currently recruiting (LAMPARA, NCT03946527).

The modest cell viability reductions in primary cultures observed during incubation with estrogen might contribute to gender-specific effects since female sex has been demonstrated to be a positive prognostic predictor in metastatic PPGL (Zheng *et al.* 2021).

The most important limitations of our primary culture model, such as the absent representation of the microenvironment and growth inhibition (disease stabilization), may be overcome by 3D organoid models but only *in vivo* models will also allow evaluation of drug toxicity.

Conclusions

We have identified several effective drugs and especially synergistic drug combinations following evaluation in human PPGL primary cultures. Interestingly, we only found minor differences in drug efficacy between cluster 1- and cluster 2-related tumors. Higher efficacy of some single anti-cancer agents (cabozantinib, selpercatinib, 5-FU) was shown in the more aggressive cluster 1-related, including *SDHB*-related, tumors. This may be due to the more aggressive behavior and more rapid cell growth of these tumors, making the cells more prone to drug interventions. Some targeted combination treatments and the re-purposed agents low-dose zoledronic acid and high-dose estrogen were more effective in cluster 2. We are aware that the human primary culture data may not be directly transferrable to drug responsivity *in vivo*, but studies are now needed to correlate and compare *in vitro* and *in vivo* data.

Supplementary materials

This is linked to the online version of the paper at https://doi.org/10.1530/ERC-21-0355.

Declaration of interest

The authors declare that there is no conflict of interest that could be perceived as prejudicing the impartiality of the research reported.

Funding

This work was supported by the German Research Foundation [Deutsche Forschungsgemeinschaft (DFG)] within the CRC/Transregio 205/2, Project number: 314061271 – TRR 205 'The Adrenal: Central Relay in Health and Disease' (to N B, S R, C G Z, J P, S R B, M K, M F, M R, G E, F B, N P, and S N). This work also received support of the Heuberg Foundation, Zurich, Switzerland (Working Title: 'Novel multidimensional models for the adrenal gland and adrenal tumors') to C H and S R B and a grant from Hochschulmedizin Zürich: Immunotherapies Targeting Endocrine Tumors (Immuno-TargET) to F B and A W.

References

Alzofon N, Koc K, Panwell K, Pozdeyev N, Marshall CB, Albuja-Cruz M, Raeburn CD, Nathanson KL, Cohen DL, Wierman ME, *et al.* 2021 Mastermind like transcriptional coactivator 3 (MAML3) drives neuroendocrine tumor progression. *Molecular Cancer Research* 1476–1485. (https://doi.org/10.1158/1541-7786.MCR-20-0992)

April-Monn SL, Wiedmer T, Skowronska M, Maire R, Schiavo Lena M, Trippel M, Di Domenico A, Muffatti F, Andreasi V, Capurso G, *et al.* 2021 Three-dimensional primary cell culture: a novel preclinical model for pancreatic neuroendocrine tumors. *Neuroendocrinology* 273–287. (https://doi.org/10.1159/000507669)

Aristizabal Prada ET, Spottl G, Maurer J, Lauseker M, Koziolek EJ, Schrader J, Grossman A, Pacak K, Beuschlein F, Auernhammer CJ, *et al.* 2018 The role of GSK3 and its reversal with GSK3 antagonism in everolimus resistance. *Endocrine-Related Cancer* 893–908. (https://doi.org/10.1530/ERC-18-0159)

Ayala-Ramirez M, Chougnet CN, Habra MA, Palmer JL, Leboulleux S, Cabanillas ME, Caramella C, Anderson P, Al Ghuzlan A, Waguespack SG, *et al.* 2012 Treatment with sunitinib for patients with progressive metastatic pheochromocytomas and sympathetic paragangliomas. *Journal of Clinical Endocrinology and Metabolism* 4040–4050. (https://doi.org/10.1210/jc.2012-2356)

Baudin E, Goichot B, Berruti A, Hadoux J, Moalla S, Laboureau S, Noelting S, Fouchardière CDL, Kienitz T, Deutschbein T, *et al.* 2021 First International Randomized Study in malignant progressive pheochromocytoma and paragangliomas (FIRSTMAPPP): an academic double-blind trial investigating sunitinib. *Annals of Oncology* S621–S625. doi:10.1016/annonc/annonc700.

Bayley JP & Devilee P 2020 Advances in paraganglioma-pheochromocytoma cell lines and xenografts. *Endocrine-Related Cancer* R433–R450. (https://doi.org/10.1530/ERC-19-0434)

Bechmann N & Eisenhofer G 2021 Hypoxia-inducible factor 2alpha: a key player in tumorigenesis and metastasis of pheochromocytoma and paraganglioma? *Experimental and Clinical Endocrinology and Diabetes* [epub]. (https://doi.org/10.1055/a-1526-5263)

Bechmann N, Ehrlich H, Eisenhofer G, Ehrlich A, Meschke S, Ziegler CG & Bornstein SR 2018 Anti-tumorigenic and anti-metastatic activity of the sponge-derived marine drugs aeroplysinin-1 and isofistularin-3 against pheochromocytoma in vitro. *Marine Drugs* 172. (https://doi.org/10.3390/md16050172)

Bechmann N, Poser I, Seifert V, Greunke C, Ullrich M, Qin N, Walch A, Peitzsch M, Robledo M, Pacak K, *et al.* 2019 Impact of extrinsic and intrinsic hypoxia on catecholamine biosynthesis in absence or presence of Hif2alpha in pheochromocytoma cells. *Cancers* 594. (https://doi.org/10.3390/cancers11050594)

© 2022 Society for Endocrinology
Published by Bioscientifica Ltd.
Printed in Great Britain

Downloaded from Bioscientifica.com at 05/11/2022 04:19:32PM
via Bodleian Library

Bechmann N, Moskopp ML, Ullrich M, Calsina B, Wallace PW, Richter S, Friedemann M, Langton K, Fliedner SMJ, Timmers HJLM, *et al.* 2020 HIF2alpha supports pro-metastatic behavior in pheochromocytomas/paragangliomas. *Endocrine-Related Cancer* **27** 625–640. (https://doi.org/10.1530/ERC-20-0205)

Bukowski RM & Vidt DG 1984 Chemotherapy trials in malignant pheochromocytoma: report of two patients and review of the literature. *Journal of Surgical Oncology* **27** 89–92. (https://doi.org/10.1002/jso.2930270207)

Burnichon N, Vescovo L, Amar L, Libé R, De Reynies A, Venisse A, Jouanno E, Laurendeau I, Parfait B, Bertherat J, *et al.* 2011 Integrative genomic analysis reveals somatic mutations in pheochromocytoma and paraganglioma. *Human Molecular Genetics* **20** 3974–3985. (https://doi.org/10.1093/hmg/ddr324)

Costello BA, Borad MJ, Qi Y, Kim GP, Northfelt DW, Erlichman C & Alberts SR 2014 Phase I trial of everolimus, gemcitabine and cisplatin in patients with solid tumors. *Investigational New Drugs* **32** 710–716. (https://doi.org/10.1007/s10637-014-0096-3)

Courtney KD, Ma Y, Diaz De Leon A, Christie A, Xie Z, Woolford L, Singla N, Joyce A, Hill H, Madhuranthakam AJ, *et al.* 2020 HIF-2 complex dissociation, target inhibition, and acquired resistance with PT2385, a first-in-class HIF-2 inhibitor, in patients with clear cell renal cell carcinoma. *Clinical Cancer Research* **26** 793–803. (https://doi.org/10.1158/1078-0432.CCR-19-1459)

Crona J, Lamarca A, Ghosal S, Welin S, Skogseid B & Pacak K 2019 Genotype-phenotype correlations in pheochromocytoma and paraganglioma: a systematic review and individual patient meta-analysis. *Endocrine-Related Cancer* **26** 539–550. (https://doi.org/10.1530/ERC-19-0024)

Deeks ED 2021 Belzutifan: first approval. *Drugs* **81** 1921–1927. (https://doi.org/10.1007/s40265-021-01606-x)

Del Curatolo A, Conciatori F, Cesta Incani U, Bazzichetto C, Falcone I, Corbo V, D'Agosto S, Eramo A, Sette G, Sperduti I, *et al.* 2018 Therapeutic potential of combined BRAF/MEK blockade in BRAF-wild type preclinical tumor models. *Journal of Experimental and Clinical Cancer Research* **37** 140. (https://doi.org/10.1186/s13046-018-0820-5)

Di Ianni N, Maffezzini M, Eoli M & Pellegatta S 2021 Revisiting the immunological aspects of temozolomide considering the genetic landscape and the immune microenvironment composition of glioblastoma. *Frontiers in Oncology* **11** 747690. (https://doi.org/10.3389/fonc.2021.747690)

Druce MR, Kaltsas GA, Fraenkel M, Gross DJ & Grossman AB 2009 Novel and evolving therapies in the treatment of malignant phaeochromocytoma: experience with the mTOR inhibitor everolimus (RAD001). *Hormone and Metabolic Research* **41** 697–702. (https://doi.org/10.1055/s-0029-1220687)

Eisenhofer G, Lenders JW, Siegert G, Bornstein SR, Friberg P, Milosevic D, Mannelli M, Linehan WM, Adams K, Timmers HJ, *et al.* 2012 Plasma methoxytyramine: a novel biomarker of metastatic pheochromocytoma and paraganglioma in relation to established risk factors of tumour size, location and SDHB mutation status. *European Journal of Cancer* **48** 1739–1749. (https://doi.org/10.1016/j.ejca.2011.07.016)

Exner S, Prasad V, Wiedenmann B & Grotzinger C 2018 Octreotide does not inhibit proliferation in five neuroendocrine tumor cell lines. *Frontiers in Endocrinology* **9** 146. (https://doi.org/10.3389/fendo.2018.00146)

Fankhauser M, Bechmann N, Lauseker M, Goncalves J, Favier J, Klink B, William D, Gieldon L, Maurer J, Spottl G, *et al.* 2019 Synergistic highly potent targeted drug combinations in different pheochromocytoma models including human tumor cultures. *Endocrinology* **160** 2600–2617. (https://doi.org/10.1210/en.2019-00410)

Fassnacht M, Assie G, Baudin E, Eisenhofer G, De La Fouchardiere C, Haak HR, De Krijger R, Porpiglia F, Terzolo M, Berruti A, *et al.* 2020 Adrenocortical carcinomas and malignant phaeochromocytomas: ESMO-EURACAN Clinical Practice Guidelines for diagnosis, treatment and follow-up. *Annals of Oncology* **31** 1476–1490. (https://doi.org/10.1016/j.annonc.2020.08.2099)

Fishbein L, Leshchiner I, Walter V, Danilova L, Robertson AG, Johnson AR, Lichtenberg TM, Murray BA, Ghayee HK, Else T, *et al.* 2017 Comprehensive molecular characterization of pheochromocytoma and paraganglioma. *Cancer Cell* **31** 181–193. (https://doi.org/10.1016/j.ccell.2017.01.001)

Gieldon L, William D, Hackmann K, Jahn W, Jahn A, Wagner J, Rump A, Bechmann N, Nolting S, Knosel T, *et al.* 2019 Optimizing genetic workup in pheochromocytoma and paraganglioma by integrating diagnostic and research approaches. *Cancers* **11** 809. (https://doi.org/10.3390/cancers11060809)

Goldstein RE, O'Neill Jr JA, Holcomb 3rd GW, Morgan 3rd WM, Neblett 3rd WW, Oates JA, Brown N, Nadeau J, Smith B, Page DL, *et al.* 1999 Clinical experience over 48 years with pheochromocytoma. *Annals of Surgery* **229** 755–764; discussion 764–766. (https://doi.org/10.1097/00000658-199906000-00001)

Hadoux J, Favier J, Scoazec JY, Leboulleux S, Al Ghuzlan A, Caramella C, Deandreis D, Borget I, Loriot C, Chougnet C, *et al.* 2014 SDHB mutations are associated with response to temozolomide in patients with metastatic pheochromocytoma or paraganglioma. *International Journal of Cancer* **135** 2711–2720. (https://doi.org/10.1002/ijc.28913)

Hamidi O, Young Jr WF, Gruber L, Smestad J, Yan Q, Ponce OJ, Prokop L, Murad MH & Bancos I 2017 Outcomes of patients with metastatic phaeochromocytoma and paraganglioma: a systematic review and meta-analysis. *Clinical Endocrinology* **87** 440–450. (https://doi.org/10.1111/cen.13434)

Hart T, Chandrashekhar M, Aregger M, Steinhart Z, Brown KR, Macleod G, Mis M, Zimmermann M, Fradet-Turcotte A, Sun S, *et al.* 2015 High-resolution CRISPR screens reveal fitness genes and genotype-specific cancer liabilities. *Cell* **163** 1515–1526. (https://doi.org/10.1016/j.cell.2015.11.015)

Helm J, Drukewitz S, Poser I, Richter S, Friedemann M, William D, Mohr H, Nölting S, Robledo M, Bornstein SR, *et al.* 2022 Treatment of pheochromocytoma cells with recurrent cycles of hypoxia: a new pseudohypoxic in vitro model. *Cells* **11** 560. (https://doi.org/10.3390/cells11030560)

Herrera-Martinez AD, Van Den Dungen R, Dogan-Oruc F, Van Koetsveld PM, Culler MD, De Herder WW, Luque RM, Feelders RA & Hofland LJ 2019 Effects of novel somatostatin-dopamine chimeric drugs in 2D and 3D cell culture models of neuroendocrine tumors. *Endocrine-Related Cancer* **26** 585–599. (https://doi.org/10.1530/ERC-19-0086)

Hescot S, Curras-Freixes M, Deutschbein T, Van Berkel A, Vezzosi D, Amar L, De La Fouchardiere C, Valdes N, Riccardi F, Do Cao C, *et al.* 2019 Prognosis of malignant pheochromocytoma and paraganglioma (MAPP-Prono study): a European network for the study of adrenal tumors retrospective study. *Journal of Clinical Endocrinology and Metabolism* **104** 2367–2374. (https://doi.org/10.1210/jc.2018-01968)

Jha A, Patel M, Baker E, Gonzales MK, Ling A, Millo C, Knue M, Civelek AC & Pacak K 2020 Role of 68Ga-DOTATATE PET/CT in a case of SDHB-related pterygopalatine fossa paraganglioma successfully controlled with octreotide. *Nuclear Medicine and Molecular Imaging* **54** 48–52. (https://doi.org/10.1007/s13139-019-00629-3)

Jiang J, Zhang J, Pang Y, Bechmann N, Li M, Monteagudo M, Calsina B, Gimenez-Roqueplo AP, Nolting S, Beuschlein F, *et al.* 2020 Sino-European differences in the genetic landscape and clinical presentation of pheochromocytoma and paraganglioma. *Journal of Clinical Endocrinology and Metabolism* **105** dgaa502. (https://doi.org/10.1210/clinem/dgaa502)

Jimenez C, Busaidy N, Habra M, Waguespack S & Jessop A 2017 A phase 2 study to evaluate the effects of cabozantinib in patients with unresectable metastatic pheochromocytomas and paragangliomas.

t hpsp ph / doi .rhg/ 1h053/ d1o5/ E/ Rr
Published by Bioscientifica Ltd.
Printed in Great Britain

Downloaded from Bioscientifica.com at 05/11/2022 04:19:32PM
via Bodleian Library

In *International Symposium on Pheochromocytoma and Paraganglioma Sydey, Australia*.

Jin XF, Spoettl G, Maurer J, Nolting S & Auernhammer CJ 2020 Inhibition of Wnt/beta-catenin signaling in neuroendocrine tumors in vitro: antitumoral effects. *Cancers* **12** 345. (https://doi.org/10.3390/cancers12020345)

John H, Ziegler WH, Hauri D & Jaeger P 1999 Pheochromocytomas: can malignant potential be predicted? *Urology* **53** 679–683. (https://doi.org/10.1016/s0090-4295(98)00612-8)

Jonasch E, Donskov F, Iliopoulos O, Rathmell WK, Narayan VK, Maughan BL, Oudard S, Else T, Maranchie JK, Welsh SJ, *et al.* 2021 Belzutifan for renal cell carcinoma in von Hippel-Lindau disease. *New England Journal of Medicine* **385** 2036–2046. (https://doi.org/10.1056/NEJMoa2103425)

Keith B, Johnson RS & Simon MC 2011 HIF1alpha and HIF2alpha: sibling rivalry in hypoxic tumour growth and progression. *Nature Reviews: Cancer* **12** 9–22. (https://doi.org/10.1038/nrc3183)

Lam AK 2017 Update on adrenal tumours in 2017 World Health Organization (WHO) of endocrine tumours. *Endocrine Pathology* **28** 213–227. (https://doi.org/10.1007/s12022-017-9484-5)

Lenders JWM, Kerstens MN, Amar L, Prejbisz A, Robledo M, Taieb D, Pacak K, Crona J, Zelinka T, Mannelli M, *et al.* 2020 Genetics, diagnosis, management and future directions of research of phaeochromocytoma and paraganglioma: a position statement and consensus of the working group on endocrine hypertension of the European Society of Hypertension. *Journal of Hypertension* **38** 1443–1456. (https://doi.org/10.1097/HJH.0000000000002438)

Li XC, Wu BS, Jiang Y, Li J, Wang ZF, Ma C, Li YR, Yao J, Jin XQ & Li ZQ 2021 Temozolomide-induced changes in gut microbial composition in a mouse model of brain glioma. *Drug Design, Development and Therapy* **15** 1641–1652. (https://doi.org/10.2147/DDDT.S298261)

Long GV, Hauschild A, Santinami M, Atkinson V, Mandala M, Chiarion-Sileni V, Larkin J, Nyakas M, Dutriaux C, Haydon A, *et al.* 2017 Adjuvant dabrafenib plus trametinib in stage III BRAF-mutated melanoma. *New England Journal of Medicine* **377** 1813–1823. (https://doi.org/10.1056/NEJMoa1708539)

Luchetti A, Walsh D, Rodger F, Clark G, Martin T, Irving R, Sanna M, Yao M, Robledo M, Neumann HP, *et al.* 2015 Profiling of somatic mutations in phaeochromocytoma and paraganglioma by targeted next generation sequencing analysis. *International Journal of Endocrinology* **2015** 138573. (https://doi.org/10.1155/2015/138573)

Mannelli M, Ianni L, Cilotti A & Conti A 1999 Pheochromocytoma in Italy: a multicentric retrospective study. *European Journal of Endocrinology* **141** 619–624. (https://doi.org/10.1530/eje.0.1410619)

Mora J, Cruz O, Parareda A, Sola T & De Torres C 2009 Treatment of disseminated paraganglioma with gemcitabine and docetaxel. *Pediatric Blood and Cancer* **53** 663–665. (https://doi.org/10.1002/pbc.22006)

Nölting S, Ullrich M, Pietzsch J, Ziegler CG, Eisenhofer G, Grossman A & Pacak K 2019 Current management of pheochromocytoma/paraganglioma: a guide for the practicing clinician in the era of precision medicine. *Cancers* **11** 1505. (https://doi.org/10.3390/cancers11101505)

Nölting S, Bechmann N, Taieb D, Beuschlein F, Fassnacht M, Kroiss M, Eisenhofer G, Grossman A & Pacak K 2022 Personalized management of pheochromocytoma and paraganglioma. *Endocrine Reviews* **43** 199–239. (https://doi.org/10.1210/endrev/bnab019)

Oh DY, Kim TW, Park YS, Shin SJ, Shin SH, Song EK, Lee HJ, Lee KW & Bang YJ 2012 Phase 2 study of everolimus monotherapy in patients with nonfunctioning neuroendocrine tumors or pheochromocytomas/paragangliomas. *Cancer* **118** 6162–6170. (https://doi.org/10.1002/cncr.27675)

O'Kane GM, Ezzat S, Joshua AM, Bourdeau I, Leibowitz-Amit R, Olney HJ, Krzyzanowska M, Reuther D, Chin S, Wang L, *et al.* 2019 A phase 2 trial of sunitinib in patients with progressive paraganglioma or pheochromocytoma: the SNIPP trial. *British Journal of Cancer* **120** 1113–1119. (https://doi.org/10.1038/s41416-019-0474-x)

Pang Y, Lu Y, Caisova V, Liu Y, Bullova P, Huynh TT, Zhou Y, Yu D, Frysak Z, Hartmann I, *et al.* 2018 Targeting NAD(+)/PARP DNA repair pathway as a novel therapeutic approach to SDHB-mutated cluster I pheochromocytoma and paraganglioma. *Clinical Cancer Research* **24** 3423–3432. (https://doi.org/10.1158/1078-0432.CCR-17-3406)

Patel M, Tena I, Jha A, Taieb D & Pacak K 2021 Somatostatin receptors and analogs in pheochromocytoma and paraganglioma: old players in a new precision medicine world. *Frontiers in Endocrinology* **12** 625312. (https://doi.org/10.3389/fendo.2021.625312)

Pavel M, Oberg K, Falconi M, Krenning EP, Sundin A, Perren A, Berruti A & ESMO Guidelines Committee. Electronic address: clinicalguidelines@esmo.org 2020 Gastroenteropancreatic neuroendocrine neoplasms: ESMO Clinical Practice Guidelines for diagnosis, treatment and follow-up. *Annals of Oncology* **31** 844–860. (https://doi.org/10.1016/j.annonc.2020.03.304)

Pham H, Kearns NA & Maehr R 2016 Transcriptional regulation with CRISPR/Cas9 effectors in mammalian cells. *Methods in Molecular Biology* **1358** 43–57. (https://doi.org/10.1007/978-1-4939-3067-8_3)

Pipas JM & Krywicki RF 2000 Treatment of progressive metastatic glomus jugulare tumor (paraganglioma) with gemcitabine. *Neuro-Oncology* **2** 190–191. (https://doi.org/10.1093/neuonc/2.3.190)

Planchard D, Kim TM, Mazieres J, Quoix E, Riely G, Barlesi F, Souquet PJ, Smit EF, Groen HJ, Kelly RJ, *et al.* 2016 Dabrafenib in patients with BRAF(V600E)-positive advanced non-small-cell lung cancer: a single-arm, multicentre, open-label, phase 2 trial. *Lancet: Oncology* **17** 642–650. (https://doi.org/10.1016/S1470-2045(16)00077-2)

Reid IR, Horne AM, Mihov B, Stewart A, Garratt E, Bastin S & Gamble GD 2020 Effects of zoledronate on cancer, cardiac events, and mortality in osteopenic older women. *Journal of Bone and Mineral Research* **35** 20–27. (https://doi.org/10.1002/jbmr.3860)

Richards S, Aziz N, Bale S, Bick D, Das S, Gastier-Foster J, Grody WW, Hegde M, Lyon E, Spector E, *et al.* 2015 Standards and guidelines for the interpretation of sequence variants: a joint consensus recommendation of the American College of Medical Genetics and Genomics and the Association for Molecular Pathology. *Genetics in Medicine* **17** 405–424. (https://doi.org/10.1038/gim.2015.30)

Rinke A, Auernhammer CJ, Bodei L, Kidd M, Krug S, Lawlor R, Marinoni I, Perren A, Scarpa A, Sorbye H, *et al.* 2021 Treatment of advanced gastroenteropancreatic neuroendocrine neoplasia, are we on the way to personalised medicine? *Gut* **70** 1768–1781. (https://doi.org/10.1136/gutjnl-2020-321300)

Slinker BK 1998 The statistics of synergism. *Journal of Molecular and Cellular Cardiology* **30** 723–731. (https://doi.org/10.1006/jmcc.1998.0655)

Srimuninnimit V & Wampler GL 1991 Case report of metastatic familial pheochromocytoma treated with cisplatin and 5-fluorouracil. *Cancer Chemotherapy and Pharmacology* **28** 217–219. (https://doi.org/10.1007/BF00685513)

Tena I, Gupta G, Tajahuerce M, Benavent M, Cifrian M, Falcon A, Fonfria M, Del Olmo M, Reboll R, Conde A, *et al.* 2018 Successful second-line metronomic temozolomide in metastatic paraganglioma: case reports and review of the literature. *Clinical Medicine Insights. Oncology* **12** 1179554918763367. (https://doi.org/10.1177/1179554918763367)

Tolcher AW, Bendell JC, Papadopoulos KP, Burris 3rd HA, Patnaik A, Jones SF, Rasco D, Cox DS, Durante M, Bellew KM, *et al.* 2015 A phase IB trial of the oral MEK inhibitor trametinib (GSK1120212) in combination with everolimus in patients with advanced solid tumors. *Annals of Oncology* **26** 58–64. (https://doi.org/10.1093/annonc/mdu482)

Tonyukuk V, Emral R, Temizkan S, Sertcelik A, Erden I & Corapcioglu D 2003 Case report: patient with multiple paragangliomas treated with long acting somatostatin analogue. *Endocrine Journal* **50** 507–513. (https://doi.org/10.1507/endocrj.50.507)

Turkova H, Prodanov T, Maly M, Martucci V, Adams K, Widimsky Jr J, Chen CC, Ling A, Kebebew E, Stratakis CA, *et al.* 2016 Characteristics

© 2022 Society for Endocrinology
Published by Bioscientifica Ltd.
Printed in Great Britain

Downloaded from Bioscientifica.com at 05/11/2022 04:19:32PM
via Bodleian Library

and outcomes of metastatic Sdhb and sporadic pheochromocytoma/paraganglioma: an National Institutes of Health study. *Endocrine Practice* **22** 302–314. (https://doi.org/10.4158/EP15725.OR)

Van den Bossche V, Jadot G, Grisay G, Pierrard J, Honoré N, Petit B, Augusto D, Sauvage S, Laes JF & Seront E 2020 c-MET as a potential resistance mechanism to everolimus in breast cancer: from a case report to patient cohort analysis. *Targeted Oncology* **15** 139–146. (https://doi.org/10.1007/s11523-020-00704-2)

van Hulsteijn LT, Van Duinen N, Verbist BM, Jansen JC, Van Der Klaauw AA, Smit JW & Corssmit EP 2013 Effects of octreotide therapy in progressive head and neck paragangliomas: case series. *Head and Neck* **35** E391–E396. (https://doi.org/10.1002/hed.23348)

Wang L, Fang D, Xu J & Luo R 2020 Various pathways of zoledronic acid against osteoclasts and bone cancer metastasis: a brief review. *BMC Cancer* **20** 1059. (https://doi.org/10.1186/s12885-020-07568-9)

Waqar SN, Gopalan PK, Williams K, Devarakonda S & Govindan R 2013 A phase I trial of sunitinib and rapamycin in patients with advanced non-small cell lung cancer. *Chemotherapy* **59** 8–13. (https://doi.org/10.1159/000348584)

Wirth LJ, Sherman E, Robinson B, Solomon B, Kang H, Lorch J, Worden F, Brose M, Patel J, Leboulleux S, *et al.* 2020 Efficacy of selpercatinib in RET-altered thyroid cancers. *New England Journal of Medicine* **383** 825–835. (https://doi.org/10.1056/NEJMoa2005651)

Yaeger R & Corcoran RB 2019 Targeting alterations in the RAF-MEK pathway. *Cancer Discovery* **9** 329–341. (https://doi.org/10.1158/2159-8290.CD-18-1321)

Yao JC, Shah MH, Ito T, Bohas CL, Wolin EM, Van Cutsem E, Hobday TJ, Okusaka T, Capdevila J, De Vries EG, *et al.* 2011 Everolimus for advanced pancreatic neuroendocrine tumors. *New England Journal of Medicine* **364** 514–523. (https://doi.org/10.1056/NEJMoa1009290)

Yao JC, Fazio N, Singh S, Buzzoni R, Carnaghi C, Wolin E, Tomasek J, Raderer M, Lahner H, Voi M, *et al.* 2016 Everolimus for the treatment of advanced, non-functional neuroendocrine tumours of the lung or gastrointestinal tract (RADIANT-4): a randomised, placebo-controlled, phase 3 study. *Lancet* **387** 968–977. (https://doi.org/10.1016/S0140-6736(15)00817-X)

Zheng L, Gu Y, Silang J, Wang J, Luo F, Zhang B, Li C & Wang F 2021 Prognostic nomograms for predicting overall survival and cancer-specific survival of patients with malignant pheochromocytoma and paraganglioma. *Frontiers in Endocrinology* **12** 684668. (https://doi.org/10.3389/fendo.2021.684668)

Received in final form 1 March 2022
Accepted 23 March 2022
Accepted Manuscript published online 23 March 2022

Published by Bioscientifica Ltd.
Printed in Great Britain

Downloaded from Bioscientifica.com at 05/11/2022 04:19:32PM
via Bodleian Library

6. Publication II

Society for Endocrinology

Endocrine-Related Cancer (2024) **31** e230041
https://doi.org/10.1530/ERC-23-0041

Received 21 February 2023
Accepted 9 November 2023
Available online 9 November 2023
Version of Record published 30 November 2023

RESEARCH

Impact of the PI3K-alpha inhibitor alpelisib on everolimus resistance and somatostatin receptor expression in an orthotopic pancreatic NEC xenograft mouse model

Ajay-Mohan Mohan[1,2], Sonal Prasad[1,2], Fabian Schmitz-Peiffer[1,2], Catharina Lange[1], Mathias Lukas[1], Eva J Koziolek[1,3], Jakob Albrecht[1,2,3], Daniel Messroghli[4,5], Ulrike Stein[3,6], Matthias Ilmer[3,7,8], Katharina Wang[9], Laura Schober[9], Astrid Reul[10], Julian Maurer[9], Juliane Friemel[11], Achim Weber[11], Richard A Zuellig[10], Constanze Hantel[9,10], Ralph Fritsch[12], Martin Reincke[9], Karel Pacak[13], Ashley B Grossman[14,15,16], Christoph J Auernhammer[9,17], Felix Beuschlein[10], Winfried Brenner[1,2,3], Nicola Beindorff[2,*] and Svenja Nölting[9,10,*]

[1]Department of Nuclear Medicine, Charité – Universitätsmedizin Berlin, Berlin, Germany
[2]Berlin Experimental Radionuclide Imaging Center (BERIC), Charité - Universitätsmedizin Berlin, Berlin, Germany
[3]German Cancer Consortium (DKTK), partner site Berlin, Berlin, Germany
[4]Department of Internal Medicine - Cardiology, Deutsches Herzzentrum Berlin, Berlin, Germany
[5]Preclinical MRI Center, Charité - Universitätsmedizin Berlin, Berlin, Germany
[6]Experimental and Clinical Research Center, Charité-Universitätsmedizin Berlin, and Max-Delbrück-Center for Molecular Medicine in the Helmholtz Association, Translational Oncology of Solid Tumours, Berlin, Germany
[7]Department of General, Visceral, and Transplantation Surgery, University Hospital, LMU Munich, Munich, Germany
[8]German Cancer Research Center (DKFZ), Heidelberg, Germany
[9]Department of Medicine IV, University Hospital, LMU Munich, Munich, Germany
[10]Department of Endocrinology, Diabetology and Clinical Nutrition, University Hospital, University of Zurich (USZ) and University of Zurich (UZH), Zurich, Switzerland
[11]Department of Pathology and Molecular Pathology, University Zurich and University Hospital Zürich, Zurich, Switzerland
[12]Department of Medical Oncology and Hematology, University Zurich and University Hospital Zürich, Zurich, Switzerland
[13]Eunice Kennedy Shriver National Institute of Child Health and Human Development, National Institute of Health (NIH), Bethesda, Maryland, USA
[14]Green Templeton College, University of Oxford, London, United Kingdom
[15]Centre for Endocrinology, Barts and the London School of Medicine, Queen Mary University of London, United Kingdom
[16]ENETS Centre of Excellence, Royal Free Hospital, London, United Kingdom
[17]ENETS Centre of Excellence, Interdisciplinary Center of Neuroendocrine Tumours of the GastroEnteroPancreatic System at the University Hospital of Munich, Munich, Germany

Correspondence should be addressed to S Nölting: svenja.noelting@usz.ch

*(N Beindorff and S Nölting contributed equally to this work)

Abstract

The mechanistic target of rapamycin complex 1 (mTORC1) inhibitor everolimus is one of the few approved therapies for locally advanced and metastatic neuroendocrine tumours (NETs). However, after initial disease stabilisation, most patients develop resistance within 1 year. Our aim was to overcome resistance to everolimus by additional treatment with the PI3K-alpha inhibitor alpelisib in an everolimus-resistant orthotopic pancreatic neuroendocrine

Published by Bioscientifica Ltd.
https://erc.bioscientifica.com
© 2023 the author(s)

Downloaded from Bioscientifica.com at 01/29/2024 11:13:29AM
via HU - Charite Berlin

Endocrine-Related Cancer (2024) **31** e230041
https://doi.org/10.1530/ERC-23-0041

carcinoma xenograft mouse model. Female SCID mice underwent laparoscopic pancreatic transplantation of everolimus-sensitive (BON1KDMSO) or everolimus-resistant (BON1RR2) NET cells. Both groups were further divided into four treatment groups: placebo, everolimus, alpelisib, and everolimus + alpelisib (combination). Oral treatment was started at a tumour volume of approximately 140 mm^3 and continued until 1900–2000 mm^3, validated by weekly MRI. Somatostatin receptor expression and tumour viability were analysed by ^{68}Ga-DOTATOC and ^{18}F-FDG PET/CT. Everolimus resistance of the BON1RR2 tumours was confirmed. In the everolimus-sensitive group, everolimus alone, alpelisib alone, and combination treatment significantly prolonged survival, compared to placebo, while in the BON1RR2 group, only combination treatment significantly prolonged survival compared to placebo, but neither everolimus nor alpelisib alone. Placebo-treated everolimus-sensitive tumours grew more rapidly (median survival 45 days), compared to placebo-treated everolimus-resistant tumours (60 days). Within the everolimus-sensitive group, the combination-treated mice showed the longest median survival (52 days). Of all groups, the everolimus-resistant combination-treated group survived longest (69 days). Combination treatment with everolimus and alpelisib seems promising to overcome everolimus resistance in neuroendocrine neoplasms, and should be further examined in a clinical trial.

Keywords alpelisib; everolimus; pancreatic NEC; pancreatic NET; everolimus resistance

Introduction

The annual incidence of all neuroendocrine tumours (NETs) is currently 8.6/100,000 and is continuously increasing (White *et al.* 2022). A previously published review describes the global differences in the incidence of NETs (Das & Dasari 2021). Pancreatic NETs (panNETs) are a subgroup of NETs that are often indolent and characterised by early lymph node and liver metastases, with 40–45% of patients showing liver metastases at initial diagnosis (Frilling *et al.* 2014). Surgery is the only curative treatment option in patients with localised panNETs. For locally advanced or metastatic disease, there are only few approved systemic treatment options, including biotherapy (somatostatin analogues, approved as anti-proliferative therapy only for a low proliferation index Ki-67 ≤10%) (Rinke *et al.* 2009, Caplin *et al.* 2014), molecularly targeted therapy (everolimus (Yao *et al.* 2011, 2016), sunitinib (Raymond *et al.* 2011)), chemotherapy with streptozotocin/5-fluorouracil (Pavel *et al.* 2020), and peptide (somatostatin) receptor radionuclide therapy (PRRT) (Strosberg *et al.* 2021). Chemotherapy schemes with capecitabine/temozolomide are also part of the guideline recommendations. The 10-year survival of panNETs is only approximately 44%, while 5-year survival post surgery is approximately 65% (de Wilde *et al.* 2012).

Everolimus, a mechanistic target of rapamycin complex 1 (mTORC1) inhibitor, is an approved systemic therapy option for locally advanced and metastatic panNETs (Yao *et al.* 2011, 2016), while in neuroendocrine carcinomas (NECs) small studies have reported only modest activity of everolimus (Panzuto *et al.* 2017, Okuyama *et al.* 2020). According to the latest World Health Organisation (WHO) classification (Rindi *et al.* 2022) NECs fall under the class of poorly differentiated neuroendocrine neoplasms which are characterised by abundant necrosis, a high Ki-67, small or large cell morphology and low expression of somatostatin receptors (SSTR), which makes them less suitable for PRRT.

After initial disease stabilisation, most patients develop resistance to everolimus within 1 year of treatment (Yao *et al.* 2011, 2016). Reversible adaptive short-term resistance mechanisms (after 24–72 h treatment with everolimus) include compensatory protein kinase B (Akt) pathway activation through different insulin-dependent feedback loops (Zitzmann *et al.* 2010, Passacantilli *et al.* 2014, Vandamme *et al.* 2016). Irreversible long-term resistance has been much less studied. Thus, we have previously established two stable everolimus-resistant human pancreatic NET cell lines, BON1RR1 and BON1RR2, in order to investigate the mechanisms of stable long-term everolimus resistance (Aristizabal Prada *et al.* 2018): after 24 weeks of permanent treatment with 10 nM everolimus, BON1RR1 and BON1RR2 cells showed stable resistance to everolimus. The control cell line (BON1KDMSO) showed continuing sensitivity to 10 nM everolimus (Aristizabal Prada *et al.* 2018). The resistant cell lines did not regain sensitivity over time and maintained persistent stable resistance after a drug holiday of 13 weeks (13 weeks without everolimus treatment). In contrast to other previously developed everolimus-resistant NET cell lines, which were not proven to be stably resistant (Passacantilli *et al.* 2014, Vandamme *et al.* 2016, Sciammarella *et al.* 2020, Vitali *et al.* 2020), our everolimus-resistant cell line model is the first one that is suitable to generate a clinically relevant everolimus-resistant orthotopic pancreatic xenograft tumour mouse model to study stable resistance to everolimus *in vivo*.

Downloaded from Bioscientifica.com at 01/29/2024 11:13:29AM
via HU - Charite Berlin

Endocrine-Related Cancer (2024) **31** e230041
https://doi.org/10.1530/ERC-23-0041

Our group has previously shown *in vitro* that in long-term resistance to everolimus there is increased activation of glycogen synthase kinase3 (GSK3, an effector protein in the PI3K-Akt signalling pathway) in combination with decreased baseline insulin receptor substrate-1 (IRS-1) protein levels, G1 cell cycle arrest, and decreased autophagy (Aristizabal Prada *et al.* 2018). Moreover, we have shown in various NET cell lines that PI3K-alpha inhibitor alpelisib (BYL719) was able to overcome everolimus resistance *in vitro*, and also led to GSK3 inhibition and upregulation of somatostatin receptor (SSTR2) expression (Nölting *et al.* 2017, Aristizabal Prada *et al.* 2018).

We have therefore now transferred our everolimus-resistant cell line (Aristizabal Prada *et al.* 2018) to an orthotopic pancreatic NEC xenograft mouse model. The aim of this current study was to further characterise this first-ever developed everolimus-resistant orthotopic pancreatic NEC xenograft mouse model, and to investigate *in vivo* whether the PI3K-alpha inhibitor alpelisib (already FDA-approved for the treatment of breast cancer) may overcome resistance to everolimus, and lead to upregulation of PRRT-relevant SSTR2 expression. In addition, we checked for potential treatment-induced nephrotoxic effects and early tumour-induced kidney damage in our animal model. Treatment-induced nephrotoxic effects have been reported in many oncological treatment regimens, e.g. proteinuria and renal failure with everolimus treatment (Launay-Vacher *et al.* 2015) and one case of grade 3 acute kidney injury after combination treatment with alpelisib, everolimus, and exemestane in a phase 1b study (Curigliano *et al.* 2021). Moreover, in order to find out how increased GSK3 activation in the resistant tumour cells may contribute to everolimus resistance, and whether mitochondrial respiration and aerobic glycolysis might be involved, we also selectively inhibited GSK3 in BON1KDMSO and BON1RR2 cells and evaluated the oxygen consumption rates and extracellular acidification rates after selective GSK3 inhibition.

Materials and methods

Cell culture

Human everolimus-sensitive BON1KDMSO and everolimus-resistant BON1RR2 undifferentiated pancreatic NET cell lines (Aristizabal Prada *et al.* 2018) (histologically, NEC cell lines) were cultured in Dulbecco's Modified Eagle Medium (DMEM, Gibco®, ThermoFisher, Berlin Germany) with 10% fetal calf serum (FCS, Sigma-Aldrich), 0.01% penicillin (Biochrom, Berlin Germany), 0.01% streptomycin (Biochrom, Berlin, Germany), and 0.04% amphotericin (Biochrom, Berlin, Germany), at a humidified temperature of 37°C with 5% CO_2. Everolimus resistance in BON1RR2 cells was maintained with the continuous administration of 10 nM everolimus (Novartis Pharma) during cell culture to ensure stability of resistance during the whole *in vivo* experiment over several weeks, although it has previously been shown that the BON1RR2 cell line shows stable resistance even after a drug holiday of 13 weeks (Aristizabal Prada *et al.* 2018). Cells were transferred to antibiotic- and anti-fungal-free medium and everolimus administration was discontinued 48 h before tumour cell inoculation into the pancreas of each mouse to reduce their influence on tumour growth in the animal. All cell lines used in the study were authenticated twice by the German Biological Centre DSMZ (DSMZ, Braunschweig, Germany) using short tandem repeat (STR) analysis.

Animals and surgery

The study protocol was approved by our local committee for animal care Landesamt for Gesundheit and Sociales (LAGeSo G0177/18) according to the German law for the protection of animals. All applicable institutional and national guidelines for the care and use of animals were followed. All procedures were conducted in 74 female 'severe combined immune deficient' (SCID) mice. Animals were housed at the Berlin Experimental Radionuclide Imaging Center (BERIC) with a 12-h light–12-h darkness circadian rhythm. The husbandry conditions have been described in detail previously (Beindorff *et al.* 2018). Animals received a standard diet (SSNIFF®, Soest, Germany) and were additionally supplied with wet food and rusk following surgery.

Mice were operated when they weighed at least 20 g. Laparotomy was performed transplanting BON1KDMSO cells in 38 animals and BON1RR2 in 36 animals. Mice were anaesthetised using isoflurane (1.5–3%, CP-Pharma, Burgdorf, Germany) and intraperitoneal ketamine (60 mg/kg, CP-Pharma, Burgdorf, Germany). For additional analgesia, subcutaneous metamizole (200 mg/kg, Ratiopharm, Ulm, Germany) and carprofen (5 mg/kg, CP-Pharma, Burgdorf, Germany) were injected. Cells (2×10^6 cells) were mixed in 20 µL of pure DMEM media and injected orthotopically into the pancreas using a microscope (M125, Leica Microsystems). Following cell injection, the site of injection was disinfected with an antiseptic solution (SERASEPT®, Serag-Wiessner, Naila, Germany) in order to prevent any leakage of cells into the abdominal cavity. Analgesic medication with carprofen was performed for 24 h, and metamizole was added to the drinking water (1.25 mg/mL) for 72 h after surgery. Body weight was monitored daily after surgery for 1 week, and then, from treatment initiation, the animals were weighed every day on weekdays (from Monday to Friday) before oral gavage. For statistical calculations, body weight measurements performed at T0 (when an animal of the respective cell line was expected to have a minimum

Downloaded from Bioscientifica.com at 01/29/2024 11:13:29AM
via HU - Charite Berlin

Endocrine-Related Cancer (2024) **31** e230041
https://doi.org/10.1530/ERC-23-0041

tumour size of approximately 60 mm^3), T1 (28 days after treatment initiation), and T2 (tumour size of almost 2000 mm^3 or 20 weeks after surgery) were used.

Oral therapy

Animals of both cell lines were divided into four treatment groups: BON1KDMSO animals with placebo (n = 10), everolimus (n = 10), alpelisib (n = 8), and the combination of everolimus and alpelisib (n = 10); and BON1RR2 animals with placebo (n = 10), everolimus (n = 8), alpelisib (n = 8), and combination of everolimus and alpelisib (n = 10).

Oral administration of the drugs was started at a minimum tumour size of approximately 140 mm^3 and continued until the tumour reached a size of 1900–2000 mm^3, which was validated by magnetic resonance (MR) imaging, or when other termination criteria (maximum of 140 days after surgery or critical health status) were reached. Minimally invasive body weight-adjusted oral drug administration was performed directly into the oral cavity by a pipette on weekdays from Monday to Friday.

The monotherapy concentrations were 0.5 mg/kg body weight for everolimus (corresponding to a standard dose of 10 mg everolimus in humans with an average weight of 60 kg, Novartis Pharma) and 60 mg/kg body weight for alpelisib (corresponding to a standard dose of 300 mg alpelisib in humans with an average weight of 60 kg, Novartis Pharma). The combination treatment contained 0.5 mg/kg body weight of everolimus and 63 mg/kg body weight of alpelisib. Stock solutions were dissolved in dimethyl sulfoxide (167 µL DMSO per amount of drug for 1 kg body weight, Sigma-Aldrich). Aliquots were frozen at −80°C and diluted in corn oil (3167 µL per amount of drug for 1 kg body weight, Sigma-Aldrich) immediately before oral treatment. This results in a total volume of 3334 µL per amount of drug for 1 kg body weight, which corresponds to an oral drug volume of 100 µL for a 30 g mouse. The placebo treatment was composed of the same concentrations of DMSO and corn oil, and the same total volume.

Magnetic resonance imaging and imaging time points

Magnetic resonance (MR) imaging (3T MRI, MRS 3047, MR Solutions, Guildford, UK) was performed in a heated bed maintained at 32°C accounting for the additional heating generated in the coil. Fast T2 spin echo sequence axial acquisitions were acquired with the following parameters: matrix 256 × 256 × 48 with dimensions 0.2 × 0.2 × 0.1 mm, repetition time (TR): 3000–5000 ms with 4 averages. Animals were imaged at 18–25 days post surgery and thereafter every 12 weeks.

Baseline imaging (T0) was defined as the time when an animal of the respective cell line was expected to have a minimum tumour size of approximately 60 mm^3. After MR baseline imaging (T0), radionuclide imaging was performed. Immediately after first radionuclide imaging, oral treatment was started for each group (at that time point the minimum tumour size was approximately 140 mm^3) and continued until a termination criterion was reached. Time point T1 was defined by the first animal reaching a tumour size of 1600 mm^3. A placebo-treated BON1KDMSO animal was the first to reach this tumour size 28 days after treatment initiation. Therefore, T1 was chosen as the time point of 4 weeks after the start of therapy for each animal, regardless of tumour size and cell line, and radionuclide imaging was performed again at that time point. The final time point was defined as T2 for each individual animal, when either a tumour size of almost 2000 mm^3 or 140 days (20 weeks) after surgery were reached. Tumour volume was determined by the cumulative volume of the primary tumour and metastases if visible.

PET/CT for imaging tumour viability and receptor expression

Radionuclide imaging with positron emission tomography/computed tomography (PET/CT) was performed in a heated mouse bed at 37°C (nanoPET/CT plus, Mediso, Budapest, Hungary) at time points T0, T1 and T2. Tumour viability was assessed by injection of ^{18}F-FDG (Life Radiopharma, f-con, Holzhausen, Germany) after a 3-h fasting period, and blood glucose was measured before injection. SSTR tumour expression was validated after injection of ^{68}Ga-DOTATOC (Jussing *et al.* 2021). Tracer injection of approximately 18 MBq of each tracer in a maximum volume of 100 µL was applied into the tail vein, and PET imaging was performed under isoflurane anaesthesia (1.5–2.0%). After an incubation period of approximately 55 min, a 30 min PET was performed, followed by a CT at 45 kVp, 240 projections, 500 ms, 1 pitch, and a binning ratio of 1:4. PET/CT images were reconstructed using the ordered subset expectation maximisation (OSEM) algorithm with 8 iterations and 6 subsets, including attenuation and random corrections.

Image analysis was performed using PMOD 3.5 (PMOD Technologies Ltd., Zurich, Switzerland).

Tumour size (MR imaging), tumour viability (^{18}F-FDG-PET), and SSTR receptor expression (^{68}Ga-DOTATOC-PET) were quantified by manual contouring of a volume of interest (VOI) over the tumour using the standard uptake value ($SUV_{max\text{-}10}$) based on the 10 voxels with the highest activity within the VOI.

Renal scintigraphy

To monitor potential treatment effects on renal function, renal semi-stationary single photon emission computed tomography/computed tomography (SPECT/CT) was

Downloaded from Bioscientifica.com at 01/29/2024 11:13:29AM
via HU - Charite Berlin

Endocrine-Related Cancer (2024) **31** e230041
https://doi.org/10.1530/ERC-23-0041

performed with approximately 29 MBq ^{99m}technetium-mercaptoacetyltriglycine (^{99m}Tc-MAG3) (NanoSPECT/CT, Mediso, Budapest, Hungary/Bioscan, Paris, France), as recently described in detail (Huang *et al.* 2018). Animals were placed in the scanner, with each detector equipped with a nine-pinhole aperture (rat high resolution, $d = 1.5$ mm) with a 22 mm SPECT scan range. Renal scintigraphy was performed first at T0. To assess treatment effects, renal scintigraphy was repeated 4 weeks after the start of treatment at T1. Each renal time activity curve was obtained by plotting the absolute activity values for each kidney VOI against time (PMOD Technologies Ltd., Zurich, Switzerland). Renal time-to-peak (T_{max}), T_{50} (50% clearance), and T_{25} (75% clearance) as well as aorta blood excretion half-life (aorta 50% clearance) were used for statistical analysis.

Histology

Sixty-nine tumours were collected in 4% buffered formalin for 48 h and then preserved in 0.1% sodium azide–phosphate buffer solution (PBS).

Tumour size was measured as maximum diameter and formalin-fixed, paraffin-embedded tissue was cut (3 µm) and mounted on SuperFrost™ slides (ThermoFisher Scientific). Conventional staining with haematoxylin–eosin (HE) was performed on all slides to evaluate tumour morphology and necrosis.

For immunohistochemistry, the slides were stained with primary antibodies directed against human Ki-67 and SSTR2. Slides were processed using the following Ventana protocols: Benchmark discovery platform (Ventana Medical Systems, Inc., Tucson, AZ, USA); Ki-67: SP-6, monoclonal (Cell Marque life screen, Hamburg, Germany), dilution 1:100, pre-treatment H2 Epitope Retrieval Solution 2 (ER2) 30 min (Leica Biosystems), incubation for 60 min, visualisation immunohistochemistry refine 3,3'-diaminobenzidine (DAB); SSTR2A: Polyclonal (Zytomed systems, Berlin, Germany), dilution 1:25, pre-treatment H2 80 min, incubation for 30 min, visualisation OptiView DAB Kit. Ki-67 scoring was performed as fraction (%) of nuclear stained cells/by the total of vital tumour cells. SSTR2 was evaluated as positive in fraction (%) of cells with membranous staining/by the total of vital tumour cells. In detail, quantification of SSTR2 expression was performed as follows: only membranous reactivity of vital tumour cells irrespective of cytoplasmatic staining was counted as positive. The percentages of membranous positivity were scored in absolute numbers (Volante score 3: >50% positive cells, Volante score 2: <50% positive cells, Volante score 1: only cytoplasmatic positivity, Volante score 0: no immunoreactivity). The slides were digitalised using a Nano Zoomer C9600 Virtual Slide Light microscope scanner by Hamamatsu and NDP View Software.

XF real-time ATP rate assay experiments (measurement of oxygen consumption rate and extracellular acidification rate)

For quantification of real-time adenosine triphosphate (ATP) production, single-cell suspensions from trypsinised early passage adherent cell cultures (BON1KDMSO and BON1RR2) were seeded into XF Cell Culture Plates (Agilent Technologies). All the experiments were performed three times in triplicate. According to the manufacturer's instructions, cells were plated at cellular densities of 8000–10,000 cells/well in XF pH-defined media and incubated overnight. Oxygen consumption rate (OCR) and extracellular acidification rate (ECAR) as measures of mitochondrial respiration and glycolysis, respectively, were monitored as well as effects of treatment with AR-A014418 (Selleckchem, S7435-50mg, Munich, Germany) (20 µM) on OCR and ECAR in both cell lines. Oligomycin, rotenon, and antimycin A were sequentially injected according to the manufacturer's instructions. Experiments were run on an XF HS Mini Analyzer (Agilent Technologies) and data analysis was performed with the Seahorse Wave 2.4 software.

Statistical analysis

Statistical analysis was conducted with Statistical Package for the Social Sciences Statistics (SPSS) software, version 28.0. Tumour growth kinetics and renal scintigraphy were analysed with R 3.1.3 (the R Foundation for Statistical Computing). Linear regression analysis was performed and median tumour volume and day were used to generate tumour growth curves. Body weight loss measurements were calculated based on the three intervention time points at T0, T1, and T2.

Descriptive parameters are represented by median (interquartile range (IQR, 25th–75th percentile), minimum and maximum). Differences between treatment groups within the everolimus-resistant and non-resistant group, respectively, and between everolimus-resistant and non-resistant tumours were analysed using non-parametric Mann–Whitney U (MWU) and Kruskal–Wallis test while intra-treatment group differences (T0, T1, T2 within a treatment group under each cell line) were tested with Wilcoxon and ANOVA. A Student's t-test was used for groups with smaller sample size. Cumulative survival curves were generated using Kaplan–Meier analysis based on T2 time points. $P \leq 0.05$ was considered as significant and $P \leq 0.1$ as a trend.

Results

Model characterisation, tumour growth kinetics, and survival analysis

Evaluation of the T2-weighted MR images showed vital tumour tissue in all animals at all three time points, regardless of cell line and treatment, but also

Downloaded from Bioscientifica.com at 01/29/2024 11:13:29AM
via HU - Charite Berlin

Endocrine-Related Cancer (2024) **31** e230041
https://doi.org/10.1530/ERC-23-0041

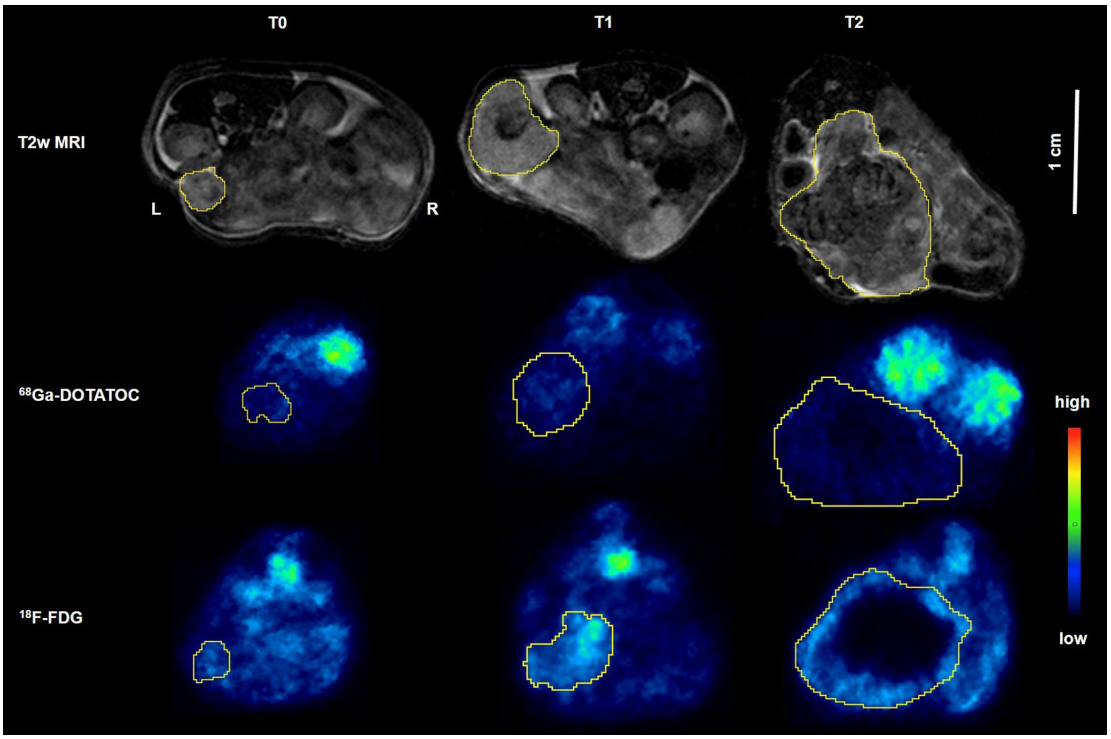

Figure 1

The images show a BON1RR2 animal on combination treatment (everolimus + alpelisib). The tumour is outlined with a yellow volume of interest (VOI). Over time, MRI clearly shows an increase of hypointense 'dark areas' corresponding to necrosis with total tumour volumes at T0 of 43 mm^3, T1 225 mm^3, and T2 1635 mm^3. MRI, ^{68}Ga-DOTATOC- and ^{18}F-FDG-PET were performed on different days at the respective time points T0 (before treatment start, minimum tumour size of approximately 60 mm^3), T1 (4 weeks after treatment start) and T2 (final time point, when termination criteria were reached). Therefore, the size and location of the tumour layers are not identical. ^{68}Ga-DOTATOC uptake (SUV): T0 = 1.01, T1 = 1.06, T2 = 0.45; ^{18}F-FDG uptake (SUV): T0 = 1.6, T1 = 3.2, T2 = 2.6.

clearly hypointense necrotic tumour tissue at T1 and T2 to varying extents, as shown in Fig. 1. This was confirmed by the histological findings, which showed 30–90% tumour necrosis in 67 of 69 animals examined. Only two animals had less than 30% necrosis. Furthermore, all tumours were classified as neuroendocrine carcinomas (NECs) based on a high Ki-67 (>20%), in the majority Ki-67 >55% (mean 85 ± 12.5%), and small cell morphology. Eight tumours (BON1KDMSO (2× everolimus, 1× combination), BON1RR2 (2× placebo, 1× everolimus, 2× combination)) were classified as mixed endocrine/exocrine tumours comparable to the human MiNEN (mixed neuroendocrine–non-neuroendocrine neoplasm of the pancreas) based on the diagnostic criteria for MiNEN as defined by the WHO digestive system tumours, fifth edition 2019 (Nagtegaal *et al.* 2020), comprising a morphological exocrine component of ≥30% such as gland formation and cystic features (Supplementary Fig. 1A, see section on supplementary materials given at the end of this article). For mouse tumours, criteria were applied based on HE slides, estimating the percentage of gland formation within vital tumour.

There was no difference in Ki-67 values between everolimus-sensitive and everolimus-resistant tumours (BON1KDMSO 90% (85–90) 30–95, BON1RR2 90% (85–90) 40–98, $P = 0.493$). There was low histological SSTR2 expression of only 10–30% in most tumours of all treatment groups regardless of the cell line. Quantification of SSTR2 expression based on Volante scoring revealed 8 tumours with a Volante score 3 (>50% of positive cells) from BON1RR2 cell line across all treatment groups (placebo, everolimus, alpelisib, combination) and 54 tumours with a Volante score 2 (<50% of positive cells). Seven tumours had a Volante score 0. Figure 2A, B, and C shows an example of HE staining (A) of a tumour with necrotic areas, Ki-67 staining (B), and SSTR2 staining (C) from a BON1KDMSO animal treated with combination on day 78. Figure 2D, E, and F shows an example of HE staining (D), highly positive Ki-67 staining (E) and SSTR2 staining (F) with negligible SSTR2 expression of a tumour from a combination-treated BON1RR2 animal.

The first MR imaging, performed between 18 and 25 days after surgery, showed that BON1KDMSO tumours grew faster than BON1RR2 tumours (trend, $P = 0.087$), as already observed in cell culture experiments and shown in Fig. 3. Consequently, T0 with a minimum target tumour size of 60 mm^3 before the first radionuclide imaging and start of oral treatment

Downloaded from Bioscientifica.com at 01/29/2024 11:13:29AM
via HU - Charite Berlin

Endocrine-Related Cancer (2024) **31** e230041
https://doi.org/10.1530/ERC-23-0041

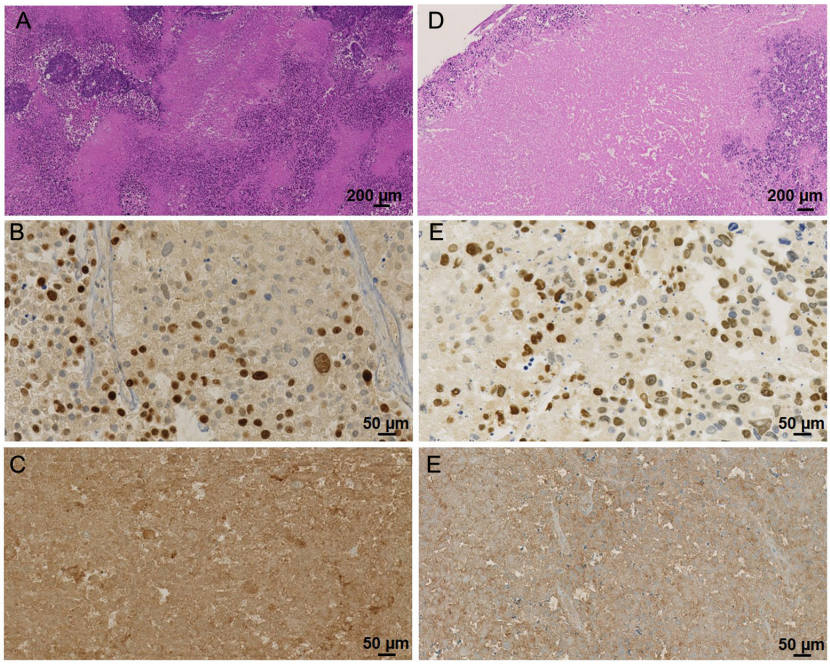

Figure 2

(A, D) HE staining, (B, E) highly positive Ki-67 staining, and (C, F) SSTR2 staining with negligible SSTR2 expression of (A, B, C) BON1KDMSO and (D, E, F) BON1RR2 combination treatment (everolimus + alpelisib) 78 days and 132 days after surgery, respectively.

occurred earlier in BON1KDMSO at day 18–28 (56 mm³ (40–79) 20–202) than in BON1RR2 animals at days 21–34 (71 mm³ (57–103) 41–216).

Kaplan–Meier survival analysis (Fig. 4) shows that placebo-treated BON1KDMSO animals had a significantly shorter median survival (42 days) than placebo-treated BON1RR2 animals (53 days) ($P < 0.001$). In BON1KDMSO animals, everolimus (44 days, $P = 0.002$), alpelisib (53 days, $P < 0.001$) and combination treatment (52 days, $P < 0.001$) significantly increased median survival, compared to placebo (42 days). There was no significant difference between alpelisib and the combination treatment ($P = 0.675$). However, both alpelisib ($P = 0.027$) and combination treatment ($P = 0.023$) significantly prolonged survival, compared to everolimus alone. In BON1RR2 animals, only combination treatment significantly prolonged median survival (69 days), compared to placebo (53 days, $P < 0.001$), to everolimus (56 days, $P < 0.001$) and to alpelisib (61 days, $P = 0.019$). There was no significant difference in survival between placebo, everolimus, and alpelisib in BON1RR2 animals. Importantly, two of ten combination-treated BON1RR2 animals survived 20 weeks (140 days) post surgery, and despite not reaching a tumour size of 2000 mm³, the trial had to be terminated according to the termination criteria (maximum 140 days after surgery). Only one of these two animals developed metastases at 20 weeks.

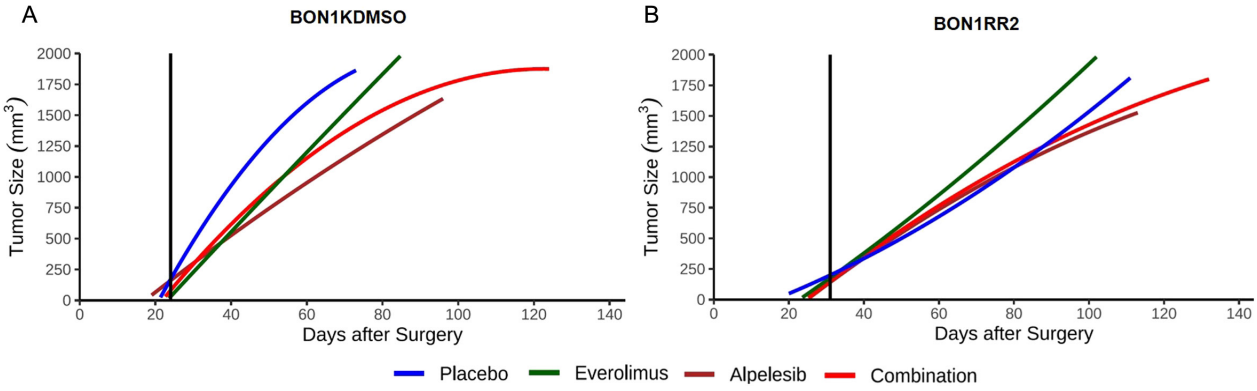

Figure 3

Tumour growth curves generated from sequential MR imaging after inoculation of BON1KDMSO and BON1RR2 cells depicting the kinetics of different treatment groups. Linear regression analysis was performed and data were generated with median tumour volume plotted against the median days after surgery. The vertical solid line represents the median start of oral treatment with 24 days in BON1KDMSO and 31 days in BON1RR2 animals.

Downloaded from Bioscientifica.com at 01/29/2024 11:13:29AM
via HU - Charite Berlin

R - r dR d e l i Rr l(2024) **31** e230041
https://doi.org/10.1530/ERC-23-0041

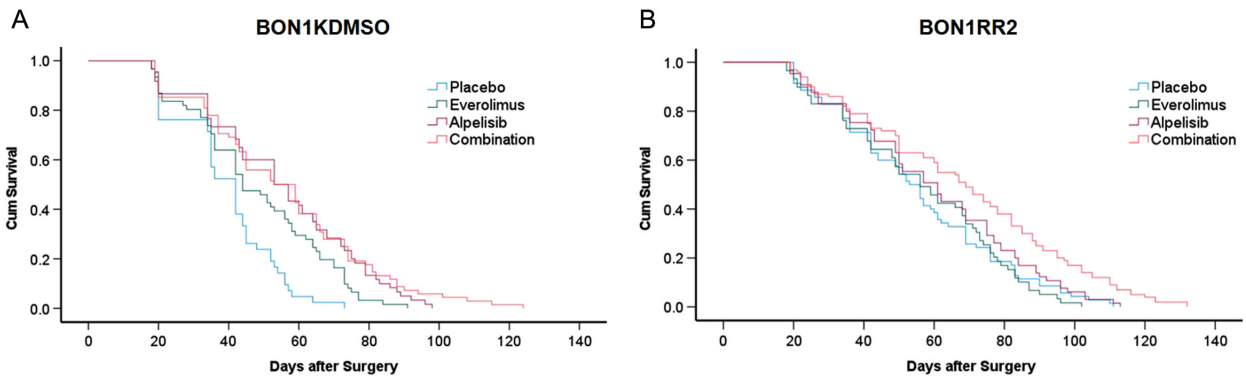

Figure 4

Tumour growth was monitored by MR imaging until a termination criterion (2000 mm³ tumour size, maximum of 140 days after surgery or critical health status) was reached. Corresponding Kaplan–Meier curves depict animal survival with (A) BON1KDMSO and (B) BON1RR2 tumours for the respective treatment group. In the BON1KDMSO group, survival was significantly prolonged by everolimus (= 0.002), alpelisib (< 0.001), and combination therapy (< 0.001) compared to placebo and by alpelisib (= 0.027) and combination therapy (= 0.023) compared to everolimus. In the BON1RR2 group, only the combination therapy significantly prolonged survival (< 0.02) compared to placebo, everolimus, and alpelisib.

Four BON1KDMSO (1× everolimus, 2× alpelisib, 1× combination treatment,) and five BON1RR2 animals (2× alpelisib, 3× combination treatment) developed metastases 58–132 days after surgery, predominantly in the liver with only one animal having additional peritoneal metastases. Histologically, the metastases showed necrosis, low SSTR2 expression and high Ki-67, similar to the primary tumour. Due to the short survival period of the placebo-treated animals, the potential formation of metastases cannot be excluded in general.

Functional imaging: tumour somatostatin-receptor expression and glucose (^{18}F-FDG) uptake (viability)

^{68}Ga-DOTATOC uptake of the respective cell line and treatment groups is summarised in Table 1. PET imaging with ^{68}Ga-DOTATOC showed no significant change in tumour uptake during the course of treatment in BON1KDMSO or BON1RR2 animals within the different treatment groups. The overall low

Table 1 ^{68}Ga-DOTATOC standard uptake values ($SUV_{max\text{-}10}$) based on 10 voxels with highest uptake activity within the volume-of-interest (VOI). Each set of data includes the median, interquartile range (IQR), minimum–maximum and number of animals of each treatment group for each cell line. Time points T0 = before treatment start (minimum tumour size of approximately 60 mm³), T1 = 4 weeks after treatment start, T2 = final time point, when termination criteria were reached. There are no significant differences within any treatment group over time.

	BON1KDMSO			BON1RR2		
	T0	T1	T2	T0	T1	T2
Placebo	0.6 (0.4–0.8) 0.3–1.3 (*R* = 6)	0.9 (0.4–1.2) 0.3–1.4 (*R* = 10)	1.5 (*R* = 1)	0.8 (0.6–0.9) 0.6–1.0 (*Rl*= 10)	1.0 (0.8–1.1) 0.8–1.4 (*R* = 10)	1.1 (0.8–1.1) 0.4–1.2 (*R* = 6)
Everolimus	0.6 (0.4–0.9) 0.3–1.6 (*R* = 8)	0.6 (0.5–0.8) 0.4–0.8 (*R* = 10)	0.9 (0.5–4.9) 0.3–7.4 (*R* = 5)	0.7 (0.5–0.9) 0.4–1.0 (*R* = 8)	0.7 (0.7–1.3) 0.5–1.6 (*R* = 8)	0.8 (0.7–1.1) 0.5–1.7 (*R* = 6)
Alpelisib	0.6 (0.5–0.7) 0.2–0.7 (*R* = 8)	0.8 (0.6–1.1) 0.3–2.9 (*R* = 8)	0.8 (0.6–4.1) 0.4–13.5 (*R* = 6)	0.7 (0.5–0.8) 0.4–0.9 (*R* = 8)	0.9 (0.7–1.2) 0.7–2.1 (*R* = 8)	0.9 (0.7–21.9) 0.7–28.9 (*R* = 4)
Combination	1.2 (0.5–1.4) 0.2–2.6 (*R* = 10)	0.8 (0.6–0.9) 0.5–1.2 (*R* = 9)	0.7 (0.5–0.8) 0.5–1.1 (*R* = 6)	0.9 (0.7–1.5) 0.6–3.3 (*R* = 10)	1.1 (0.8–1.4) 0.5–16.2 (*R* = 10)	0.8 (0.5–1.0) 0.4–2.1 (*R* = 7)

Downloaded from Bioscientifica.com at 01/29/2024 11:13:29AM
via HU - Charite Berlin

l Ri rl œ- a el i d (2024) **31** e230041
https://doi.org/10.1530/ERC-23-0041

Table 2 ^{18}F-FDG standard uptake values ($SUV_{max\text{-}10}$) based on 10 voxels with highest uptake activity within the volume of interest (VOI). Each set of data includes the median, interquartile range (IQR), minimum–maximum and number of animals of each treatment group for each cell line. Time points T0 = before treatment start (minimum tumour size of approximately 60 mm^3), T1 = 4 weeks after treatment start, T2 = final time point, when termination criteria were reached.

	BON1KDMSO			BON1RR2		
	T0	T1	T2	T0	T1	T2
Placebo	3.1	5.0	3.4	3.5[a]	4.6	4.3
	(2.9–3.4)	(4.4–5.5)		(2.3–3.9)	(3.7–5.4)	(3.6–4.9)
	2.5–4.1	3.5–9.3		1.8–4.0	3.0–5.9	3.2–5.0
	(*l* = 6)	(*l* = 9)	(*l* = 1)	(*l* = 10)	(*l* = 10)	(*l* = 6)
Everolimus	3.5	3.9	4.4	2.4[b]	4.5	4.3
	(2.4–3.8)	(2.8–5.6)	(3.1–5.3)	(2.1–3.4)	(4.0–5.4)	(3.6–5.8)
	1.4–4.0	2.3–6.0	2.5–6.1	1.4–3.4	0.5–8.2	2.9–6.2
	(*l* = 7)	(*l* = 10)	(*l* = 5)	(*l* = 8)	(*l* = 8)	(*l* = 6)
Alpelisib	3.5	3.7	2.4	2.5[a]	4.3	2.8
	(3.1–3.7)	(2.7–5.3)	(1.8–3.5)	(2.2–3.2)	(2.8–5.7)	(2.0–4.0)
	2.3–3.9	1.6–5.6	1.1–4.5	1.6–3.7	2.1–7.5	2.0–4.1
	(*l* = 6)	(*l* = 8)	(*l* = 6)	(*l* = 8)	(*l* = 8)	(*l* = 4)
Combination	3.1	4.4	2.7	2.4[a]	3.9	2.8
	(2.9–3.6)	(2.4–5.1)	(1.4–3.7)	(1.5–3.4)	(3.3–4.9)	(2.6–4.2)
	1.7–4.1	2.2–5.6	1.0–4.8	0.8–3.8	2.4–6.5	2.3–4.6
	(*l* = 10)	(*l* = 9)	(*l* = 6)	(*l* = 10)	(*l* = 9)	(*l* = 7)

[a]$E < 0.01$ between T0 and T1 within a treatment group; [b]$E = 0.051$ between T0 and T1 within a treatment group.

^{68}Ga-DOTATOC uptake is clearly demonstrated in Fig. 1. Overall, there was no significant correlation between *in vivo* ^{68}Ga-DOTATOC uptake and histological SSTR2 expression ($P > 0.05$).

^{18}F-FDG uptake for assessing tumour viability is shown in Table 2. Due to higher ^{18}F-FDG uptake of the tumours compared to ^{68}Ga-DOTATOC, tumours can be clearly delineated in the ^{18}F-FDG-PET image and necrotic areas can be localised, as shown in Fig. 1. In contrast to the individual treatment groups, pooled data at T0 revealed a significantly higher ^{18}F-FDG uptake of BON1KDMSO (3.3 (2.9–3.7) 1.4–4.1) compared to BON1RR2 tumours (2.5 (2.2–3.4) 0.8–4.0; $P = 0.025$) indicating more aggressive behaviour/faster growth of BON1KDMSO tumours as also demonstrated by MRI. We did not find a statistically significant difference in ^{18}F-FDG uptake at time points T1 and T2 between pooled BON1KDMSO and BON1RR2 animals. In BON1KDMSO animals, ^{18}F-FDG-PET showed no difference in uptake between the different time points within either treatment group. In contrast, in BON1RR2 animals, there was a significant increase in ^{18}F-FDG uptake from T0 to T1 for placebo ($P = 0.003$), alpelisib ($P = 0.035$), and the combination treatment ($P = 0.006$), and a trend for higher ^{18}F-FDG uptake for everolimus ($P = 0.051$). No significant changes were observed in the further course (T2) of the respective treatment groups. Inter-treatment significance was only found in BON1RR2 tumours at T2, with placebo showing a higher tumour uptake compared to alpelisib ($P = 0.05$), while everolimus-treated tumours showing a significantly increased ^{18}F-FDG uptake, compared to alpelisib ($P = 0.041$) and the combination ($P = 0.047$). This may reflect a higher rate of aerobic glycolysis (Warburg effect) by increased GSK3 activation in everolimus resistance (see 'Oxygen consumption rate and extracellular acidification rate measurements' section).

Oxygen consumption rate and extracellular acidification rate measurements

The selective GSK3 inhibitor AR-A014418 more strongly inhibited survival of the resistant BON1RR1/BON1RR2 cells which show increased GSK3 activation (Aristizabal Prada *et al.* 2018), compared to the sensitive BON1KDMSO cells (data not shown), indicating a pivotal role of GSK3 in everolimus resistance.

Seahorse ATP real-time rate assays show that selective GSK3 inhibition by AR-A01441 leads to a significant increase in the oxygen consumption rate (OCR, mitochondrial respiration, red line in Fig. 5) ($P \leq 0.03$) and a significant decrease in extracellular acidification rate (ECAR, aerobic glycolysis, Warburg effect, red line in Fig. 5) ($P \leq 0.03$) in BON1KDMSO and BON1RR2 cells, indicating GSK3-mediated impairment of mitochondrial respiration and increase in aerobic glycolysis (Warburg effect) (Fig. 5).

Effects of treatment and tumour growth on body weight and blood glucose

Regardless of cell line or treatment, animals significantly lost weight between T0 and T1 (4 weeks after the start of treatment) (pooled BON1KDMSO T0 19.6 g ((18.8–21.0)

Downloaded from Bioscientifica.com at 01/29/2024 11:13:29AM
via HU - Charite Berlin

l Ri rl œ- a el i d(2024) **31** e230041
https://doi.org/10.1530/ERC-23-0041

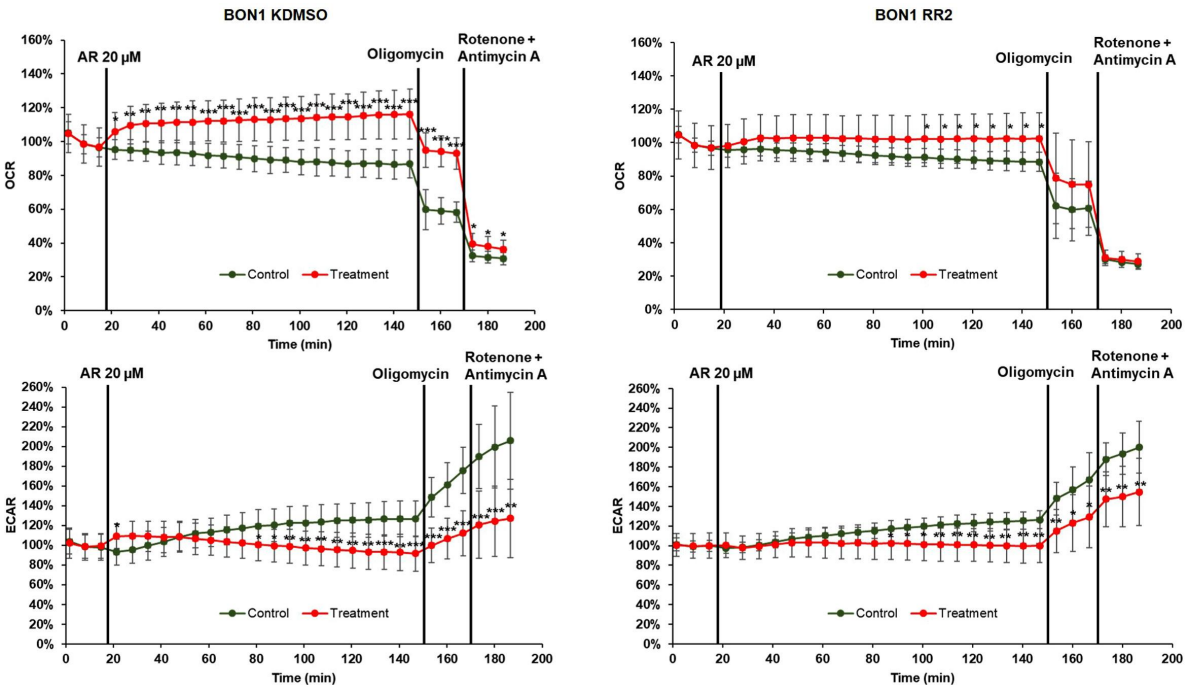

Figure 5

ATP Real-time rate assay results from BON1KDMSO und BON1RR2 cells after stimulation with the selective GSK3-inhibitor AR-A014418 20 µM (red line) and without stimulation (green line). Each experiment was performed three times in triplicate. Measurement of 20 cycles was performed, followed by three cycles of oligomycin (1.5 µM) and 3 cycles of rotenone + antimycin A (0.5 µM), consecutively. The three experiments started at different baseline oxygen consumption rates (OCR, in pmol/min) and different baseline extracellular acidification rates (ECAR, in mpH/min), respectively, although the same cell numbers (10,000/well) were seeded. For better comparability, we calculated the mean baseline OCR and ECAR of all three experiments before the start of treatment and set the mean baseline OCR and ECAR at 100%. All changes in OCR and ECAR due to treatment are expressed in percentages. In both cell lines, there was a significant increase in OCR and a significant decrease in ECAR after selective GSK3 inhibition, compared to the control, corresponding to a shift to higher mitochondrial respiration and lower glycolysis. ATP inhibitor = oligomycin, mitochondrial function inhibitor = rotenone, ***n <0.001; **n < 0.01; *n < 0.05 between control and treatment.

16.6–24.2) vs T1 18.1 g ((16.9–19.2) 14.2–22.8), $P < 0.001$; pooled BON1RR2 T0 19.9 g ((19.0–20.6) 17.0–22.8) vs T1 17.7 g ((16.5–18.6) 14.2–22.2), $P < 0.001$). When comparing T1 between the different treatment groups of BON1KDMSO animals, no weight difference was observed ($P = 0.55$). BON1RR2 animals at T1 under alpelisib alone (16.5 g (15.0–17.3) 13.7–18.1) weighed significantly less, compared to the other BON1RR2 treatment groups ($P < 0.02$) and compared to alpelisib-treated BON1KDMSO animals (17.8 g (16.3–18.3) 15.3–20.1; $P = 0.017$). Animals under alpelisib treatment regained weight by the end of the trial (T2 – either a tumour size of almost 2000 mm³ or 140 days after surgery): BON1KDMSO 18.5 g (17.6–20.2) 16.9–21.5, $P = 0.077$ and BON1RR2 18.9 g (18.5–19.7) 18.0–20.8, $P < 0.001$. After T1, animal weight gain was rather dependent on tumour growth than on better health of the animals.

Since everolimus resistance is associated with increased activation of the GSK-3 pathway (Aristizabal Prada *et al.* 2018) and alpelisib may induce hyperglycaemia (Hedges *et al.* 2021), blood glucose levels were determined. When comparing the everolimus-sensitive with the everolimus-resistant group, there was no significant difference at T0 between the pooled data of BON1KDMSO (123 mg/dL (109–137) 80–159) and BON1RR2 animals (117 mg/dL (100–129) 94–207, $P = 0.215$) or between the individual groups of each cell line. Only at T1, 4 weeks after treatment initiation, significantly *lower* glucose levels occurred in the alpelisib-treated BON1RR2 animals (83 mg/dL (75–90) 67–103) compared to alpelisib-treated BON1KDMSO (145 mg/dL (115–177) 93–254, $P < 0.001$) possibly explaining the transient weight loss. Moreover, in BON1RR2 animals, there was a significant decrease in blood glucose under everolimus at T1 (100 mg/dL (65–114) 54–116) compared to T0 (117 mg/dL (104–117) 97–152, $P = 0.04$).

Effects of treatment and tumour growth on renal function

Pooled BON1KDMSO and BON1RR2 renal data of T_{max}, T_{50}, and T_{25} as well as T_{50} of the aorta are summarised in Table 3. Regardless of the treatment, no effect of therapy on T_{max} could be detected by kidney scintigraphy. Only alpelisib caused significantly delayed T_{50} (6.1 min (4.3–8.5) 3.8–25.8; $P = 0.013$) and T_{25}

Downloaded from Bioscientifica.com at 01/29/2024 11:13:29AM
via HU - Charite Berlin

Endocrine-Related Cancer (2024) **31** e230041
https://doi.org/10.1530/ERC-23-0041

Table 3 The table shows pooled data of BON1KDMSO and BON1RR2 cells. ^{99m}Tc-MAG3 aorta blood excretion half-life with respect to treatment is expressed as $T_{50aorta}$ in seconds. ^{99m}Tc-MAG3 kidney uptake with respect to treatment is expressed as time-to-peak (T_{max}), T_{50}, and T_{25} in minutes. Each set of data includes the median, interquartile range (IQR), minimum–maximum, and number of animals.

	Placebo		Everolimus		Alpelisib		Combination	
	T0	T1	T0	T1	T0	T1	T0	T1
Aorta excretion (s)								
$T_{50aorta}$	28 (16–66) 12–77 (*n* = 15)	19 (16–45) 11–93 (*n* = 15)	29 (23–44) 17–69 (*n* = 15)	34 (23–41) 18–76 (*n* = 17)	31 (25–48) 18–80 (*n* = 14)	34 (18–51) 14–88 (*n* = 15)	44 (32–66) 10–139 (*n* = 19)	32 (21–49) 9–117 (*n* = 18)
Kidney uptake (min)								
T_{max}	1.8 (1.6–2.1) 1.4–5.6	1.6 (1.5–3.2) 1.3–7.7	1.4 (1.2–1.8) 1.1–3.3	1.4 (1.3–1.9) 1.1–2.1	1.7 (1.3–2.4) 1.1–4.2	1.7 (1.4–2.5) 1.3–10.9	1.5 (1.3–1.6) 1.2–2.3	1.6 (1.3–2.1) 1.2–5.7
T_{50}	5.1 (4.2–7.2) 3.3–15.3	4.8 (3.9–8.7) 2.7–18.3	4.0 (2.6–5.1) 2.3–6.2	3.8 (3.2–4.7) 2.3–6.3	4.1[a] (3.7–5.7) 2.5–8.7	6.1 (4.3–8.5) 3.8–25.8	3.7 (3.3–4.8) 3.1–5.8	4.33 (3.4–5.3) 2.3–14.3
T_{25}	8.9 (6.9–11.5) 5.1–26.3 (*n* = 15)	8.3 (6.4–14.3) 4.1–29.2 (*n* = 15)	6.5 (4.1–8.2) 2.5–10.6 (*n* = 15)	6.8 (5.1–7.7) 3.5–10.1 (*n* = 17)	6.8[a] (6.0–9.6) 4.2–14.8 (*n* = 14)	10.1 (7.3–17.9) 6.2–44.2 (*n* = 15)	6.2 (5.3–8.0) 5.0–9.9 (*n* = 19)	7.3 (5.7–9.3) 3.5–22.6 (*n* = 18)

[a]$P < 0.02$ between T0 (before treatment, minimum tumour size of approximately 60 mm^3) and T1 (4 weeks after treatment start) within a treatment group.

(10.1 min (7.3–17.9) 6.2–44.2; $P = 0.013$) at T1, compared to T0 (T_{50} 4.1 min (3.7–5.7) 2.5–8.7; T_{25} 6.8 min (6.0–9.6) 4.2–14.8) when all alpelisib-treated animals were pooled. This influence of alpelisib on renal excretion was no longer observed when BON1KDMSO and BON1RR2 animals were evaluated separately, nor in animals treated with the alpelisib/everolimus combination.

Moreover, the influence of tumour size on kidney function was evaluated: 4 weeks after the start of treatment at the time of greatest variability in tumour size, the aorta blood excretion half-life ($T_{50aorta}$) was reached earlier with increasing tumour size ($\rho = -0.45$, $P < 0.001$). However, no correlation of tumour size with renal T_{max}, T_{50}, and T_{25} was found.

Discussion

We have successfully established the first robust everolimus-resistant orthotopic pancreatic human NEC xenograft mouse model by utilising our previously established everolimus-resistant human pancreatic NET cell line (BON1RR2) (Aristizabal Prada *et al.* 2018). In contrast to other previously established everolimus-resistant NET cell lines, our resistant cell line is the first one proven to be stably resistant, even after a drug holiday of 13 weeks and thus suitable for *in vivo* testing (Passacantilli *et al.* 2014, Vandamme *et al.* 2016, Sciammarella *et al.* 2020, Vitali *et al.* 2020).

Kaplan–Meier analysis revealed that everolimus significantly prolonged survival in the animals with everolimus-sensitive tumours, but not in those with everolimus-resistant tumours. In the everolimus-sensitive animals, alpelisib alone and combination treatment also significantly prolonged survival, compared to placebo and – interestingly – even to everolimus. In the everolimus-resistant BON1RR2 animals, there was no significant survival benefit after treatment with everolimus or alpelisib alone, but there was after combination treatment. Thus, both everolimus resistance and overcoming everolimus resistance by combination treatment could be demonstrated *in vivo*. Furthermore, combination treatment had neither adverse effects on body weight nor on the kidney function of the mice. Alpelisib as single treatment, however, caused significantly delayed excretion time points T_{50} and T_{25} after 4 weeks of treatment, which is in line with the frequently observed increased serum creatinine levels in clinical studies on alpelisib in breast cancer patients (FDA 2019, Markham 2019). Interestingly, significant tumour growth from approximately 100 mm^3 to 1600 mm^3 during 4 weeks of placebo treatment did not cause any significant changes in kidney scintigraphic parameters T_{max}, T_{50}, and T_{25}, while the aorta blood excretion half-life ($T_{50aorta}$) was reached earlier with increasing tumour size. Fast-growing orthotopic pancreatic tumours and their tumour vessel system with a high blood flow obviously

Downloaded from Bioscientifica.com at 01/29/2024 11:13:29AM
via HU - Charite Berlin

Endocrine-Related Cancer (2024) **31** e230041
https://doi.org/10.1530/ERC-23-0041

increase the tracer extraction from the abdominal aorta resulting in a shorter aortic excretion half-life.

Our group has previously shown a synergistic anti-tumour potential of mTORC1 inhibitor everolimus and the PI3K-alpha inhibitor alpelisib *in vitro*, as they act to inhibit complementary signalling pathways in human pancreatic NET (BON1), everolimus-resistant BON1RR1/BON1RR2 and murine phaeochromocytoma cell lines; this effect was also seen in patient phaeochromocytoma/paraganglioma primary cultures and spheroid models (Nölting *et al.* 2017, Aristizabal Prada *et al.* 2018, Fankhauser *et al.* 2019, Wang *et al.* 2022). These findings can now be extended to our *in vivo* model, explaining the prolonged survival under combination treatment in BON1KDMSO and BON1RR2 animals. The present data are also consistent with other *in vivo* studies whereby combination treatment with mTORC1 and PI3K inhibitors showed synergistic anti-tumour effects, resulting in increased survival compared to monotherapy (Yang *et al.* 2011, Djukom *et al.* 2014, Kim *et al.* 2020). Djukom *et al.* also reported decreased progression of liver metastases during such combination therapy in a BON1 mouse liver metastasis model (Djukom *et al.* 2014). However, importantly, in contrast to our model, in these studies the tumours did not show *a priori* resistance to mTORC1 inhibitors.

Besides overcoming everolimus resistance, we also aimed to decipher the potential mechanism of everolimus resistance. Our previous *in vitro* studies in BON1RR1/BON1RR2 cell lines have revealed some potential mechanisms of everolimus resistance (Aristizabal Prada *et al.* 2018) such as G1 cell cycle arrest associated with reduced CDK1 (cdc2) expression in the everolimus-resistant cell line (Aristizabal Prada *et al.* 2018), which is consistent with the observed slower growth rate and lower baseline ^{18}F-FDG/glucose uptake of the everolimus-resistant tumours, compared to the sensitive ones. However, there was no difference in Ki-67 values between everolimus-sensitive and resistant tumours which might explain these differential ^{18}F-FDG uptake values. As another potential mechanism of resistance, there was increased activation of GSK3 associated with reduced IRS-1 protein levels in the everolimus-resistant cell lines *in vitro*: this may explain the increase in ^{18}F-FDG/glucose uptake in BON1RR2 tumours between T0 and T1 *in vivo* irrespective of the type of treatment. Such an increase was not observed in BON1KDMSO tumours. Moreover, there was a significantly higher ^{18}F-FDG/glucose uptake at T2 after everolimus treatment, compared to alpelisib and the combination, in the resistant tumours only. Cellular stress (drug treatment or tumour growth itself) may lead to increased glucose uptake in the resistant tumours via an increased Warburg effect (aerobic glycolysis) through increased activation of GSK3 and negative regulation of mitochondrial respiration (Yang *et al.* 2017, Papadopoli *et al.* 2021). Increased activation of GSK3 has been reported to be associated with depleted mitochondrial function (Chiara & Rasola 2013, Yang *et al.* 2017, Papadopoli *et al.* 2021). Consistently, the oxygen consumption rate and extracellular acidification rate measurements showed that selective GSK3 inhibition led to an increase in mitochondrial respiration and a decrease in aerobic glycolysis (Warburg effect) in BON1KDMSO and BON1RR2 cells *in vitro*. Thus, we speculate that the increase in ^{18}F-FDG uptake during tumour growth (between T0 and T1) only in the resistant tumours could be attributed to the GSK3-mediated depleted mitochondrial function, and an increased Warburg effect during stress, in contrast to the higher mitochondrial respiration found in the everolimus-sensitive tumours. Everolimus itself has also been shown to impair mitochondrial respiration (Pelicano *et al.* 2014), and this may be partly compensated by increased activation of GSK3 and a stress-induced shift to higher aerobic glycolysis in the everolimus-resistant cells and tumours compared to the everolimus-sensitive tumours. Consistently, the resistant cell lines and tumours grew more slowly, and the resistant cell lines were more vulnerable to GSK3 inhibition, compared to the sensitive cell lines.

For further phenotype characterisation of our everolimus-resistant orthotopic pancreatic NEC mouse model, and to find out if combination treatment with everolimus and alpelisib leads to tumour cell differentiation and SSTR2 upregulation as shown *in vitro* (Nölting *et al.* 2017), ^{68}Ga-DOTATOC-PET imaging was performed. ^{68}Ga-DOTATOC imaging plays a significant role in the diagnosis, staging and follow-up of well-differentiated SSTR2 positive NETs, while ^{18}F-FDG plays a more important role in the diagnostic workflow of NET G3 (Ki-67 >20%) and NEC (mostly Ki-67 >55%), with low SSTR2 expression and increased metabolic turnover with high glucose intake and thus high ^{18}F-FDG uptake (Kayani *et al.* 2008, Rindi *et al.* 2018, Liu *et al.* 2020, Yu *et al.* 2022). The NET PET scoring system has been found to serve as a predictor of overall survival with high histological correlation (Chan *et al.* 2017, Bailey *et al.* 2019): ^{68}Ga-DOTATOC positive/^{18}F-FDG negative tumours had a better prognosis and prolonged survival compared to other groups (Chan *et al.* 2017). These findings are consistent with a higher ^{18}F-FDG than ^{68}Ga-DOTATOC tumour uptake in our study in which all of the tumours revealed a NEC morphology with increased Ki-67 (mostly 70–90%), poor differentiation, and necrosis (Fig. 1). Only 9% of all animals in our study showed a visually positive ^{68}Ga-DOTATOC PET, and there was no significant correlation between ^{68}Ga-DOTATOC imaging and histological SSTR2 expression. Although we have previously shown *in vitro* that combination treatment with everolimus and alpelisib led to NET cell (BON1) differentiation and strongly increased SSTR2 expression (Nölting *et al.* 2017), no increased expression of SSTR2 could be observed after combination treatment in our *in vivo* model. These findings might be explained by the fact that increased SSTR2 expression at a molecular level may not necessarily lead to increased

Downloaded from Bioscientifica.com at 01/29/2024 11:13:29AM
via HU - Charite Berlin

cellular surface expression accessible for radiolabelled receptor ligand molecules.

Interestingly, our study demonstrated liver metastasis formation in 17% of animals undergoing treatment, but no metastases were seen in the placebo-treated groups. Eight out of nine animals with metastases were found to be either from the alpelisib ($n = 4$) or the combination treatment group ($n = 4$), and one animal from the everolimus group. Previous animal studies have reported 50–70% metastases formation in a rat NET tumour model undergoing everolimus treatment, while no metastases occurred during treatment with ^{177}Lu-DOTATATE (Pool *et al.* 2013, Bison *et al.* 2014). One could hypothesise that, on the one hand, highly effective treatment (e.g. ^{177}Lu-DOTATATE) may prevent the formation of metastases, but on the other hand, the longer survival times of animals under targeted treatments might enhance their likelihood to develop metastases compared to placebo-treated animals. Accordingly, only effective targeted treatments (e.g. everolimus, alpelisib, and the combination in BON1KDMSO animals, as well as alpelisib and mostly combination in BON1RR2 animals), but not placebo treatment, led to metastasis formation. There was no significant difference regarding metastasis formation between BON1KDMSO and BON1RR2 animals *in vivo*.

In contrast to these preclinical findings, clinical data from the phase III RADIANT-3 trial in patients with pNETs have not demonstrated an increased risk of new metastasis in patients treated with everolimus vs placebo, reporting new metastases without/with tumour growth of preexisting target lesions in 45% vs 49%, respectively (Yao *et al.* 2011).

It is worth noting that both everolimus (FDA-approved for NET treatment) and alpelisib (FDA-approved for breast cancer treatment) are already in clinical use. As observed in our study, alpelisib-treated animals survived significantly longer with no additional side effects compared to the animals treated with everolimus, as recommended by the current guidelines. This suggests high anti-tumour potential of alpelisib in the treatment of NET/NEC. A phase 2 clinical study investigating alpelisib vs everolimus in NET/NEC would be the logical next step to provide further information on survival and toxicity in a clinical setting. We further conclude that combination treatment with everolimus and alpelisib seems promising to overcome everolimus resistance in neuroendocrine neoplasms and should also be further examined in a phase 2 clinical study. A dose-escalation phase 1b clinical study to determine the maximum tolerated/recommended dose of alpelisib in combination with everolimus, assessing the safety, preliminary efficacy, and effects of alpelisib on the pharmacokinetics of everolimus in solid tumours including pNETs, has already been published in 2021 (Curigliano *et al.* 2021): in the pNET cohort, the 16-week progression-free survival under combination treatment was 35.3%.

In the future, it would be, moreover, very interesting to perform the reverse experiment of our current study in order to determine if treatment resistance to alpelisib may be overcome by everolimus.

Supplementary materials

This is linked to the online version of the paper at https://doi.org/10.1530/ERC-23-0041.

Declaration of interest

The authors declare that there is no conflict of interest that could be perceived as prejudicing the impartiality of the study reported.

Acknowledgements

This work was supported by the Else Kröner-Fresenius-Stiftung (2018_A79) (to SN), the German Research Foundation (Deutsche Forschungsgemeinschaft (DFG)) within the CRC/Transregio 205/2, Project number: 314061271 – TRR 205 'The Adrenal: Central Relay in Health and Disease' (to SN, FB and MR), Technologiestiftung Berlin (TSB) for SPECT/CT use, the Deutsche Forschungsgemeinschaft (DFG) for nanoScan PET/CT (INST 335/454-1 FUGG) and 3T MRI system MRS 3017 (INST 335/516-1 FUGG) use, the Else Kröner-Fresenius-Stiftung (2019_A130) and Wilhelm Sander-Stiftung (2019.022.1) (to MI), the Hochschulmedizin Zurich as part of the Immuno-TargET project (to SN and FB). The BERIC and Preclinical MRI Center are supported by Charité 3R – Replace, Reduce, Refine. Ajay-Mohan Mohan is supported by a grant from Deutscher Akademischer Austausch Dienst (DAAD) for participation in the DFG-funded Berlin School of Integrative Oncology (BSIO) PhD program. Everolimus and alpelisib were provided by Novartis Pharma.

References

Aristizabal Prada ET, Spottl G, Maurer J, Lauseker M, Koziolek EJ, Schrader J, Grossman A, Pacak K, Beuschlein F, Auernhammer CJ, *et al.* 2018 The role of GSK3 and its reversal with GSK3 antagonism in everolimus resistance. *Endocrine-Related Cancer* **25** 893–908. (https://doi.org/10.1530/ERC-18-0159)

Bailey D, Chan D, Roach P, Schembri G, Bernard E, Hsiao E, Hayes A, Khasraw M, Samra J & Pavlakis N 2019 The prognostic impact of dual FDG/somatostatin receptor PET in metastatic neuroendocrine tumours: updated overall survival from the NETPET study. *Journal of Nuclear Medicine* **60** 505.

Beindorff N, Bartelheimer A, Huang K, Lukas M, Lange C, Huang EL, Aschenbach JR, Eary JF, Steffen IG & Brenner W 2018 Normal values of thyroid uptake of 99mTechnetium pertechnetate SPECT in mice with respect to age, sex, and circadian rhythm. *Nuklearmedizin. Nuclear Medicine* **57** 181–189. (https://doi.org/10.3413/Nukmed-0978-18-05)

Bison SM, Pool SE, Koelewijn SJ, van der Graaf LM, Groen HC, Melis M & de Jong M 2014 Peptide receptor radionuclide therapy (PRRT) with [(177)Lu-DOTA(0),Tyr(3)]octreotate in combination with RAD001 treatment: further investigations on tumor metastasis and response in the rat pancreatic CA20948 tumor model. *EJNMMI Research* **4** 21. (https://doi.org/10.1186/s13550-014-0021-y)

Caplin ME, Pavel M, Cwikla JB, Phan AT, Raderer M, Sedlackova E, Cadiot G, Wolin EM, Capdevila J, Wall L, *et al.* 2014 Lanreotide in metastatic enteropancreatic neuroendocrine tumors. *New England Journal of Medicine* **371** 224–233. (https://doi.org/10.1056/NEJMoa1316158)

Chan DL, Pavlakis N, Schembri GP, Bernard EJ, Hsiao E, Hayes A, Barnes T, Diakos C, Khasraw M, Samra J, *et al.* 2017 Dual somatostatin

Downloaded from Bioscientifica.com at 01/29/2024 11:13:29AM
via HU - Charite Berlin

receptor/FDG PET/CT imaging in metastatic neuroendocrine tumours: proposal for a novel grading scheme with prognostic significance. *Theranostics* **7** 1149–1158. (https://doi.org/10.7150/thno.18068)

Chiara F & Rasola A 2013 GSK-3 and mitochondria in cancer cells. *Frontiers in Oncology* **3** 16. (https://doi.org/10.3389/fonc.2013.00016)

Curigliano G, Martin M, Jhaveri K, Beck JT, Tortora G, Fazio N, Maur M, Hubner RA, Lahner H, Donnet V, *et al.* 2021 Alpelisib in combination with everolimus +/- exemestane in solid tumours: phase Ib randomised, open-label, multicentre study. *European Journal of Cancer* **151** 49–62. (https://doi.org/10.1016/j.ejca.2021.03.042)

Das S & Dasari A 2021 Epidemiology, incidence, and prevalence of neuroendocrine neoplasms: are there global differences? *Current Oncology Reports* **23** 43. (https://doi.org/10.1007/s11912-021-01029-7)

de Wilde RF, Edil BH, Hruban RH & Maitra A 2012 Well-differentiated pancreatic neuroendocrine tumors: from genetics to therapy. *Nature Reviews Gastroenterology and Hepatology* **9** 199–208. (https://doi.org/10.1038/nrgastro.2012.9)

Djukom C, Porro LJ, Mrazek A, Townsend CM, Hellmich MR & Chao C 2014 Dual inhibition of PI3K and mTOR signaling pathways decreases human pancreatic neuroendocrine tumor metastatic progression. *Pancreas* **43** 88–92. (https://doi.org/10.1097/MPA.0b013e3182a44ab4)

Fankhauser M, Bechmann N, Lauseker M, Goncalves J, Favier J, Klink B, William D, Gieldon L, Maurer J, Spottl G, *et al.* 2019 Synergistic highly potent targeted drug combinations in different pheochromocytoma models including human tumor cultures. *Endocrinology* **160** 2600–2617. (https://doi.org/10.1210/en.2019-00410)

FDA 2019 Highlights of prescribing information. Silver Spring, MD, USA: Food and Drug Administration. (available at: https://www.accessdata.fda.gov/drugsatfda_docs/label/2019/212526s000lbl.pdf)

Frilling A, Modlin IM, Kidd M, Russell C, Breitenstein S, Salem R, Kwekkeboom D, Lau WY, Klersy C, Vilgrain V, *et al.* 2014 Recommendations for management of patients with neuroendocrine liver metastases. *Lancet. Oncology* **15** e8–e21. (https://doi.org/10.1016/S1470-2045(13)70362-0)

Hedges CP, Boix J, Jaiswal JK, Shetty B, Shepherd PR & Merry TL 2021 Efficacy of providing the PI3K p110alpha inhibitor BYL719 (alpelisib) to middle-aged mice in their diet. *Biomolecules* **11**. (https://doi.org/10.3390/biom11020150)

Huang K, Lukas M, Steffen IG, Lange C, Huang EL, Dorau V, Brenner W & Beindorff N 2018 Normal Values of Renal Function measured with 99mTechnetium mercaptoacetyltriglycine SPECT in Mice with Respect to Age, Sex and Circadian Rhythm. *Nuklearmedizin. Nuclear Medicine* **57** 224–233. (https://doi.org/10.3413/Nukmed-0999-18-09)

Jussing E, Milton S, Samen E, Moein MM, Bylund L, Axelsson R, Siikanen J & Tran TA 2021 Clinically applicable cyclotron-produced gallium-68 gives high-yield radiolabeling of DOTA-based tracers. *Biomolecules* **11**. (https://doi.org/10.3390/biom11081118)

Kayani I, Bomanji JB, Groves A, Conway G, Gacinovic S, Win T, Dickson J, Caplin M & Ell PJ 2008 Functional imaging of neuroendocrine tumors with combined PET/CT using 68ga-DOTATATE (DOTA-DPhe1,Tyr3-octreotate) and 18F-FDG. *Cancer* **112** 2447–2455. (https://doi.org/10.1002/cncr.23469)

Kim HJ, Gong MK, Yoon CY, Kang J, Yun M, Cho NH, Rha SY & Choi YD 2020 Synergistic antitumor effects of combined treatment with HSP90 inhibitor and PI3K/mTOR dual inhibitor in cisplatin-resistant human bladder cancer cells. *Yonsei Medical Journal* **61** 587–596. (https://doi.org/10.3349/ymj.2020.61.7.587)

Launay-Vacher V, Aapro M, de Castro G, Cohen E, Deray G, Dooley M, Humphreys B, Lichtman S, Rey J, Scotte F, *et al.* 2015 Renal effects of molecular targeted therapies in oncology: a review by the Cancer and the Kidney International Network (C-KIN). *Annals of Oncology* **26** 1677–1684. (https://doi.org/10.1093/annonc/mdv136)

Liu X, Li N, Jiang T, Xu H, Ran Q, Shu Z, Wu J, Li Y, Zhou S & Zhang B 2020 Comparison of gallium-68 somatostatin receptor and (18) F-fluorodeoxyglucose positron emission tomography in the diagnosis of neuroendocrine tumours: a systematic review and meta-analysis. *Hellenic Journal of Nuclear Medicine* **23** 188–200. (https://doi.org/10.1967/s002449912108)

Markham A 2019 Alpelisib: first global approval. *Drugs* **79** 1249–1253. (https://doi.org/10.1007/s40265-019-01161-6)

Nagtegaal ID, Odze RD, Klimstra D, Paradis V, Rugge M, Schirmacher P, Washington KM, Carneiro F, Cree IA & Board Whocote 2020 The 2019 WHO classification of tumours of the digestive system. *Histopathology* **76** 182–188. (https://doi.org/10.1111/his.13975)

Nölting S, Rentsch J, Freitag H, Detjen K, Briest F, Mobs M, Weissmann V, Siegmund B, Auernhammer CJ, Aristizabal Prada ET, *et al.* 2017 The selective PI3Kalpha inhibitor BYL719 as a novel therapeutic option for neuroendocrine tumors: results from multiple cell line models. *PLoS One* **12** e0182852. (https://doi.org/10.1371/journal.pone.0182852)

Okuyama H, Ikeda M, Okusaka T, Furukawa M, Ohkawa S, Hosokawa A, Kojima Y, Hara H, Murohisa G, Shioji K, *et al.* 2020 A Phase II trial of everolimus in patients with advanced pancreatic neuroendocrine carcinoma refractory or intolerant to platinum-containing chemotherapy (NECTOR trial). *Neuroendocrinology* **110** 988–993. (https://doi.org/10.1159/000505550)

Panzuto F, Rinzivillo M, Spada F, Antonuzzo L, Ibrahim T, Campana D, Fazio N & Delle Fave G 2017 Everolimus in pancreatic neuroendocrine carcinomas G3. *Pancreas* **46** 302–305. (https://doi.org/10.1097/MPA.0000000000000762)

Papadopoli D, Pollak M & Topisirovic I 2021 The role of GSK3 in metabolic pathway perturbations in cancer. *Biochimica et Biophysica Acta. Molecular Cell Research* **1868** 119059. (https://doi.org/10.1016/j.bbamcr.2021.119059)

Passacantilli I, Capurso G, Archibugi L, Calabretta S, Caldarola S, Loreni F, Delle Fave G & Sette C 2014 Combined therapy with RAD001 e BEZ235 overcomes resistance of PET immortalized cell lines to mTOR inhibition. *Oncotarget* **5** 5381–5391. (https://doi.org/10.18632/oncotarget.2111)

Pavel M, Oberg K, Falconi M, Krenning EP, Sundin A, Perren A, Berruti A & ESMO Guidelines Committee. Electronic address: clinicalguidelines@esmo.org 2020 Gastroenteropancreatic neuroendocrine neoplasms: ESMO Clinical Practice Guidelines for diagnosis, treatment and follow-up. *Annals of Oncology* **31** 844–860. (https://doi.org/10.1016/j.annonc.2020.03.304)

Pelicano H, Zhang W, Liu J, Hammoudi N, Dai J, Xu RH, Pusztai L & Huang P 2014 Mitochondrial dysfunction in some triple-negative breast cancer cell lines: role of mTOR pathway and therapeutic potential. *Breast Cancer Research* **16** 434. (https://doi.org/10.1186/s13058-014-0434-6)

Pool SE, Bison S, Koelewijn SJ, van der Graaf LM, Melis M, Krenning EP & de Jong M 2013 mTOR inhibitor RAD001 promotes metastasis in a rat model of pancreatic neuroendocrine cancer. *Cancer Research* **73** 12–18. (https://doi.org/10.1158/0008-5472.CAN-11-2089)

Raymond E, Dahan L, Raoul JL, Bang YJ, Borbath I, Lombard-Bohas C, Valle J, Metrakos P, Smith D, Vinik A, *et al.* 2011 Sunitinib malate for the treatment of pancreatic neuroendocrine tumors. *New England Journal of Medicine* **364** 501–513. (https://doi.org/10.1056/NEJMoa1003825)

Rindi G, Klimstra DS, Abedi-Ardekani B, Asa SL, Bosman FT, Brambilla E, Busam KJ, de Krijger RR, Dietel M, El-Naggar AK, *et al.* 2018 A common classification framework for neuroendocrine neoplasms: an International Agency for Research on Cancer (IARC) and World Health Organization (WHO) expert consensus proposal. *Modern Pathology* **31** 1770–1786. (https://doi.org/10.1038/s41379-018-0110-y)

Rindi G, Mete O, Uccella S, Basturk O, La Rosa S, Brosens LAA, Ezzat S, De Herder WW, Klimstra DS, Papotti M, *et al.* 2022 Overview of the 2022

Downloaded from Bioscientifica.com at 01/29/2024 11:13:29AM
via HU - Charite Berlin

WHO classification of neuroendocrine neoplasms. *Endocrine Pathology* **33** 115–154. (https://doi.org/10.1007/s12022-022-09708-2)

Rinke A, Muller HH, Schade-Brittinger C, Klose KJ, Barth P, Wied M, Mayer C, Aminossadati B, Pape UF, Blaker M, *et al.* 2009 Placebo-controlled, double-blind, prospective, randomized study on the effect of octreotide LAR in the control of tumor growth in patients with metastatic neuroendocrine midgut tumors: a report from the PROMID Study Group. *Journal of Clinical Oncology* **27** 4656–4663. (https://doi.org/10.1200/JCO.2009.22.8510)

Sciammarella C, Luce A, Riccardi F, Mocerino C, Modica R, Berretta M, Misso G, Cossu AM, Colao A, Vitale G, *et al.* 2020 Lanreotide induces cytokine modulation in intestinal neuroendocrine tumors and overcomes resistance to everolimus. *Frontiers in Oncology* **10** 1047. (https://doi.org/10.3389/fonc.2020.01047)

Strosberg JR, Caplin ME, Kunz PL, Ruszniewski PB, Bodei L, Hendifar A, Mittra E, Wolin EM, Yao JC, Pavel ME, *et al.* 2021 (177)Lu-Dotatate plus long-acting octreotide versus highdose long-acting octreotide in patients with midgut neuroendocrine tumours (NETTER-1): final overall survival and long-term safety results from an open-label, randomised, controlled, phase 3 trial. *Lancet Oncology* **22** 1752–1763.

Vandamme T, Beyens M, de Beeck KO, Dogan F, van Koetsveld PM, Pauwels P, Mortier G, Vangestel C, de Herder W, Van Camp G, *et al.* 2016 Long-term acquired everolimus resistance in pancreatic neuroendocrine tumours can be overcome with novel PI3K-AKT-mTOR inhibitors. *British Journal of Cancer* **114** 650–658. (https://doi.org/10.1038/bjc.2016.25)

Vitali E, Boemi I, Tarantola G, Piccini S, Zerbi A, Veronesi G, Baldelli R, Mazziotti G, Smiroldo V, Lavezzi E, *et al.* 2020 Metformin and everolimus: a promising combination for neuroendocrine tumors treatment. *Cancers (Basel)* **12**. (https://doi.org/10.3390/cancers12082143)

Wang K, Schutze I, Gulde S, Bechmann N, Richter S, Helm J, Lauseker M, Maurer J, Reul A, Spoettl G, *et al.* 2022 Personalized drug testing in human pheochromocytoma/paraganglioma primary cultures. *Endocrine-Related Cancer* **29** 285–306. (https://doi.org/10.1530/ERC-21-0355)

White BE, Rous B, Chandrakumaran K, Wong K, Bouvier C, van Hemelrijck M, George G, Russell B, Srirajaskanthan R & Ramage JK 2022 Incidence and survival of neuroendocrine neoplasia in England 1995–2018: a retrospective, population-based study. *Lancet Regional Health. Europe* **23** 100510. (https://doi.org/10.1016/j.lanepe.2022.100510)

Yang S, Xiao X, Meng X & Leslie KK 2011 A mechanism for synergy with combined mTOR and PI3 kinase inhibitors. *PLoS One* **6** e26343. (https://doi.org/10.1371/journal.pone.0026343)

Yang K, Chen Z, Gao J, Shi W, Li L, Jiang S, Hu H, Liu Z, Xu D & Wu L 2017 The key roles of GSK-3beta in regulating mitochondrial activity. *Cellular Physiology and Biochemistry* **44** 1445–1459. (https://doi.org/10.1159/000485580)

Yao JC, Shah MH, Ito T, Bohas CL, Wolin EM, Van Cutsem E, Hobday TJ, Okusaka T, Capdevila J, de Vries EG, *et al.* 2011 Everolimus for advanced pancreatic neuroendocrine tumors. *New England Journal of Medicine* **364** 514–523. (https://doi.org/10.1056/NEJMoa1009290)

Yao JC, Fazio N, Singh S, Buzzoni R, Carnaghi C, Wolin E, Tomasek J, Raderer M, Lahner H, Voi M, *et al.* 2016 Everolimus for the treatment of advanced, non-functional neuroendocrine tumours of the lung or gastrointestinal tract (RADIANT-4): a randomised, placebo-controlled, phase 3 study. *Lancet* **387** 968–977. (https://doi.org/10.1016/S0140-6736(15)00817-X)

Yu J, Cao F, Zhao X, Xie Q, Lu M, Li J, Yang Z & Sun Y 2022 Correlation and comparison of somatostatin receptor Type 2 immunohistochemical scoring systems with 68ga-DOTATATE positron emission tomography/computed tomography imaging in gastroenteropancreatic neuroendocrine neoplasms. *Neuroendocrinology* **112** 358–369. (https://doi.org/10.1159/000517530)

Zitzmann K, Ruden J, Brand S, Goke B, Lichtl J, Spottl G & Auernhammer CJ 2010 Compensatory activation of Akt in response to mTOR and Raf inhibitors - a rationale for dual-targeted therapy approaches in neuroendocrine tumor disease. *Cancer Letters* **295** 100–109. (https://doi.org/10.1016/j.canlet.2010.02.018)

Downloaded from Bioscientifica.com at 01/29/2024 11:13:29AM
via HU - Charite Berlin

7. Appendix (Publication III)

The Journal of Clinical Endocrinology & Metabolism, 2022, **107**, 2963–2972
https://doi.org/10.1210/clinem/dgac471
Advance access publication 17 August 2022
Mini-Review

Targeted Therapies in Pheochromocytoma and Paraganglioma

Katharina Wang,[1] Joakim Crona,[2] Felix Beuschlein,[1,6] Ashley B. Grossman,[3,4] Karel Pacak,[5] and Svenja Nölting[1,6]

[1]Department of Internal Medicine IV, University Hospital, LMU Klinikum, Ludwig Maximilian University of Munich, 80336 Munich, Germany
[2]Department of Medical Sciences, Uppsala University, 75185 Uppsala, Sweden
[3]Green Templeton College, University of Oxford, Oxford OX2 6HG, United Kingdom
[4]NET Unit, ENETS Centre of Excellence, Royal Free Hospital, London NW3 2QG, United Kingdom
[5]Eunice Kennedy Shriver National Institute of Child Health and Human Development, National Institutes of Health, Bethesda, Maryland 20892-1109, USA; and
[6]Department of Endocrinology, Diabetology and Clinical Nutrition, University Hospital Zurich (USZ) and University of Zurich (UZH), 8091 Zurich, Switzerland

Correspondence: Svenja Nölting, MD, Department of Endocrinology, Diabetology and Clinical Nutrition, University Hospital Zurich (USZ) and University of Zurich (UZH), Rämistrasse 100, CH 8091 Zurich, Switzerland. Email: svenja.noelting@usz.ch

Abstract

Molecular targeted therapy plays an increasingly important role in the treatment of metastatic pheochromocytomas and paragangliomas (PPGLs), which are rare tumors but remain difficult to treat. This mini-review provides an overview of established molecular targeted therapies in present use, and perspectives on those currently under development and evaluation in clinical trials. Recently published research articles, guidelines, and expert views on molecular targeted therapies in PPGLs are systematically reviewed and summarized. Some tyrosine kinase inhibitors (sunitinib, cabozantinib) are already in clinical use with some promising results, but without formal approval for the treatment of PPGLs. Sunitinib is the only therapeutic option which has been investigated in a randomized placebo-controlled clinical trial. It is clinically used as a first-, second-, or third-line therapeutic option for the treatment of progressive metastatic PPGLs. Some other promising molecular targeted therapies (hypoxia-inducible factor 2 alpha [HIF2α] inhibitors, tumor vaccination together with checkpoint inhibitors, antiangiogenic therapies, kinase signaling inhibitors) are under evaluation in clinical trials. The HIF2α inhibitor belzutifan may prove to be particularly interesting for cluster 1B-/*VHL/EPAS1*-related PPGLs, whereas antiangiogenic therapies seem to be primarily effective in cluster 1A-/*SDHx*-related PPGLs. Some combination therapies currently being evaluated in clinical trials, such as temozolomide/olaparib, temozolomide/talazoparib, or cabozantinib/atezolizumab, will provide data for novel therapy for metastatic PPGLs. It is likely that advances in such molecular targeted therapies will play an essential role in the future treatment of these tumors, with more personalized therapy options paving the way towards improved therapeutic outcomes.

Key Words: molecular targeted therapy, metastatic, pheochromocytoma, paraganglioma

Abbreviations: ccRCC, clear cell renal cell carcinoma; CT, computed tomography; CVD, cyclophosphamide/vincristine/dacarbazine; DCR, disease control rate; FDA, US Food and Drug Administration; [^{18}F]-FDOPA PET/CT, [^{18}F]-fluorodihydroxyphenylalanine positron emission tomography-CT; HIF2α, hypoxia-inducible factor 2 alpha; HSA, high specific activity; MRI, magnetic resonance imaging; NET, neuroendocrine tumor; ORR, objective response rate; PARP, poly (ADP-ribose) polymerase; PFS, progression-free survival; PPGL, pheochromocytoma and paraganglioma; PRRT, peptide (somatostatin) receptor (SSTR)-based radionuclide therapy; RCC, renal cell carcinoma; SSTR, somatostatin receptor; TKI, tyrosine kinase inhibitor; VHL, von Hippel-Lindau; [^{68}Ga]-DOTA-SSA PET/CT, ^{68}Gallium-labeled somatostatin analogue positron emission tomography-computed tomography

Pheochromocytomas and paragangliomas are a group of neuroendocrine neoplasms that originate from the adrenal medulla (pheochromocytomas) or the sympathetic or parasympathetic extra-adrenal paraganglia (paragangliomas). These tumors, collectively referred to as PPGLs, show the highest rate of heritability or genetically known causes among all endocrine tumors.

In recent years, an increasing number of variants in genes involved in PPGL tumor pathogenesis have been discovered, as previously reviewed (1). Germline mutations are known to be present in up to 30% to 35% of PPGL patients, whereas somatic mutations in similar genes can be found in up to one-half of patients (2-8). Thus, around 70% to 80% of all patients show germline or somatic mutations in known PPGL disease-causing genes, and genetic testing is recommended for every patient because this may guide their management and improve their clinical outcome (9-12).

PPGLs can be assigned to 1 of 3 main molecular clusters depending on their genetic signature: pseudohypoxia-related cluster 1 (1A or 1B), kinase signaling-related cluster 2, or Wnt signaling-related cluster 3 (**Fig. 1**). These clusters are associated with distinct biochemical profiles, imaging-related functionalities, clinical presentations, and prognostic differences. Genetic profiling of PPGLs therefore allows for personalized diagnostics and follow-up of these tumors. Although cluster-specific biochemical phenotyping, imaging, and follow-up have already entered routine clinical practice

Received: 29 May 2022. **Editorial Decision:** 2 August 2022. **Corrected and Typeset:** 26 August 2022
© The Author(s) 2022. Published by Oxford University Press on behalf of the Endocrine Society. All rights reserved. For permissions, please e-mail: journals.permissions@oup.com

Downloaded from https://academic.oup.com/jcem/article/107/11/2963/6668850 by Universitaetsbibliothek Muenchen user on 31 January 2024

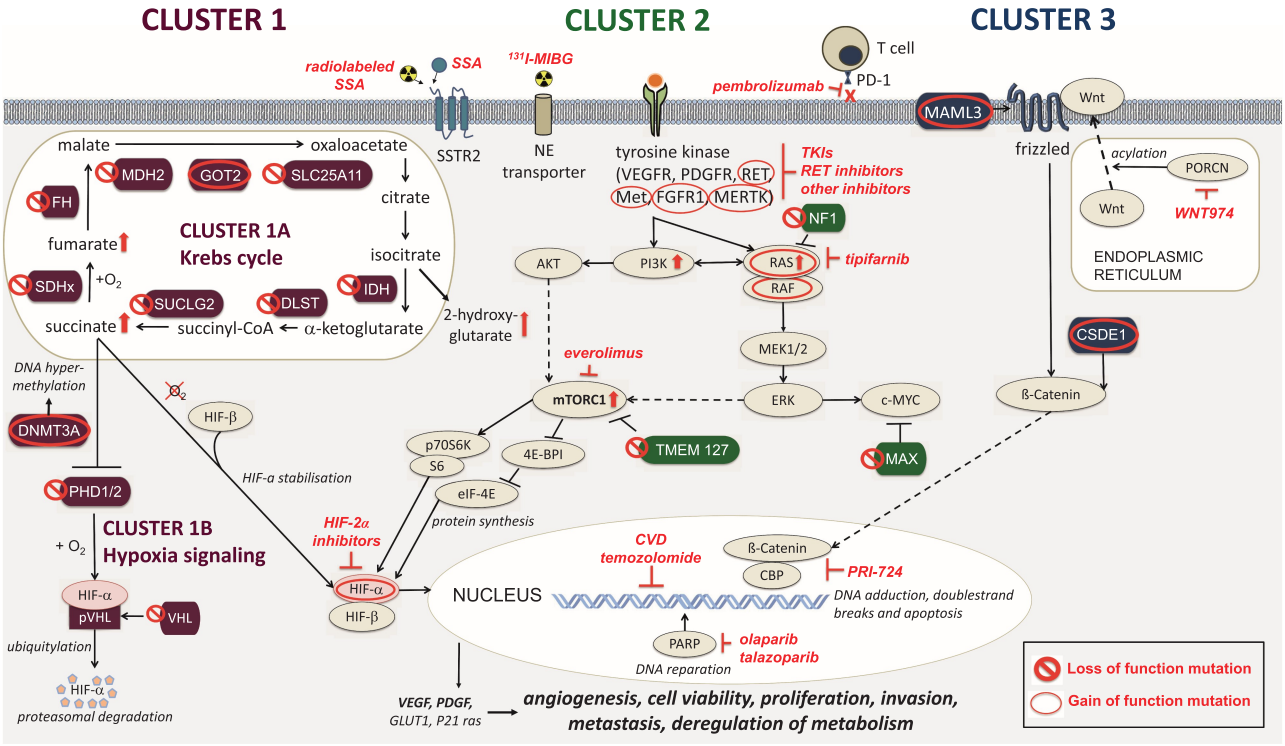

Figure 1. The 3 main molecular clusters of PPGLs and their associated gain (○) or loss (⊘) of function mutations. Cluster 1 mutations (crimson) include mutations in cluster 1A/Krebs cycle-related genes (*SDHx, FH, MDH2, GOT2, SLC25A11, IDH, DLST, SUCLG2*) and cluster 1B/hypoxia signaling-related genes (*PHD1/2, VHL, HIF2A/EPAS1*). These mutations lead to an accumulation of oncometabolites, increased DNS hypermethylation, decreased HIF-α degradation and HIF-α stabilization. Cluster 2 mutations (green) disrupt the kinase signaling pathway and lead to their overactivation (*RET, MET, FGFR1, MERTK, NGFR, NF1, HRAS, BRAF, TMEM127, MAX*). Cluster 3 mutations (blue) affect the Wnt signaling pathway (*MAML3, CSDE1*). All mutations may lead to increased angiogenesis, cell proliferation, invasion, metastasis, and deregulation of metabolism. Potential therapies are shown in red. ⇧ protein activation or upregulation; ⊥ protein inhibition.

(12), therapy has largely remained nonspecific and unrelated to mutation status.

In terms of treatment, options are overall still limited for PPGL patients with metastatic disease, and there are no treatment options that may offer a complete cure to this disease. The only officially approved therapy currently available is high specific activity (HSA) [^{131}I]-MIBG therapy that is approved only in the United States (13). Around 10% to 15% of all patients with pheochromocytomas, plus a significantly higher proportion of patients with paragangliomas (35%-40%), develop metastases (14-21). Although cluster 1 tumors, particularly *SDHB*- and *SDHA*-mutant PPGLs, show a high metastatic risk of up to 75% (2, 20, 22-24), of the 3 clusters, cluster 2 tumors are associated with the lowest metastatic risk of 3% to 10% (2, 24, 25). Cluster 3 tumors are relatively rare but show aggressive behavior and a high metastatic risk (2, 26). Overall, 5- and 10-year mortality rates for metastatic patients have been reported to be 37% and 29%, respectively (27), with *SDHB* mutations in particular associated with decreased survival in metastatic PPGL patients (28).

Therefore, with only few established therapeutic options available for metastatic PPGLs, novel therapeutic approaches are urgently needed (12, 29, 30). In recent years, personalized and genetically guided therapy has become increasingly investigated, with some molecular targeted therapies already playing a role in the therapy of metastatic PPGLs. Molecular targeted therapy is defined as a treatment that targets specific molecules that play key roles in cancer growth and survival, leading to an inhibition of tumor cell growth and progression, or a promotion of tumor cell death (31, 32).

This mini-review focuses on molecular targeted therapies for metastatic PPGLs, providing an overview of existing therapeutic options and their efficacy, and highlights the current development of novel personalized molecular targeted therapies. Recently published research articles, guidelines, and expert views on molecular targeted therapies in PPGLs were systematically reviewed, and are summarized in this mini-review.

Management of Metastatic PPGLs

The diagnosis of metastatic PPGL patients is based, similarly to nonmetastatic PPGL patients, either on their clinical presentation with typical signs and symptoms, on the presence of an adrenal incidentaloma, or following surveillance because of a personal or family history (11). However, compared with nonmetastatic PPGL patients, metastatic disease may more often lead to a clinical presentation with severe hypertension or fluctuation in blood pressure because of a higher tumor burden (11, 33). To confirm or rule out a PPGL, subsequent biochemical testing and imaging is indicated (34).

The management of metastatic PPGLs is highly dependent on their biochemical phenotype, ideally determined by measurement of plasma-free metanephrines using liquid chromatography-tandem mass spectrometry (12). Cluster 1 PPGLs predominantly present with a noradrenergic phenotype, defined by an increase of normetanephrine either

Downloaded from https://academic.oup.com/jcem/article/107/11/2963/6668850 by Universitaetsbibliothek Muenchen user on 31 January 2024

without an increase in metanephrines or with an increase of metanephrine less than 5% of the increase in both metabolites (35). Less commonly, 3-methoxytyramine may also be increased—defining a dopaminergic phenotype (36). Cluster 2 PPGLs are predominantly adrenergic, defined by an increase in plasma metanephrine more than 5% of the increase of all metabolites (35, 36). The precise biochemical phenotype of cluster 3 PPGLs is still unknown (12).

The imaging modalities chosen for screening are dependent on many factors including primary tumor location (adrenal vs extra-adrenal), mutation and patient age. Computed tomography (CT) imaging is preferred for the screening of adrenal tumors and shows higher sensitivity than magnetic resonance imaging (MRI) scans in the detection of lung metastases (12). MRI is now the preferred imaging modality for the screening of extra-adrenal tumors and for the detection of liver metastases. MRI is also preferably used in children and for long-term follow-up of all patients (37). If functional imaging is indicated, the use of the ^{68}Gallium-labeled somatostatin analogue positron emission tomography-CT ([^{68}Ga]-DOTA-SSA PET/CT) is recommended for cluster 1A-related PPGL patients, whereas [^{18}F]-fluorodihydroxyphenylalanine positron emission tomography-CT ([^{18}F]-FDOPA PET/CT) is recommended as first-line functional imaging for cluster 1B- and cluster 2-related PPGL patients (12, 38).

Following the initial diagnosis of a PPGL, genetic counseling and testing should be recommended for every patient (9, 12). Certain mutations (eg, *SDHB*, *ARTX*) as well as a tumor size >5 cm, multifocality, previously detected metastases, or a noradrenergic/dopaminergic biochemical phenotype, are all characteristics associated with a higher risk of the development of future metastases (28, 39-41).

Individualized therapy decisions, particularly for metastatic patients, should be made in a multidisciplinary tumor board, preferably in a specialized center (9, 12). In general, surgery is the only curative therapy available, and is indicated as first-line therapy for locoregional disease or maybe oligometastatic disease in selected cases, but may also be used to provide symptomatic relief (eg, by lowering catecholamine levels) in the case of catecholamine-related signs and symptoms, or to reduce tumor mass effects for patients with widespread metastases (12, 42). Furthermore, some studies have suggested resection of the primary tumor and of the metastases to be beneficial for metastatic PPGL patients (39, 43-46); however, more conclusive evidence is still needed.

In functional PPGLs, alpha-adrenoreceptor blockade is usually indicated for 7 to 14 days before any treatment intervention, surgical or otherwise, and should be continued for at least 3 days after ablative or systemic therapies (9, 11, 42). Moreover, alpha-adrenoreceptor blockade should be considered in each patient with metastatic disease with catecholamine-related signs and symptoms.

Because there are no officially approved systemic therapies available for metastatic PPGLs, apart from HSA [^{131}I]-MIBG therapy in the United States, therapy is largely based on past practice and experience.

Therapy of Metastatic PPGLs With a Special Focus on Molecular Targeted Therapies

The treatment algorithm for metastatic PPGL patients should be personalized, based on the rate of progression, overall tumor burden, location of metastases, and the general condition of each patient including assessment of co-morbidities. A flow chart of the practical therapy standards is shown in **Fig. 2**. The original data and studies supporting the practical therapy standards are summarized and reviewed in Nölting et al (12).

Various modalities can be used to affect symptomatic control, including those from mass effects and catecholamine-related signs and symptoms, in appropriate circumstances; these would include palliative resection of the primary or metastases, alpha-adrenoreceptor blockade, interventional radiology, or radiotherapy (12).

Although molecular targeted therapy is being increasingly studied in patients with metastatic PPGLs, systemic therapy is still largely based on conventional chemotherapy or based on some specific characteristics as with targeted radionuclide therapy. Moreover, such practical therapy standards are mostly based on retrospective data, with few prospective trials and only 1 completed randomized placebo-controlled clinical trial (FIRST-MAPPP) (47).

Molecular targeted therapies include therapeutic approaches such as antiangiogenic agents and hypoxia-inducible factor 2 alpha (HIF2α) inhibitors, especially for cluster 1 tumors, inhibitors of kinase signaling pathways (PI3K/AKT/mTOR, Ras/Raf/MEK/ERK), especially for cluster 2 tumors, and potentially Wnt signaling inhibitors for cluster 3 tumors. All ongoing clinical trials investigating molecular targeted therapy in PPGL patients are listed in **Table 1**.

Chemotherapy

Cytotoxic chemotherapy using cyclophosphamide/vincristine/dacarbazine (CVD, *Averbuch* scheme) or temozolomide are conventional therapeutic options for metastatic PPGL patients. These therapies are only briefly mentioned here to give an overview of the practical therapy standards but are not considered targeted therapy. For metastatic PPGLs with rapid progression and a high visceral tumor burden, CVD chemotherapy may be the treatment of choice (12, 42). The largest meta-analysis on CVD therapy reported a partial response concerning tumor volume in 37% of patients (4 studies), and a partial response concerning catecholamine excess in 40% of patients (2 studies) (48). However, complete responses regarding tumor volume and catecholamine excess were only seen in 4% and 14%, respectively.

Although temozolomide has also shown promising efficacy in metastatic, particularly *SDHB*-mutant, PPGLs in retrospective studies (49, 50), prospective data are still lacking. At present, probably the main place of temozolomide is in patients showing slow-to-moderate progression and who are not eligible for peptide (somatostatin) receptor (SSTR)-based radionuclide therapy (PRRT) or MIBG therapy, or who show slow-to-moderate progression after such treatment (12, 49, 50).

Combination therapy: temozolomide plus poly (ADP-ribose) inhibitor (targeted therapy)

A preclinical study showed that combining temozolomide with a poly (ADP-ribose) polymerase (PARP) inhibitor may be a novel therapeutic approach in *SDHB*-mutant PPGLs (51), and a prospective randomized clinical phase 2 study investigating temozolomide vs temozolomide plus the PARP inhibitor olaparib in metastatic PPGL is currently recruiting

Downloaded from https://academic.oup.com/jcem/article/107/11/2963/6668850 by Universitaetsbibliothek Muenchen user on 31 January 2024

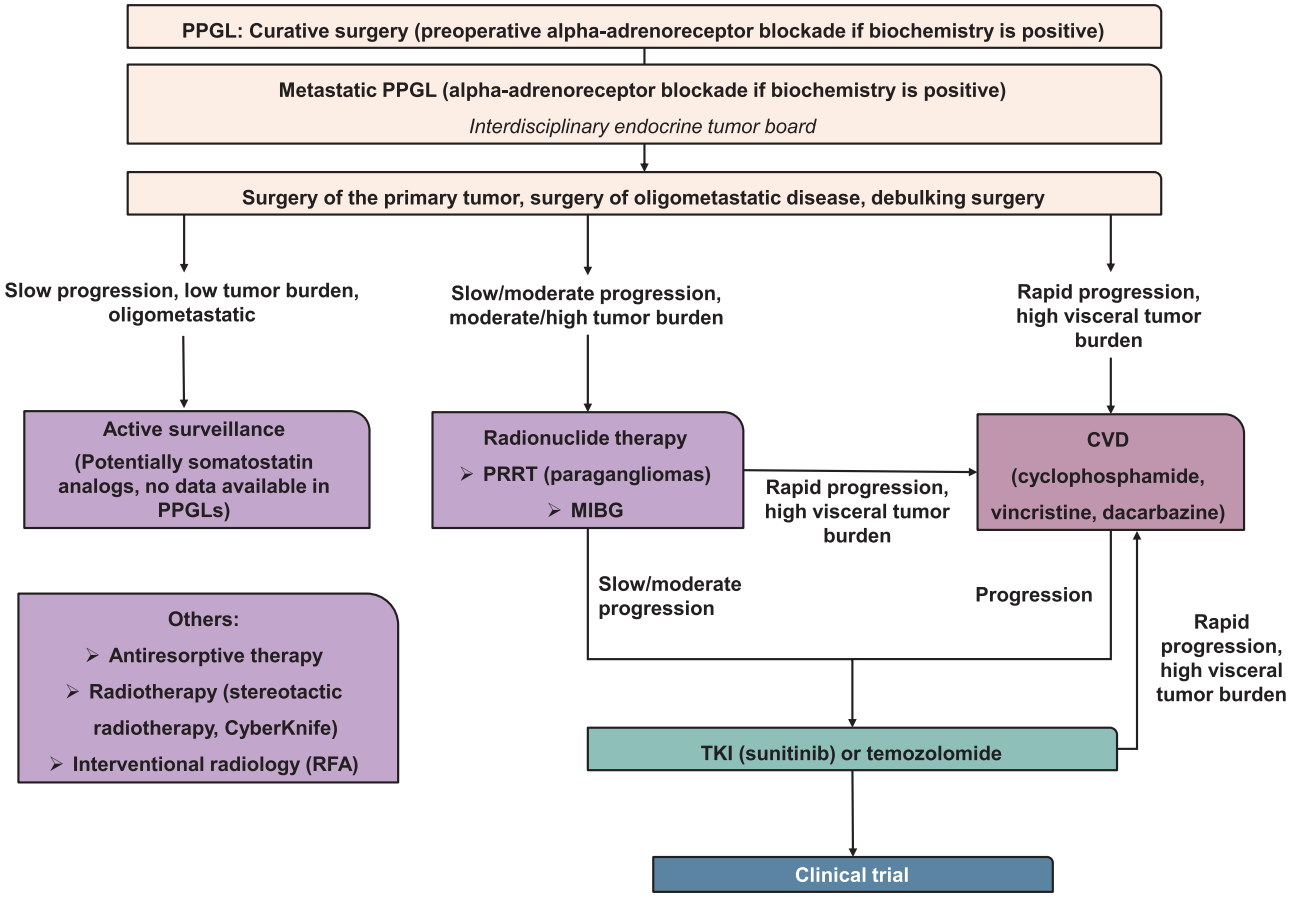

Figure 2. Simplified flow chart of the practical therapy standards in metastatic PPGLs (12). Each metastatic PPGL patient should be discussed in an interdisciplinary endocrine tumor board. Surgery of the primary tumor, of oligometastatic disease or debulking surgery, should always be considered. In the case of slow progression, low tumor burden and oligometastatic disease, active surveillance may be considered. In patients with slow-to-moderate progression, moderate-to-high tumor burden and positivity on SSTR2 or MIBG imaging, radionuclide therapy using either PRRT or MIBG (depending on avidity on molecular imaging) may be applied. For slowly/moderately progressing tumors that are not eligible for PRRT or MIBG, TKIs or temozolomide may be considered as first-line therapies. In the case of rapid progression or high visceral tumor burden, CVD chemotherapy may be applied. In the case of slow-to-moderate progression following radionuclide therapy, TKIs or temozolomide may be considered. In the case of rapid progression and high visceral tumor burden following other systemic therapies, CVD should be considered. Following progression to CVD, TKIs, or temozolomide may be considered. In case of further progression, inclusion in clinical trials may be considered. MIBG, meta-[^{131}I] iodobenzylguanidine; PRRT, somatostatin receptor-based radionuclide therapy; RFA, radiofrequency ablation; TKI, tyrosine kinase inhibitor.

(NCT04394858). Another phase 2 trial investigating temozolomide in combination with the PARP inhibitor talazoparib in advanced cancers, including PPGLs, is also now recruiting (RARE 2, NCT05142241).

Targeted Radionuclide Therapy

In patients with slow-to-moderate progression and moderate-to-high tumor burden, targeted radionuclide therapy using peptide PRRT or meta-[^{131}I] iodobenzylguanidine ([^{131}I]-MIBG) may currently be used as first-line therapeutic options (11-13). However, such PPRT is only indicated if the tumor is positive on [^{68}Ga]-DOTA-SSA imaging (12, 52), whereas HSA or conventional [^{131}I]-MIBG therapy may be applied in patients with tumors that show uptake on [^{123}I]-MIBG imaging (13, 42).

HSA [^{131}I]-MIBG therapy has been US Food and Drug Administration (FDA)-approved based on a phase 2 study with good results (n = 64, partial response or stable disease in 92%, median overall survival 36.7 months) (13). However, studies have shown that metastatic cluster 1-, particularly *SDHB*-related, PPGLs may be less frequently positive on [^{123}I]-MIBG imaging (53). Therefore, other radionuclide therapies, such as PRRT, may be particularly interesting for cluster 1-related PPGLs, which often show strong SSTR2 expression and positivity on [^{68}Ga]-DOTA-SSA imaging (38, 54, 55). A prospective study has also shown particularly long overall survival (82 months) in metastatic paraganglioma patients (n = 28) following [^{90}Y] DOTATOC therapy, further suggesting a high therapeutic potential of PRRT in metastatic paragangliomas (56).

Other types of PRRT are now also being evaluated. PRRT using alpha-particle emitting radionuclides such as ^{225}Ac-DOTATATE has shown promising results in metastatic gastro-enteropancreatic neuroendocrine tumor (NET) patients who are refractory to or have reached the maximum therapy cycles of ^{177}Lu-DOTATATE therapy and may also prove to be valuable for metastatic PPGL patients (57). PRRT using SSTR antagonists, which may have higher tumor-binding affinity than SSTR agonists (58), has been shown to be clinically feasible and effective (59). However, there are still no completed or active clinical trials investigating these types of PRRT in patients with metastatic PPGL.

Downloaded from https://academic.oup.com/jcem/article/107/11/2963/6668850 by Universitaetsbibliothek Muenchen user on 31 January 2024

Table 1. Ongoing clinical trials investigating molecular targeted therapy in PPGLs, listed in order of their mention in the text

Ongoing clinical trials	Intervention/treatment	Study design	Phase	Location[a]	Status
NCT04394858	Olaparib (PARP inhibitor) plus temozolomide (chemotherapeutic)	Prospective	2	US	Recruiting
NCT05142241 (RARE 2)	Talazoparib (PARP inhibitor) plus temozolomide (chemotherapeutic)	Prospective	2	US	Recruiting
NCT00107289	[^{131}I]-MIBG	Prospective	2	US	Recruiting
NCT01850888	[^{131}I]-MIBG in palliative patients	Prospective	NA	US	Recruiting
NCT04770831	[^{131}I]-MIBG	Prospective	2	US	Recruiting
NCT00874614	HSA [^{131}I]-MIBG	Prospective	2	US	Unknown
NCT03206060	[^{177}Lu] DOTATATE (PRRT)	Prospective	2	US	Recruiting
NCT04276597	[^{177}Lu] DOTATOC (PRRT)	Prospective	2	US	Recruiting
NCT04711135	[^{177}Lu] DOTATATE (PRRT) in adolescents	Prospective	2	US, Europe, UK	Recruiting
NCT04029428	[^{177}Lu] DOTATATE vs [^{90}Y] DOTATATE vs mix of 50% each (PRRT)	Prospective	2	Poland	Unknown
NCT00843037 (SNIPP)	Sunitinib (TKI)	Prospective	2	Canada, Netherlands	Active, not recruiting
NCT02302833	Cabozantinib s-malate (TKI)	Prospective	2	US	Recruiting
NCT01371201 (FIRST-MAPPP)	Sunitinib (TKI)	Randomized, double-blind, placebo-controlled	2	Europe	Closed (data arriving soon)
NCT03946527 (LAMPARA)	Lanreotide (SSTR analog)	Prospective	2	US	Recruiting
NCT03839498	Axitinib (TKI)	Prospective	2	US	Recruiting
NCT03008369	Lenvatinib (TKI)	Prospective	2	US	Active, not recruiting
NCT04860700	Anlotinib (TKI)	Prospective	2	China	Recruiting
NCT05133349	Anlotinib (TKI)	Prospective	2	China	Recruiting
NCT02721732	Pembrolizumab (Immunotherapeutic)	Prospective	2	US	Active, not recruiting
NCT04400474 (CABATEN)	Cabozantinib (TKI) plus atezolizumab (immunotherapeutic)	Prospective	2	Spain	Recruiting
NCT04924075 (MK-6482-015)	Belzutifan (HIF2α inhibitor)	Prospective	2	US, Canada, Europe, UK, Russia, Turkey	Recruiting
NCT04895748	DFF332 (HIF2α inhibitor) plus everolimus (mTORC1 inhibitor) or DFF332 plus spartalizumab (immunotherapeutic) plus taminadenant (A2A receptor antagonist)	Prospective	1	US, Europe, Japan, Singapore	Recruiting
NCT04284774 (MATCH)	Tipifarnib (farnesyltransferase inhibitor)	Prospective	2	US	Recruiting
NCT04187404 (Spencer)	EO2401 (therapeutic vaccine) plus nivolumab (immunotherapeutic)	Prospective	1/2	US and Europe	Recruiting
NCT03034200	ONC201 (small molecule DRD2 antagonist)	Prospective	2	US	Active, not recruiting

Abbreviations: HSA, high specific activity; HIF2α, hypoxia-inducible factor 2 alpha; MIBG, meta-iodobenzylguanidine; NA, not applicable; PARP, poly (ADP-ribose) polymerase; PRRT, peptide receptor radionuclide therapy; TKI, tyrosine kinase inhibitor.
[a]Trial locations at the timepoint of the writing of this paper.

Several clinical trials further investigating [^{131}I]-MIBG therapy and PRRT in metastatic PPGL patients (adult or adolescent) are now recruiting (**Table 1**).

For slowly/moderately progressing tumors that are not eligible for PRRT or MIBG, tyrosine kinase inhibitors (TKIs) or temozolomide may be considered as first-line therapeutic options (12).

Tyrosine kinase inhibitors

In the case of progression to CVD or radionuclide therapy, TKIs may be used (12). Targeting angiogenesis, which is a hallmark of metastatic PPGL development (60), by using TKIs is an important therapeutic strategy since both cluster 1, particularly *SDHB*, and cluster 2 mutations may predispose to angiogenesis (61, 62).

Sunitinib is a clinically available TKI that has been investigated in prospective phase 2 trials in PPGL patients: 1 prospective phase 2 trial (SNIPP trial, NCT00843037) showed a partial response of 13% (n = 25, disease control rate [DCR] over 12 weeks, 83% median progression-free survival [PFS] 13.4 months), and all *SDHx*-mutant patients showed partial responses or stable disease (63). The first randomized placebo-controlled phase 2 study in patients with metastatic PPGL (FIRST-MAPPP, NCT01371201) investigated sunitinib

Downloaded from https://academic.oup.com/jcem/article/107/11/2963/6668850 by Universitaetsbibliothek Muenchen user on 31 January 2024

vs placebo, and demonstrated promising preliminary results (PFS at 12 months: sunitinib group 35.9% vs placebo 18.9%; median PFS sunitinib 8.9 months vs placebo 3.6 months) (abstract) (47). A retrospective clinical trial described a partial response to sunitinib in 21% of patients, with 62.5% of cases with stable disease or a partial response in *SDHB* mutation carriers (64).

The TKI cabozantinib is also in clinical use and is being investigated in a clinical phase 2 trial in metastatic PPGL (NCT02302833) with promising preliminary results (partial response 37%, stable disease 55%, DCR 92%, PFS 16 months; responders included *SDHB*-mutant patients [preliminary data published in a review]) (62). Consistent with these data, our preclinical study on human PPGL primary cultures showed significantly stronger efficacy of cabozantinib in cluster 1 tumors, particularly *SDHB*-related tumors, compared with cluster 2 tumors (65).

Although the prospective and retrospective studies, as well as our preclinical study on human PPGL primary cultures, indicated particular efficacy of sunitinib and cabozantinib in cluster 1 *SDHx*-, particularly *SDHB*-related tumors (63-66), it still remains to be seen from the FIRST-MAPPP trial whether patients with these mutations are the best candidates for sunitinib (final detailed data are awaited). Moreover, it has to be kept in mind that patients with cluster 1-related PPGLs are often younger and have more aggressive tumors, compared with patients with cluster 2-related tumors. This may add to the better efficacy and tolerability of some drugs in patients with cluster 1-related tumors.

Other TKIs, including axitinib, pazopanib, lenvatinib, and anlotinib, have not been extensively clinically used in PPGLs as yet, but have shown moderate efficacy in small phase 2 trials (axitinib, n = 9, partial response in 3/9 patients [abstract]; pazopanib, n = 6, partial response in 1/6 patients, study halted from poor recruitment) (67, 68). Another phase 2 trial on axitinib is now recruiting (NCT03839498). A small retrospective study on the TKI lenvatinib showed promising results (n = 11, 5/11 *SDHB*-mutant, n = 8 with measurable disease, PFS at 12 months 61.4%, median PFS 14.7 months, partial response 5/8, stable disease 3/8), but a worsening of hypertension in the majority of patients (9/11) (69). Lenvatinib is currently being studied in another small phase 2 trial in metastatic PPGLs (NCT03008369). Two phase 2 trials studying TKI anlotinib in advanced PPGLs are now recruiting (NCT04860700, NCT05133349).

Immunotherapy

Pembrolizumab, a monoclonal antibody targeting PD-1, showed modest efficacy in 2 clinical phase 2 studies (n = 11, objective response rate [ORR] 9%, DCR 73%, median PFS 5.7 months and n = 9, ORR 0%, DCR 75% over 4 months, PFS at 27 weeks 43%, respectively) (NCT02721732) (70, 71).

Combination therapy: immunotherapy plus TKI

Because antiangiogenic therapy, through targeting vascular endothelial growth factor, promotes immune cell mobilization and enhances the efficacy of immunotherapy (62), the evaluation of TKIs in combination with immunotherapeutics may be of particular interest for metastatic PPGL patients. TKI plus immunotherapeutic combination therapies have already been approved for the therapy of advanced renal cell carcinoma (lenvatinib/pembrolizumab and cabozantinib/nivolumab) (72, 73), but there are only limited data available in PPGLs. One case study showed that cabozantinib plus nivolumab resulted in a major response in a metastatic PPGL patient until the end of the observation period (22 months after combination therapy initiation) (74). Furthermore, a multicohort phase 2 study of cabozantinib plus the immunotherapeutic atezolizumab in advanced endocrine tumors, including PPGLs, is currently recruiting, and may provide important clinical data (CABATEN, NCT04400474).

HIF2α Inhibitors

The HIF2α inhibitor belzutifan has received FDA approval for therapy of cancers associated with von Hippel-Lindau (VHL) disease (75), based on promising results from a phase 2 study on VHL-associated renal cell carcinoma (RCC) (n = 61, ORR 49%, partial response in 49% of patients, PFS at 24 months 96%) (MK-6482-004, NCT03401788) (76). Although PPGL patients have not been included in the studies so far, another phase 2 trial on belzutifan in advanced PPGLs and NETs is now recruiting (MK-6482-015, NCT04924075). Although some preclinical in vitro studies have shown a lack of efficacy of HIF2α inhibitors in PPGL cells, this was possibly because of the limitations of in vitro experiments (24, 65).

Other HIF2α inhibitors currently under investigation include PT2385, evaluated in a phase 2 study in VHL-associated clear cell (cc)RCC patients (NCT03108066), and DFF332 (in combination with either the mTORC1 inhibitor everolimus or the immunotherapeutic spartalizumab, plus the adenosine A2A receptor antagonist taminadenant), investigated in a phase 1 trial in tumor patients with HIF-stabilizing mutations, including PPGLs (NCT04895748).

Although there are currently no clinical data available concerning the efficacy of HIF2α inhibitors in PPGLs, these drugs theoretically offer important treatment potential for metastatic, particularly cluster 1-associated tumors (24, 77, 78), and the MK-6482-015 trial is likely to provide highly relevant data for metastatic PPGL patients.

Combination therapy: HIF2α inhibitor plus TKI

A potentially interesting combination therapy—belzutifan plus the TKI cabozantinib—is currently being investigated in a phase 2 trial in patients with advanced ccRCC (MK-6482-003, NCT03634540), with promising preliminary results (n = 41, ORR 22%, DCR 92.7% over 6 months, median PFS 16.8 months, PFS at 6 months 78.3% [in abstract]) (79).

Kinase Signaling Inhibitors

The kinase signaling pathways PI3K/AKT/mTOR or Ras/Raf/MEK/ERK are often overactivated in cluster 2-related PPGLs, and may be targeted by kinase signaling inhibitors (3, 12). TKIs have been discussed previously and may be used in both cluster 1- and cluster 2-related tumors.

The mTORC1 inhibitor everolimus is approved for the therapy of progressive NETs but has shown only slight to moderate efficacy in PPGLs in a small prospective and another small retrospective study (n = 4, DCR 25% and n = 7, DCR 71%, median PFS 3.8 months, respectively) (80, 81).

The selective RET inhibitor selpercatinib is approved for treatment of *RET*-mutant lung and thyroid cancers on the basis of a phase 1/2 clinical study in *RET*-mutant solid tumors, and medullary thyroid carcinomas (LIBRETTO-001, NCT03157128) (82). Although selpercatinib has also shown strong efficacy in a case report of a *RET* fusion-positive metastatic PPGL patient (83), our preclinical studies found

Downloaded from https://academic.oup.com/jcem/article/107/11/2963/6668850 by Universitaetsbibliothek Muenchen user on 31 January 2024

only moderate efficacy of selpercatinib in *RET*-mutant PPGL primary cultures (65), although this was based on a small sample size. Moreover, it is worth mentioning that the *RET*-mutant tumors in the primary culture study were all nonmetastatic tumors and, in general, cluster 2-related PPGLs show a very low metastatic risk (3%-10%) (2, 24, 25).

Tipifarnib, a farnesyl-transferase inhibitor that disrupts HRAS function, particularly in *HRAS*-mutant cancers, has received FDA "breakthrough therapy" designation for the treatment of recurrent or metastatic *HRAS*-mutant head-and-neck squamous cell carcinoma, based on the results of a phase 2 study (84). A phase 2 pediatric trial studying tipifarnib in patients with *HRAS*-mutant pheochromocytomas, among others, is now recruiting (MATCH, NCT04284774), and should provide important data for PPGL therapy.

Combination therapy: mTOR inhibitor plus TKI

Because everolimus usually leads to the development of resistance in patients with NETs after less than 1 year, through compensatory activation of other kinase signaling pathways (85, 86), the combination of mTOR inhibitors with TKIs may be a promising therapeutic option for NETs and also PPGLs, as shown by our preclinical studies in patient-derived PPGL primary cultures (a synergistic effect of everolimus plus cabozantinib was observed and an additive effect of everolimus plus sunitinib) (65, 87). Moreover, combination therapy of a TKI (lenvatinib) plus an mTOR inhibitor (everolimus) has been approved for other cancers (88), showing good efficacy and tolerability (89).

The combination of sunitinib plus the mTOR inhibitor rapamycin is also clinically well tolerated (90) and showed efficacy in at least 1 *SDHB*-mutant metastatic PPGL patient described in the literature (64). Stable disease was observed until the end of the observation period (3 years after initiating sunitinib, 18 months after addition of rapamycin), suggesting that molecular targeted combination therapies may prolong PFS at effective and clinically well-tolerated low doses. However, further clinical studies are warranted in metastatic PPGLs.

Combination therapy: tipifarnib plus TKI

A phase 1 trial of tipifarnib plus the TKI sorafenib in thyroid cancer showed good tolerability and promising results through inhibition of Ras/Raf/MAPK kinase/ERK and RET kinase pathways (n = 35, 8 *BRAF*-mutant, 8 *RET*-mutant, median PFS 18 months, overall survival at 24 months 80%) (91). These results also suggest a particular efficacy of combination therapy using inhibitors of the kinase signaling pathways, and this may potentially be transferable to PPGL patients. Furthermore, our preclinical studies in PPGL primary cultures have also shown notable efficacy of molecular targeted combination therapy, especially in cluster 2-, but also in cluster 1-related, PPGL primary cultures, through multiple targeting of kinase signaling pathways (65, 87).

Wnt Signaling Inhibitors

Because cluster 3-related PPGLs are relatively rare, there are no established specific therapies available for these tumors at the current time. However, targeting Wnt signaling is another therapeutic approach that should be further explored because these PPGLs harbor an aggressive phenotype with high metastatic potential (3, 26). Potential therapies include the Porcupine O-Acyltransferase inhibitor WNT974 and ß-catenin inhibitor PRI-724, which have shown good efficacy in a preclinical study in neuroendocrine tumor cell lines (92).

Bone-targeted Agents

Because metastatic PPGLs commonly spread to the skeletal system, the treatment of bone metastases, particularly if symptomatic and progressive, is also an important part of PPGL therapy. The use of bone-targeted agents such as the monoclonal antibody denosumab or the bisphosphonate zoledronic acid, may be considered as standard practice (42) because they are effective in reducing the risk of pathologic fractures and the need for radiation compared with placebo, as shown in a network meta-analysis (93). Moreover, zoledronic acid may also reduce neoplastic progression (both breast cancers and nonbreast cancers), as shown in osteopenic postmenopausal women (hazard ratio 0.67) (94), through inhibition of cancer cell proliferation and viability (65, 95). Our own PPGL primary culture studies have also revealed an antitumor effect of zoledronic acid in PPGLs (65). Other therapeutic options in the case of metastases, in the skeleton or other locations, include conventional external beam radiation therapy, stereotactic radiosurgery, and interventional radiology (radiofrequency ablation, cryoablation) (12, 96, 97).

Biotherapy: Somatostatin Analogs

The use of SSTR analogs may be considered in patients with strong SSTR2 expression (often cluster 1 *SDHx*-related PPGL) (12, 42). The rationale comes from patients with metastatic NETs where both lanreotide and octreotide prolonged PFS (median PFS lanreotide not reached vs placebo 18 months, estimated PFS lanreotide at 24 months 65.1% vs placebo 33.0%; median PFS octreotide LAR 14.3 months vs placebo 6 months) (98, 99). For PPGL patients, data are still lacking: only a few case reports have been published so far (100-103). However, a phase 2 trial on lanreotide in metastatic PPGL patients is now recruiting (LAMPARA, NCT03946527). One could consider the use of such analogs in patients with slow progression before the use of other systemic therapies, given its paucity of adverse effects.

Outlook and Conclusions

Although cluster specific pathogenesis, biochemical phenotyping, diagnostics, and follow-up are already widely used for PPGLs, much therapy still remains largely nonspecific (12).

Two anecdotal reports highlight the importance of mutational analysis in determining the optimal therapeutic strategy for individual PPGL patients. A metastatic PPGL patient with a novel germline *ALK* mutation received individualized molecular targeted therapy with the ALK inhibitor brigatinib, leading to disease remission and a sustained partial response until the end of the observation period (10 months after therapy initiation) (104). Another metastatic nonhereditary PPGL patient with a novel somatic *RET-SEPTIN9* fusion was accordingly treated with the selective RET inhibitor selpercatinib, resulting in a partial response after 12 weeks of treatment and an ongoing treatment response until week 23 (83). Such individualized (particularly molecular targeted) therapy may therefore follow genetic testing and the molecular classification of metastatic PPGLs, but both germline and somatic mutation testing will need to be widely implemented in the management of PPGLs for this to be practicable.

Ongoing trials investigating molecular targeted therapies, as well as other therapeutic strategies (eg, novel therapeutic

Downloaded from https://academic.oup.com/jcem/article/107/11/2963/6668850 by Universitaetsbibliothek Muenchen user on 31 January 2024

tumor vaccines together with check-point inhibitors; Spencer, NCT04187404) and small molecules, such as the DRD2 antagonist ONC201 (NCT03034200), will also provide important novel data regarding the therapy of metastatic PPGLs.

In conclusion, this mini-review has provided an overview of the current development and use of novel and promising molecular targeted therapies in metastatic PPGL patients. Molecular targeted therapeutics are now being increasingly clinically applied and are often effective and well tolerated. Combined molecular targeted therapies are also being studied with promising results, with a need for awareness of adverse events. With therapeutic strategies constantly being optimized and novel treatment strategies being developed and tested, the outlook for these rare tumors seems promising.

Funding

This work was supported by the German Research Foundation (Deutsche Forschungsgemeinschaft [DFG]) within the CRC/Transregio 205/2, Project number: 314061271 – TRR 205 'The Adrenal: Central Relay in Health and Disease' (to S.N. and F.B.) and the Immuno-TargET project under the umbrella of University Medicine Zurich (to S.N. and F.B.).

Disclosures

The authors have nothing to disclose.

Data Availability

Data sharing is not applicable to this article as no datasets were generated or analyzed during the current study.

References

1. Jhawar S, Arakawa Y, Kumar S, *et al*. New insights on the genetics of pheochromocytoma and paraganglioma and its clinical implications. *Cancers* 2022;14(3). doi 10.3390/cancers14030594 [published Online First: Epub Date]|
2. Crona J, Lamarca A, Ghosal S, Welin S, Skogseid B, Pacak K. Genotype-phenotype correlations in pheochromocytoma and paraganglioma: a systematic review and individual patient meta-analysis. *Endocr Relat Cancer.* 2019;26(5):539-550.
3. Fishbein L, Leshchiner I, Walter V, *et al*. Comprehensive molecular characterization of pheochromocytoma and paraganglioma. *Cancer Cell* 2017;31(2):181-193.
4. Luchetti A, Walsh D, Rodger F, *et al*. Profiling of somatic mutations in phaeochromocytoma and paraganglioma by targeted next generation sequencing analysis. *Int J Endocrinol* 2015;2015:138573. doi:10.1155/2015/138573 [published Online First: Epub Date]|
5. Gieldon L, William D, Hackmann K, *et al*. Optimizing genetic workup in pheochromocytoma and paraganglioma by integrating diagnostic and research approaches. *Cancers* 2019;11(6). doi 10.3390/cancers11060809 [published Online First: Epub Date]|
6. Jiang J, Zhang J, Pang Y, *et al*. Sino-European differences in the genetic landscape and clinical presentation of pheochromocytoma and paraganglioma. *J Clin Endocrinol Metab*. 2020;105(10): 3295–3307.
7. Jochmanova I, Pacak K. Genomic landscape of pheochromocytoma and paraganglioma. *Trends Cancer* 2018;4(1):6-9.
8. Burnichon N, Vescovo L, Amar L, *et al*. Integrative genomic analysis reveals somatic mutations in pheochromocytoma and paraganglioma. *Hum Mol Genet*. 2011;20(20):3974-3985.
9. Lenders JW, Duh QY, Eisenhofer G, *et al*. Pheochromocytoma and paraganglioma: an Endocrine Society clinical practice guideline. *J Clin Endocrinol Metab*. 2014;99(6):1915-1942.
10. Buffet A, Ben Aim L, Leboulleux S, *et al*. Positive impact of genetic test on the management and outcome of patients with paraganglioma and/or pheochromocytoma. *J Clin Endocrinol Metab*. 2019;104(4):1109-1118.
11. Lenders JWM, Kerstens MN, Amar L, *et al*. Genetics, diagnosis, management and future directions of research of phaeochromocytoma and paraganglioma: a position statement and consensus of the Working Group on Endocrine Hypertension of the European Society of Hypertension. *J Hypertens*. 2020;38(8):1443-1456.
12. Nölting S, Bechmann N, Taieb D, *et al*. Personalized management of pheochromocytoma and paraganglioma. *Endocr Rev*. 2022;43(2):199-239.
13. Pryma DA, Chin BB, Noto RB, *et al*. Efficacy and safety of high-specific-activity (131)I-MIBG therapy in patients with advanced pheochromocytoma or paraganglioma. *J Nucl Med*. 2019;60(5):623-630.
14. Eisenhofer G, Lenders JW, Siegert G, *et al*. Plasma methoxytyramine: a novel biomarker of metastatic pheochromocytoma and paraganglioma in relation to established risk factors of tumour size, location and SDHB mutation status. *Eur J Cancer*. 2012;48(11):1739-1749.
15. Patel D, Phay JE, Yen TWF, *et al*. Update on pheochromocytoma and paraganglioma from the SSO Endocrine/Head and Neck Disease-Site Work Group. Part 1 of 2: advances in pathogenesis and diagnosis of pheochromocytoma and paraganglioma. *Ann Surg Oncol*. 2020;27(5):1329-1337.
16. Remine WH, Chong GC, Van Heerden JA, Sheps SG, Harrison EG Jr. Current management of pheochromocytoma. *Ann Surg*. 1974;179(5):740-748.
17. Proye CA, Vix M, Jansson S, Tisell LE, Dralle H, Hiller W. "The" pheochromocytoma: a benign, intra-adrenal, hypertensive, sporadic unilateral tumor. Does it exist? *World J Surg*. 1994;18(4):467-472.
18. Goldstein RE, O'Neill JA, Jr., Holcomb GW, 3rd, *et al*. Clinical experience over 48 years with pheochromocytoma. *Ann Surg*. 1999;229(6):755-764; discussion 64-6.
19. Mannelli M, Ianni L, Cilotti A, Conti A. Pheochromocytoma in Italy: a multicentric retrospective study. *Eur J Endocrinol*. 1999;141(6):619-624.
20. Amar L, Servais A, Gimenez-Roqueplo AP, Zinzindohoue F, Chatellier G, Plouin PF. Year of diagnosis, features at presentation, and risk of recurrence in patients with pheochromocytoma or secreting paraganglioma. *J Clin Endocrinol Metab*. 2005;90(4):2110-2116.
21. Edstrom Elder E, Hjelm Skog AL, Hoog A, Hamberger B. The management of benign and malignant pheochromocytoma and abdominal paraganglioma. *Eur J Surg Oncol*. 2003;29(3):278-283.
22. Brouwers FM, Eisenhofer G, Tao JJ, *et al*. High frequency of SDHB germline mutations in patients with malignant catecholamine-producing paragangliomas: implications for genetic testing. *J Clin Endocrinol Metab*. 2006;91(11):4505-4509.
23. Schovanek J, Martucci V, Wesley R, *et al*. The size of the primary tumor and age at initial diagnosis are independent predictors of the metastatic behavior and survival of patients with SDHB-related pheochromocytoma and paraganglioma: a retrospective cohort study. *BMC Cancer* 2014;14:523. doi:10.1186/1471-2407-14-523.
24. Bechmann N, Moskopp ML, Ullrich M, *et al*. HIF2alpha supports pro-metastatic behavior in pheochromocytomas/paragangliomas. *Endocr Relat Cancer*. 2020;27(11):625-640.
25. Kumar S, Lila AR, Memon SS, *et al*. Metastatic cluster 2-related pheochromocytoma/paraganglioma: a single-center experience and systematic review. *Endocr Connect* 2021;10(11):1463-1476.
26. Alzofon N, Koc K, Panwell K, *et al*. Mastermind like transcriptional coactivator 3 (MAML3) drives neuroendocrine tumor progression. *Mol Cancer Res*. 2021;19(9):1476-1485 doi:10.1158/1541-7786.MCR-20-0992.
27. Hamidi O, Young WF, Jr., Gruber L, *et al*. Outcomes of patients with metastatic phaeochromocytoma and paraganglioma: a systematic review and meta-analysis. *Clin Endocrinol* 2017;87(5):440-50.
28. Turkova H, Prodanov T, Maly M, *et al*. Characteristics and outcomes of metastatic sdhb and sporadic pheochromocytoma/

Downloaded from https://academic.oup.com/jcem/article/107/11/2963/6668850 by Universitaetsbibliothek Muenchen user on 31 January 2024

paraganglioma: an National Institutes of Health Study. *Endocr Pract*. 2016;22(3):302-314.
29. Nölting S, Ullrich M, Pietzsch J, *et al*. Current management of pheochromocytoma/paraganglioma: a guide for the practicing clinician in the era of precision medicine. *Cancers* 2019;11(10). Doi: 10.3390/cancers11101505 [published Online First: Epub Date]|
30. Nölting S, Grossman A, Pacak K. Metastatic phaeochromocytoma: spinning towards more promising treatment options. *Exp Clin Endocrinol Diabetes*. 2018;127(2-03):117-128.
31. Lee YT, Tan YJ, Oon CE. Molecular targeted therapy: treating cancer with specificity. *Eur J Pharmacol*. 2018;834:188-196. doi:10.1016/j.ejphar.2018.07.034.
32. Rosland GV, Engelsen AS. Novel points of attack for targeted cancer therapy. *Basic Clin Pharmacol Toxicol*. 2015;116(1):9-18.
33. Lenders JW, Eisenhofer G, Mannelli M, Pacak K. Phaeochromocytoma. *Lancet* 2005;366(9486):665-675.
34. Pacak K, Linehan WM, Eisenhofer G, Walther MM, Goldstein DS. Recent advances in genetics, diagnosis, localization, and treatment of pheochromocytoma. *Ann Intern Med*. 2001;134(4):315-329.
35. Eisenhofer G, Klink B, Richter S, Lenders JW, Robledo M. Metabologenomics of phaeochromocytoma and paraganglioma: an integrated approach for personalised biochemical and genetic testing. *Clin Biochem Rev* 2017;38(2):69-100.
36. Eisenhofer G, Deutschbein T, Constantinescu G, *et al*. Plasma metanephrines and prospective prediction of tumor location, size and mutation type in patients with pheochromocytoma and paraganglioma. *Clin Chem Lab Med*. 2020;59(2):353-363.
37. Amar L, Pacak K, Steichen O, *et al*. International consensus on initial screening and follow-up of asymptomatic SDHx mutation carriers. *Nat Rev Endocrinol*. 2021;17(7):435-444.
38. Taieb D, Hicks RJ, Hindie E, *et al*. European Association of Nuclear Medicine Practice Guideline/Society of Nuclear Medicine and Molecular Imaging Procedure Standard 2019 for radionuclide imaging of phaeochromocytoma and paraganglioma. *Eur J Nucl Med Mol Imaging*. 2019;46(10):2112-2137.
39. Hamidi O, Young WF, Jr., Iniguez-Ariza NM, *et al*. Malignant pheochromocytoma and paraganglioma: 272 patients over 55 years. *J Clin Endocrinol Metab* 2017;102(9):3296-305.
40. Hescot S, Curras-Freixes M, Deutschbein T, *et al*. Prognosis of Malignant Pheochromocytoma and Paraganglioma (MAPP-Prono Study): a European Network for the study of adrenal tumors retrospective study. *J Clin Endocrinol Metab*. 2019;104(6):2367-2374.
41. Mei L, Khurana A, Al-Juhaishi T, *et al*. Prognostic factors of malignant pheochromocytoma and paraganglioma: a combined SEER and TCGA databases review. *Horm Metab Res*. 2019;51(7):451-457.
42. Fishbein L, Del Rivero J, Else T, *et al*. The North American Neuroendocrine Tumor Society Consensus Guidelines for surveillance and management of metastatic and/or unresectable pheochromocytoma and paraganglioma. *Pancreas* 2021;50(4):469-493.
43. Roman-Gonzalez A, Zhou S, Ayala-Ramirez M, *et al*. Impact of surgical resection of the primary tumor on overall survival in patients with metastatic pheochromocytoma or sympathetic paraganglioma. *Ann Surg*. 2018;268(1):172-178.
44. Strajina V, Dy BM, Farley DR, *et al*. Surgical treatment of malignant pheochromocytoma and paraganglioma: retrospective case series. *Ann Surg Oncol*. 2017;24(6):1546-1550.
45. Wei S, Wu D, Yue J. Surgical resection of multiple liver metastasis of functional malignant pheochromocytoma: a case report and literature review. *J Cancer Res Ther*. 2013;9(Suppl):S183-S185.
46. Arnas-Leon C, Sanchez V, Santana Suarez AD, Quintana Arroyo S, Acosta C, Martinez Martin FJ. Complete remission in metastatic pheochromocytoma treated with extensive surgery. *Cureus* 2016;8(1):e447.
47. Baudin E, Goichot B, Berruti A, *et al*. First International Randomized Study in Malignant Progressive Pheochromocytoma and Paragangliomas (FIRSTMAPPP): an academic double-blind trial investigating sunitinib. *Ann Oncol*. 2021;32:S621-S25. Doi: 10.1016/annonc/annonc700
48. Niemeijer ND, Alblas G, van Hulsteijn LT, Dekkers OM, Corssmit EP. Chemotherapy with cyclophosphamide, vincristine and dacarbazine for malignant paraganglioma and pheochromocytoma: systematic review and meta-analysis. *Clin Endocrinol* 2014;81(5):642-651.
49. Hadoux J, Favier J, Scoazec JY, *et al*. SDHB mutations are associated with response to temozolomide in patients with metastatic pheochromocytoma or paraganglioma. *Int J Cancer*. 2014;135(11):2711-2720.
50. Kulke MH, Stuart K, Enzinger PC, *et al*. Phase II study of temozolomide and thalidomide in patients with metastatic neuroendocrine tumors. *J Clin Oncol*. 2006;24(3):401-406.
51. Pang Y, Lu Y, Caisova V, *et al*. Targeting NAD(+)/PARP DNA repair pathway as a novel therapeutic approach to SDHB-mutated cluster i pheochromocytoma and paraganglioma. *Clin Cancer Res*. 2018;24(14):3423-3432.
52. Kong G, Grozinsky-Glasberg S, Hofman MS, *et al*. Efficacy of peptide receptor radionuclide therapy for functional metastatic paraganglioma and pheochromocytoma. *J Clin Endocrinol Metab*. 2017;102(9):3278-3287.
53. Fonte JS, Robles JF, Chen CC, *et al*. False-negative (1)(2)(3)I-MIBG SPECT is most commonly found in SDHB-related pheochromocytoma or paraganglioma with high frequency to develop metastatic disease. *Endocr Relat Cancer*. 2012;19(1):83-93.
54. Ziegler CG, Brown JW, Schally AV, *et al*. Expression of neuropeptide hormone receptors in human adrenal tumors and cell lines: antiproliferative effects of peptide analogues. *Proc Natl Acad Sci USA*. 2009;106(37):15879-15884.
55. Van Essen M, Krenning EP, De Jong M, Valkema R, Kwekkeboom DJ. Peptide Receptor Radionuclide Therapy with radiolabelled somatostatin analogues in patients with somatostatin receptor positive tumours. *Acta Oncol*. 2007;46(6):723-734.
56. Imhof A, Brunner P, Marincek N, *et al*. Response, survival, and long-term toxicity after therapy with the radiolabeled somatostatin analogue [90Y-DOTA]-TOC in metastasized neuroendocrine cancers. *J Clin Oncol*. 2011;29(17):2416-2423.
57. Ballal S, Yadav MP, Bal C, Sahoo RK, Tripathi M. Broadening horizons with (225)Ac-DOTATATE targeted alpha therapy for gastroenteropancreatic neuroendocrine tumour patients stable or refractory to (177)Lu-DOTATATE PRRT: first clinical experience on the efficacy and safety. *Eur J Nucl Med Mol Imaging*. 2020;47(4):934-946.
58. Fani M, Braun F, Waser B, *et al*. Unexpected sensitivity of sst2 antagonists to N-terminal radiometal modifications. *J Nucl Med*. 2012;53(9):1481-1489.
59. Wild D, Fani M, Fischer R, *et al*. Comparison of somatostatin receptor agonist and antagonist for peptide receptor radionuclide therapy: a pilot study. *J Nucl Med*. 2014;55(8):1248-1252.
60. Jimenez C. Treatment for patients with malignant pheochromocytomas and paragangliomas: a perspective from the hallmarks of cancer. *Front Endocrinol* 2018;9:277. doi:10.3389/fendo.2018.00277.
61. Favier J, Igaz P, Burnichon N, *et al*. Rationale for anti-angiogenic therapy in pheochromocytoma and paraganglioma. *Endocr Pathol*. 2012;23(1):34-42.
62. Jimenez C, Fazeli S, Roman-Gonzalez A. Antiangiogenic therapies for pheochromocytoma and paraganglioma. *Endocr Relat Cancer*. 2020;27(7):R239-R254.
63. O'Kane GM, Ezzat S, Joshua AM, *et al*. A phase 2 trial of sunitinib in patients with progressive paraganglioma or pheochromocytoma: the SNIPP trial. *Br J Cancer*. 2019;120(12):1113-1119.
64. Ayala-Ramirez M, Chougnet CN, Habra MA, *et al*. Treatment with sunitinib for patients with progressive metastatic pheochromocytomas and sympathetic paragangliomas. *J Clin Endocrinol Metab*. 2012;97(11):4040-4050.
65. Wang K, Schutze I, Gulde S, *et al*. Personalized drug testing in human pheochromocytoma/paraganglioma primary cultures. *Endocr Relat Cancer*. 2022;29(6):285-306. doi:10.1530/ERC-21-0355.
66. Jimenez C, Busaidy N, Habra M, Waguespack S, Jessop A. A phase 2 study to evaluate the effects of cabozantinib in patients with unresectable metastatic pheochromocytomas and paragangliomas.

Downloaded from https://academic.oup.com/jcem/article/107/11/2963/6668850 by Universitaetsbibliothek Muenchen user on 31 January 2024

In: International Symposium on Pheochromocytoma and Paraganglioma Sydney, Australia, 2017.
67. Burotto Pichun ME, Edgerly M, Velarde M, *et al*. Phase II clinical trial of axitinib in metastatic pheochromocytomas and paragangliomas (P/PG): preliminary results. *J Clin Oncol*. 2015;33(7_suppl):457-457.
68. Jasim S, Suman VJ, Jimenez C, *et al*. Phase II trial of pazopanib in advanced/progressive malignant pheochromocytoma and paraganglioma. *Endocrine* 2017;57(2):220-225.
69. Hassan Nelson L, Fuentes-Bayne H, Yin J, *et al*. Lenvatinib as a therapeutic option in unresectable metastatic pheochromocytoma and paragangliomas. *J Endocr Soc*. 2022;6(5):bvac044.
70. Jimenez C, Subbiah V, Stephen B, *et al*. Phase II clinical trial of pembrolizumab in patients with progressive metastatic pheochromocytomas and paragangliomas. *Cancers* 2020;12(8). doi 10.3390/cancers12082307.
71. Naing A, Meric-Bernstam F, Stephen B, *et al*. Phase 2 study of pembrolizumab in patients with advanced rare cancers. *J ImmunoTher Cancer*. 2020;8(1). doi 10.1136/jitc-2019-000347.
72. Motzer R, Alekseev B, Rha SY, *et al*. Lenvatinib plus pembrolizumab or everolimus for advanced renal cell carcinoma. *N Engl J Med*. 2021;384(14):1289-1300.
73. Choueiri TK, Powles T, Burotto M, *et al*. Nivolumab plus cabozantinib versus sunitinib for advanced renal-cell carcinoma. *N Engl J Med*. 2021;384(9):829-841.
74. Economides MP, Shah AY, Jimenez C, Habra MA, Desai M, Campbell MT. A durable response with the combination of nivolumab and cabozantinib in a patient with metastatic paraganglioma: a case report and review of the current literature. *Front Endocrinol* 2020;11:594264. doi:10.3389/fendo.2020.594264 [published Online First: Epub Date]|.
75. Deeks ED. Belzutifan: first approval. *Drugs*. 2021;81(16):1921-1927.
76. Jonasch E, Donskov F, Iliopoulos O, *et al*. Belzutifan for renal cell carcinoma in von Hippel-Lindau disease. *N Engl J Med*. 2021;385(22):2036-2046.
77. Toledo RA. New HIF2alpha inhibitors: potential implications as therapeutics for advanced pheochromocytomas and paragangliomas. *Endocr Relat Cancer* 2017;24(9):C9-C19.
78. Peng S, Zhang J, Tan X, *et al*. The VHL/HIF axis in the development and treatment of pheochromocytoma/paraganglioma. *Front Endocrinol* 2020;11:586857. doi:10.3389/fendo.2020.586857 [published Online First: Epub Date]|.
79. Choueiri TK, Bauer TM, McDermott DF, *et al*. Phase 2 study of the oral hypoxia-inducible factor 2α (HIF-2α) inhibitor MK-6482 in combination with cabozantinib in patients with advanced clear cell renal cell carcinoma (ccRCC). *J Clin Oncol*. 2021;39(6_suppl):272-272.
80. Druce MR, Kaltsas GA, Fraenkel M, Gross DJ, Grossman AB. Novel and evolving therapies in the treatment of malignant phaeochromocytoma: experience with the mTOR inhibitor everolimus (RAD001). *Horm Metab Res*. 2009;41(9):697-702.
81. Oh DY, Kim TW, Park YS, *et al*. Phase 2 study of everolimus monotherapy in patients with nonfunctioning neuroendocrine tumors or pheochromocytomas/paragangliomas. *Cancer* 2012;118(24):6162-6170.
82. Wirth LJ, Sherman E, Robinson B, *et al*. Efficacy of selpercatinib in RET-altered thyroid cancers. *N Engl J Med*. 2020;383(9):825-835.
83. Mweempwa A, Xu H, Vissers JHA, *et al*. Novel RET fusion RET-SEPTIN9 predicts response to selective RET inhibition with selpercatinib in malignant pheochromocytoma. *JCO Precis Oncol* 2021;5:1160-1165. doi:10.1200/PO.21.00127 [published Online First: Epub Date]|.
84. Ho AL, Brana I, Haddad R, *et al*. Tipifarnib in head and neck squamous cell carcinoma with HRAS mutations. *J Clin Oncol*. 2021;39(17):1856-1864.
85. Yao JC, Shah MH, Ito T, *et al*. Everolimus for advanced pancreatic neuroendocrine tumors. *N Engl J Med*. 2011;364(6):514-523.
86. Yao JC, Fazio N, Singh S, *et al*. Everolimus for the treatment of advanced, non-functional neuroendocrine tumours of the lung or gastrointestinal tract (RADIANT-4): a randomised, placebo-controlled, phase 3 study. *Lancet* 2016;387(10022):968-977.
87. Fankhauser M, Bechmann N, Lauseker M, *et al*. Synergistic highly potent targeted drug combinations in different pheochromocytoma models including human tumor cultures. *Endocrinology* 2019;160(11):2600-2617.
88. Motzer RJ, Hutson TE, Glen H, *et al*. Lenvatinib, everolimus, and the combination in patients with metastatic renal cell carcinoma: a randomised, phase 2, open-label, multicentre trial. *Lancet Oncol*. 2015;16(15):1473-1482.
89. Wiele AJ, Bathala TK, Hahn AW, *et al*. Lenvatinib with or without everolimus in patients with metastatic renal cell carcinoma after immune checkpoint inhibitors and vascular endothelial growth factor receptor-tyrosine kinase inhibitor therapies. *Oncologist* 2021;26(6):476-482.
90. Waqar SN, Gopalan PK, Williams K, Devarakonda S, Govindan R. A phase I trial of sunitinib and rapamycin in patients with advanced non-small cell lung cancer. *Chemotherapy* 2013;59(1):8-13.
91. Hong DS, Cabanillas ME, Wheler J, *et al*. Inhibition of the Ras/Raf/MEK/ERK and RET kinase pathways with the combination of the multikinase inhibitor sorafenib and the farnesyltransferase inhibitor tipifarnib in medullary and differentiated thyroid malignancies. *J Clin Endocrinol Metab*. 2011;96(4):997-1005.
92. Jin XF, Spoettl G, Maurer J, Nolting S, Auernhammer CJ. Inhibition of Wnt/beta-catenin signaling in neuroendocrine tumors in vitro: antitumoral effects. *Cancers* 2020;12(2). doi 10.3390/cancers12020345.
93. Wang Z, Qiao D, Lu Y, *et al*. Systematic literature review and network meta-analysis comparing bone-targeted agents for the prevention of skeletal-related events in cancer patients with bone metastasis. *Oncologist* 2015;20(4):440-449.
94. Reid IR, Horne AM, Mihov B, *et al*. Effects of zoledronate on cancer, cardiac events, and mortality in osteopenic older women. *J Bone Miner Res*. 2020;35(1):20-27.
95. Wang L, Fang D, Xu J, Luo R. Various pathways of zoledronic acid against osteoclasts and bone cancer metastasis: a brief review. *BMC Cancer* 2020;20(1):1059.
96. Kohlenberg J, Welch B, Hamidi O, *et al*. Efficacy and safety of ablative therapy in the treatment of patients with metastatic pheochromocytoma and paraganglioma. *Cancers* 2019;11(2). doi 10.3390/cancers11020195.
97. Breen W, Bancos I, Young WF Jr, *et al*. External beam radiation therapy for advanced/unresectable malignant paraganglioma and pheochromocytoma. *Adv Radiat Oncol* 2018;3(1):25-29.
98. Caplin ME, Pavel M, Cwikla JB, *et al*. Lanreotide in metastatic enteropancreatic neuroendocrine tumors. *N Engl J Med*. 2014;371(3):224-233.
99. Rinke A, Muller HH, Schade-Brittinger C, *et al*. Placebo-controlled, double-blind, prospective, randomized study on the effect of octreotide LAR in the control of tumor growth in patients with metastatic neuroendocrine midgut tumors: a report from the PROMID Study Group. *J Clin Oncol*. 2009;27(28):4656-4663.
100. Tonyukuk V, Emral R, Temizkan S, Sertcelik A, Erden I, Corapcioglu D. Case report: patient with multiple paragangliomas treated with long acting somatostatin analogue. *Endocr J*. 2003;50(5):507-513.
101. van Hulsteijn LT, van Duinen N, Verbist BM, *et al*. Effects of octreotide therapy in progressive head and neck paragangliomas: case series. *Head Neck* 2013;35(12):E391-E396.
102. Tena I, Gupta G, Tajahuerce M, *et al*. Successful second-line metronomic temozolomide in metastatic paraganglioma: case reports and review of the literature. *Clin Med Insights Oncol* 2018;12. doi:10.1177/1179554918763367.
103. Jha A, Patel M, Baker E, *et al*. Role of (68)Ga-DOTATATE PET/CT in a case of SDHB-related pterygopalatine fossa paraganglioma successfully controlled with octreotide. *Nucl Med Mol Imaging* 2020;54(1):48-52.
104. Heregger R, Huemer F, Hutarew G, *et al*. Sustained response to brigatinib in a patient with refractory metastatic pheochromocytoma harboring R1192P anaplastic lymphoma kinase mutation: a case report from the Austrian Group Medical Tumor Therapy next-generation sequencing registry and discussion of the literature. *ESMO Open* 2021;6(4):100233.

Downloaded from https://academic.oup.com/jcem/article/107/11/2963/6668850 by Universitaetsbibliothek Muenchen user on 31 January 2024

Acknowledgements

Firstly, I would like to express my sincere gratitude to my thesis supervisor and mentor Prof. Svenja Nölting for this fascinating research topic and her continuous support, advice, and outstanding guidance during my research project.

I am also grateful to Prof. Christoph Auernhammer for additionally providing valuable expertise and support.

This project would not have been possible without Prof. Martin Reincke and Prof. Thomas Knösel who played important roles as part of my supervision committee.

I would also like to extend special thanks to Julian Maurer, Astrid Reul and Gerald Spöttl for their valuable help and the enjoyable time spent together in the laboratory.

Additionally, I am grateful to Prof. Ashley Grossman for kindly proofreading my thesis.

Finally, I would like to thank my family and partner for their encouragement and support throughout my studies. In particular, I am deeply grateful to my parents for their everlasting love and support.